Improvement of Body on Frame Chassis of Bishoftu Pickup Truck for Crashworthiness during Front and Side Impact

Ermias Diresie Wolde

A Thesis Submitted to

The Department of Mechanical Engineering

School of Mechanical, Chemical and Materials Engineering

Presented in Partial Fulfillment of the Requirement for Master of Science in Automotive Engineering

Office of Graduate Studies

Adama Science and Technology University

July, 2024

Adama, Ethiopia

Improvement of Body on Frame Chassis of Bishoftu Pickup Truck for of Crashworthiness during Front and Side Impact

Ermias Diresie Wolde

Advisor. Dr. Amana Wako

A Thesis Submitted to
The Department of Mechanical Engineering
School of Mechanical, Chemical and Materials Engineering

Presented in Partial Fulfillment of the Requirement for Master of Science in Automotive Engineering

Office of Graduate Studies
Adama Science and Technology University

July, 2024
Adama, Ethiopia

DECLARATION

I hereby declare that this Master Thesis entitled “Improvement of Body on Frame Chassis of Bishoftu Pickup Truck for of Crashworthiness during Front and Side Impact” is my original work. That is, it has not been submitted for the award of any academic degree, diploma, or certificate in any other university. All sources of materials that are used for this thesis have been duly acknowledged through citation.

Ermias Diresie Wolde	_____	_____
Name of student	Signature	Date

RECOMMENDATION

We, the advisors of this thesis, hereby certify that we have read the revised version of the thesis entitled "Improvement of Body on Frame Chassis of Bishoftu Pickup Truck for of Crashworthiness during Front and Side Impact" prepared under our guidance by Ermias Diresie submitted in partial fulfillment of the requirements for Master of Science in automotive engineering. Therefore, we recommend the submission of the revised version of the thesis to the department following the applicable procedures.

_____	_____	_____
Major Advisor	Signature	Date
_____	_____	_____
Co - Advisor	Signature	Date

APPROVAL PAGE

We, the advisors of the thesis entitled “Improvement of Body on Frame Chassis of Bishoftu Pickup Truck for of Crashworthiness during Front and Side Impact” and developed by Ermias Diresie, hereby certify that the recommendation and suggestions made by the board of examiners are appropriately incorporated into the final version of the thesis.

Major Advisor	Signature	Date
Co - Advisor	Signature	Date

We, the undersigned, members of the Board of Examiners of the thesis by Ermias Diresie have read and evaluated the thesis entitled “Improvement of Body on Frame Chassis of Bishoftu Pickup Truck for of Crashworthiness during Front and Side Impact” and examined the candidate during the open defense. This is, therefore, to certify that the thesis is accepted for partial fulfillment of the requirement of Master of Science in Automotive Engineering.

Chairperson	Signature	Date
Internal Examiner	Signature	Date
External Examiner	Signature	Date

Finally, approval and acceptance of the thesis is contingent upon submission of its final copy to the Office of Postgraduate Studies (OPGS) through the Department Graduate Council (DGC) and School Graduate Committee (SGC).

Department Head	Signature	Date
School Dean	Signature	Date
Office of Postgraduate Studies, Dean	Signature	Date

ACKNOWLEDGMENT

I would like to start by extending my deepest gratitude to God for enabling me to undertake my studies and this research. I would like to sincerely thank my advisor Dr. Amana Wako who continually conveyed constructive advice and scholarly support, without his persistent advice and guidance this research paper would not have been possible. In addition, I am grateful for my teachers who have emotionally encouraged me to complete my studies and my friends for your significant contribution, support, and advice.

Table of Contents

LIST OF TABLES

LIST OF FIGURES

ACRONYMS

CAD	Computer-Aided Design
CP	Crash pulse
EA	Energy absorption
FEA	Finite element analysis
FMVSS	Federal Motor Vehicle Safety Standard
HE	Hourglass energy
HIC	Head injury criteria
IIHS	Insurance Institute for Highway Safety
LMS	Lumped mass spring
NCAC	National crash analysis center
NHTSA	National Highway Traffic Safety Administration

NOMENCLATURE

Ed	Damping energy (kJ)
Eh	Hourglass energies (kJ)
E_{ke}	Kinetic energy (kJ)
E_s	Interface sliding (dissipated contact energy) (kJ)
F	Force of vehicles (N)
F	Instantaneous Impact Force
G	Acceleration Due to Gravity (m/s^2)
a_{max}	Peak Acceleration
F_{max}	Peak Crash Force
ρ	Foam density (kg/mm^3)
E	Young's modulus (GPa)
PR	Poisson's ratio
Y**S**	Yield strength (stress) (GPa)

ABSTRACT

The crashworthiness of vehicle chassis for crashworthiness is a crucial aspect of vehicle design and safety engineering. It involves enhancing the vehicle's ability to protect occupants during a collision by minimizing impact forces and reducing the risk of injury. This is achieved through advanced engineering techniques, materials, and structural design. This allows to strike a balance between structural strength, energy absorption, and occupant protection during a crash. Most researches focus on improving the efficiency of the vehicle by reducing the weight of the chassis but it is necessary to balance crashworthiness and weight reduction of the chassis. The main objective of this thesis work is to analysis Bishoftu Pickup vehicle chassis structure crashworthiness and analyze its performance using numerical methods. The CAD design done using SOLIDWORKS 18; and finite element analysis be conducted using LS-DYNA software. This involves modeling the chassis structure, simulating crash analysis in different conditions, and comparing the analysis results to develop an optimized design. The research aims to balance crashworthiness and weight reduction of the chassis to improve passenger vehicle passive safety performance. While the limitation is the lack of experimental evaluation. The results from the analysis the modified model shows better protection by deforming less as compared to the existing model, it gives protection to the occupant compartment after collision. Among the initial kinetic energy, 102.2kN-mm of kinetic energy which is 60.8% is lost in the existing model where as for the modified model; the loss of kinetic energy is 124.3kN-mm which is 74% of the total energy or the initial kinetic energy during frontal collision. The total deformation by the existing is 56.1 mm and the modified model is 40.5mm. Their difference in deformation is 15.6 mm (27.8% improvement in deformation). Additionally, the total energy absorbed by the modified model is more as compared to the existing model. Their difference in absorption is 21.8kN-mm (19.5% improvement in energy absorption). The maximum impact force occur on the existing model is equal to 549kN, whereas the modified produced 770kN, the difference is 221kN this is due to the reinforcement which increases the overall thickness of the chassis. It also recommended that the government and relevant bodies implement crash and safety regulations and quality evaluations for pickups. Additionally, in future research, the response of other major parts exposed to collision should be evaluated and study has to be conducted considering the effect of rear impact on the chassis.

Keywords. Chassis, Crashworthiness, Optimization, Reinforcement, Bishoftu Pickup Truck

CHAPTER ONE

INTRODUCTION

1.1 Background of the Study

Automotive chassis is a skeletal frame on which various mechanical parts like engine, tires, axle assemblies, brakes, steering, etc. are bolted. The chassis is considered to be the most significant component of an automobile (Baskar et al., 2014). It is the most crucial element that gives strength and stability to the vehicle under different conditions. The backbone of any automobile, the body of an engine, axle assemblies is fixed to the supporting frame (Liao et al., 2006). Tie bars, which are essential parts of automotive frames, are fasteners that bind different auto parts together. Automotive frames are manufactured from steel (Grzegorz et al., 2014). Aluminum is another raw material that has increasingly become popular for manufacturing these auto frames. Automobile chassis helps keep an automobile rigid, stiff, and unbending (Jeong et al., 2011). Auto chassis ensures low levels of noise, vibrations, and harshness throughout the automobile (Ren et al., 2005).

In automobile design, crash and structural analysis are the two most important engineering processes in developing a high-quality vehicle. Optimization for structural crashworthiness and energy absorption has become an important topic of research attributable to its proven benefits to public safety and social economy (Fang et al., 2017). Vehicle crash brings increasing concerns from socioeconomic aspects. Each year vehicle crash leads to about 1.2 million deaths and many more injuries worldwide, becoming one of the biggest public health issues facing modern society (Fang et al., 2017).

Crashworthiness is a designed characteristic that has the aim of dissipating energy, which is applied to a vehicle during a collision. The desirable outcome is energy being absorbed via crumple zones or chassis components that have the purpose of deforming, this results in the occupants of the vehicle experiencing less of the impact energy and an improvement in safety (Mamalis et al., 1998). As it is shown in the study conducted by O'Neill (2009), crashworthiness design of vehicle structures has proven highly effective, through which at least 43 % of potential fatalities could have been prevented and much more injuries avoided, making crashworthiness research and development draw growing interest over recent years.

According to the research conducted by Ossiander et al. (2014), Occupants of passenger vehicles that crashed with compact unibody were at an 18% lower risk of death compared to those that crashed with a compact body on frame. Therefore, since Occupants of compact unibody were at a lower risk of death compared to occupants of a body on frame, this research focus on optimization of a body on frame chassis and analyzes its performance numerically using LS- DYNA software. The main objective of this thesis is to analyze body on frame passenger vehicle chassis crashworthiness using numerical methods. The CAD design done using SOLIDWORKS 18; and finite element analysis be conducted using LS-DYNA software. The crashworthiness analysis aims to provide an optimized chassis structure that can absorb the crash energy by controlled structure deformation and achieved by redesigning by using composite material which give the chassis structure a better performance.

1.2 Statement of the Problem

Most researches focus on improving the efficiency of the vehicle by reducing the weight of the chassis but it is necessary to balance crashworthiness and weight reduction of the chassis. Vehicle crash brings increasing concerns from socioeconomic aspects. Each year vehicle crash leads to about 1.2 million deaths and many more injuries worldwide, becoming one of the biggest public health issues facing modern society (Fang et al., 2017). In addition, since Safety is compromised in a body on a framed vehicle more impact energy is passed into the cabin and to the other vehicle during a crash because the rails do not deform under impact. Therefore, to reduce injury and death occurred during vehicle crashes, it is necessary to improve passenger vehicle passive safety performance. This can be achieved by the crashworthiness design of the chassis to absorb as much as energy to reduce the kinetic energy transmitting to the occupants.

1.3 Objectives of the Study

1.3.1 General Objective

The general objective of this thesis work is to Improvement of Body on Frame Chassis of Bishoftu Pickup Truck for of Crashworthiness during Front and Side Impact by using LS-DYNA software.

1.3.2 Specific Objectives

The main objective of this research achieved through the following specific objectives.

- To model the existing structure of Bishoftu pickup to simulate the crashworthiness using SOLIDWORKS 18.
- To simulate the crash analysis of the CAD design using LS-DYNA software in different crash conditions.
- To analyze the existing frame structural responses for different speed ranges of the pickup using nonlinear FEM during frontal and side collision.
- To model the modified structure of Bishoftu pickup to simulate the crashworthiness using SOLIDWORKS 18.
- To analyze the modified frame structural responses for different speed ranges of the pickup using nonlinear FEM during frontal and side collision.
- To compere the analysis result and modified design.

1.4 Significance of the Study

Crashworthiness is a designed characteristic that has the aim of dissipating energy, which is applied to a vehicle during a collision. As it is shown in the study conducted by O'Neill (2009), crashworthiness design of vehicle structures has proven highly effective, through which at least 43 % of potential fatalities could have been prevented and much more injuries avoided, making crashworthiness research and development draw growing interest over recent years. Therefore, the main significances of this thesis are.

- To reduce occupant's death and injury by absorbing the crash energy and the chassis components.

1.5 Scope and Limitation of the Study

1.5.1 Scope of the study

The scope of this work includes CAD modeling of the chassis structure using SOLIDWORKS software. The crash analysis carried out using LS-DYNA software. Energy absorption, specific energy absorption, peak impact force, and, crash force efficiency, are considered as quantitative criteria for crashworthiness evaluation. The crash analysis simulation and results can be used to assess both the crashworthiness of the frame and to investigate ways to improve the design.

1.5.2 Limitation of the Study

Experimental evaluation of the actual work is inquired for the validity of the result. Nevertheless, hence experimental setups inquire a high amount of budget and lab facility. In this study, the experimental evaluation is not carried out.

1.6 Organization of the Thesis

This thesis is organized into six chapters. The First Chapter presents the introduction of the study, a statement of the problem, the general and specific objectives, the significance, the Scope and Limitation of the Study, and finally organization of the thesis. Literature about chassis frame, Crashworthiness, Types of Crash, Crashworthiness, and Energy Absorption and literature summary are reviewed in Chapter Two. Chapter Three elaborates on the materials and methodology of the work including data collection. Chapter Four presents the structural design and optimization of pick-up chassis frame and the modeling of existing chassis frame. Results and discussions are presented in Chapter Five. Chapter Six presents the major conclusions of the work conducted in this thesis, highlighting the findings and concluding with recommendations for further work.

CHAPTER TWO

LITERATURE REVIEW

2.1 Introduction

A vehicle frame, also known as its chassis, is the main supporting structure of a motor vehicle to which all other components are attached. Until the 1930s, virtually every (motor) vehicle had a structural frame, separate from the car's body. This construction design is known as body-on- frame. A vehicle without a body is called Chassis. The components of the vehicle like Power plant, Transmission System, Axles, Wheels and Tires, Suspension, Controlling Systems like Braking, Steering, and electrical system parts are mounted on the Chassis frame. It is the main mounting for all the components including the body. Therefore, it is also called as Carrying Unit (Babu and Narasimha, 2016).

Functions of the chassis frame.

- To carry the load of the passengers or goods carried in the body.
- To support the load of the body, engine, gearbox, etc.,
- To withstand the forces caused due to the sudden braking or acceleration
- To withstand the stresses caused due to the bad road condition.
- To withstand centrifugal force while cornering

Crashworthiness is the ability of a structure to protect its occupants during an impact. This is commonly tested when investigating the safety of vehicles. Depending on the nature of the impact and the vehicle involved, different criteria are used to determine the crashworthiness of the structure. Crashworthiness may be assessed either prospectively, using computer models (LS-DYNA, PAM-CRASH, MSC DYTRAN, MADYMO) or experiments, or retrospectively by analyzing crash outcomes. Several criteria are used to assess crashworthiness prospectively, including the deformation patterns of the vehicle structure, the acceleration experienced by the vehicle during an impact, and the probability of injury predicted by human body models.

Injury probability is defined using criteria, which are mechanical parameters (force, acceleration, or deformation) that correlate with injury risk. Optimization for structural crashworthiness and energy absorption has become an important topic of research attributable to its proven benefits to public safety and social economy (Fang et al., 2017). Vehicle crash brings increasing concerns from socioeconomic aspects.

Each year vehicle crash leads to about 1.2 million deaths and many more injuries worldwide, becoming one of the biggest public health issues facing modern society (Fang et al., 2017). Such a high socioeconomic burden places increasing attention on road and vehicle safety. As it is shown in the study conducted by O'Neill (2009), crashworthiness design of vehicle structures has proven highly effective, through which at least 43 % of potential fatalities could have been prevented and much more injuries avoided, making crashworthiness research and development draw growing interest over recent years.

Yet the question remaining to be addressed is whether their crashworthiness meets the requirements or there is a solution in balancing crashworthiness and light-weighting most effectively. Over the past two decades, design optimization has been developed as a powerful tool to seek the highest possible crashworthiness and lightest possible structure for various vehicles (Fang et al., 2017).

2.2 Types of Crash

2.2.1 Frontal Impact

Frontal impact is the most common type of crash. Statistics from NHTSA indicate that 51% of impacts resulting in injury or fatalities are fontal collisions. The act that frontal crashes are the most common is the reason that the earliest crashworthiness research focused on this type of collision. Although 51% of crashes resulting in fatalities or injury are frontal collisions, they account for only 31% of fatalities. This indicates that some success has ken achieved in the improvement of the crashworthiness of vehicles for this type of impact (Koora, et al., 2016).

NHTSA’s frontal crash standard specifies that the full front of a vehicle impact a rigid barrier. However, according to National Automotive Sampling System (NASS) estimates, 42 percent of frontal crashes are full-frontal crashes and about 56 percent are offset frontal crashes (Hershman, 2001).

2.2.2 Side Impact

Side impacts are less common than frontal crashes, comprising 25% of collisions resulting in injury or fatality. On the other hand, they account for 34% of the fatalities, indicating that protecting drivers from side impact is more difficult than fontal impact. This is likely because of the comparatively smaller crumple volume available to absorb energy is this type of impact (Koora, et al., 2016).

2.2.3 Rear Impact

Rear impacts account for a small percentage of vehicle collisions, and are usually low speed impacts. Fatality rates for this type of impact are low, only 2% of fatalities are caused by rear impact. Whiplash is the most common injury resulting from this type of impact, but the injury mechanism is not well understood (Koora, et al., 2016).

The several cross sections used in frame construction include channels, boxes, caps, double channels and I-sections. Stress analysis is performed on the frame to find the critical point with maximum pressure. The critical point is the critical factor that causes the fatigue failure of the chassis frame. The most commonly used materials for the frame are steel and aluminum. However, carbon fibers have been found to be more beneficial than these conventional materials because carbon fibers have greater strength and rigidity and are also lighter in weight. They can be easily made in various shapes. The lightweight chassis reduces the vehicle's fuel consumption, thereby increasing its fuel efficiency. Therefore, an ultra-lightweight carbon fiber chassis is preferred to build chassis to increase the strength and stability of the vehicle.

2.3 Types of Chassis Structure

Chassis structure is mainly divided into two types body on frame and unibody. The body-on-frame concept was used until the early 1960s by nearly all cars in the world. The frame looks like a ladder, two longitudinal rails connected by several lateral and cross braces. The longitude members are the main stress member. They deal with the load and the longitudinal forces caused by acceleration and braking. The lateral and cross members provide resistance to lateral forces and increase the torsional rigidity (The Aluminum Automotive Manual, 2013). Body on frame is used on trucks because of its overall strength and ability to sustain weight.

The disadvantage of the body on frame design is that.

- It is usually heavy and the torsional body stiffness needs to be improved.
- In addition, the frame tends to take up a lot of valuable space and forces the center of gravity to go up.
- Safety is also compromised in a body on a framed vehicle because the rails do not deform under impact; i.e., more impact energy is passed into the cabin and to the other vehicle (Aluminum Automotive Manual, 2013). Figure 2.1 Shows Body on frame chassis.

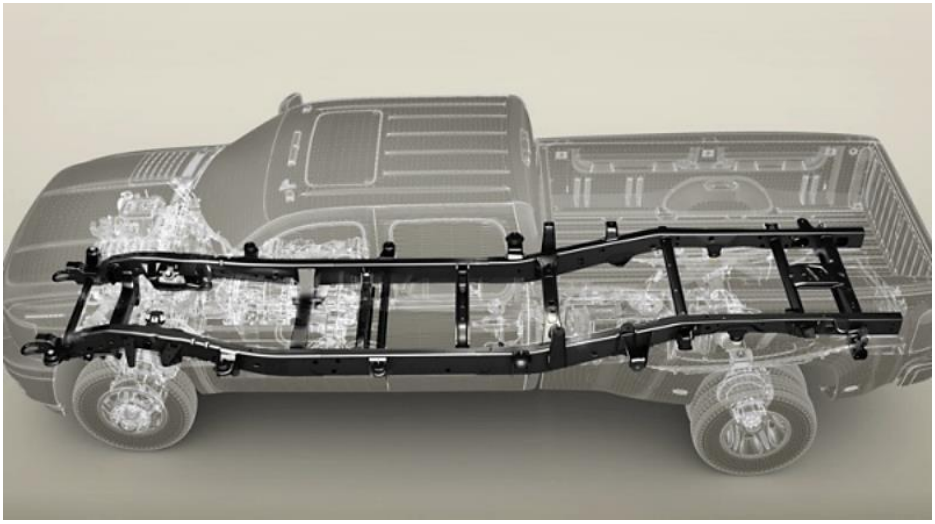

Figure 2.1. Body on frame chassis (Aluminum Automotive Manual, 2013)

2.4. Design Criteria for Crashworthiness and Energy Absorption

2.4.1. Classification of Crashworthiness Criteria

I. Injury-based metrics

From a biomechanics point of view, occupants' responses to a crash can be measured by such indices as head injury criteria (HIC), chest acceleration, chest deflection, and femur loads under the impact (Bois et al., 2004). The vehicle crash pulse (CP), the magnitude of intrusion (Intr) into the occupant compartment, restraint system, and vehicle interiors, affects these indices. Among them, CP and Intr are the direct consequences of structural crashworthiness. As a variant of intrusion velocity is also utilized as a design criterion. In general, a high acceleration implies a large impact force exerted on occupants and can result in a high risk of injury to occupants. For this reason, peak acceleration (amax) and peak crash force (Fmax) during impact are extensively employed as design criteria for optimization (Fang et al., 2017).

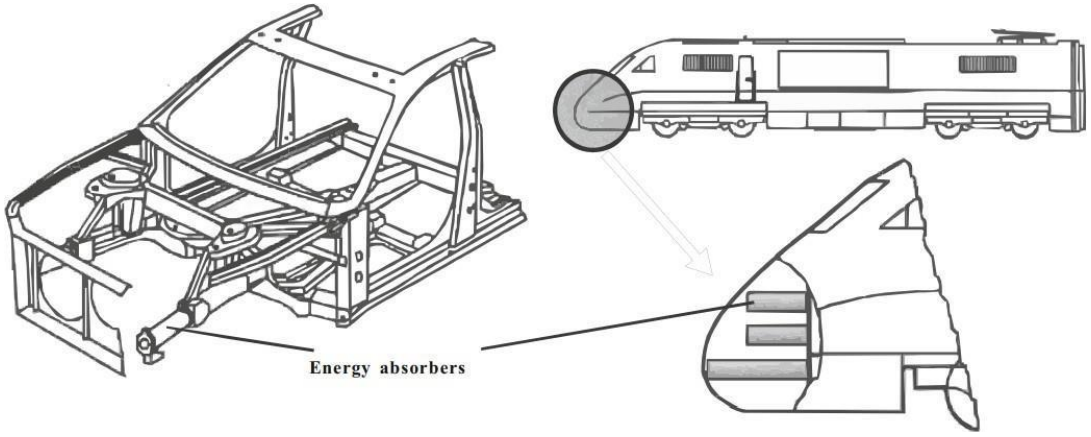

Figure 2.2. Energy absorbers in automobile/train structures (Marsolek and Reimerdes, 2004)

II. Energy-based metrics

The crashworthy structures are expected to absorb as much energy as possible to reduce the kinetic energy transmitting to the occupants. Hence, the amount of energy absorption (EA) has been drawn to exhaustive attention by researchers (Fang et al., 2017).

$$EA(d) = \int_0^d F(s)\mathrm{d}s$$

Where. ***F*** is the instantaneous impact force at the crash distance ***s*** and ***d***, the total crash displacement is concerned for measuring the energy absorption (Fang et al., 2017).

2.4.2 Remarks on Design Criteria

The selection of design criteria before optimization has been considered critically important to obtain the most beneficial optimal design (Fang et al., 2017). Taking the front side rails in frontal impact as an example, if they deform too much, the passenger compartment might be intruded severely by the engine booth. On the other hand, if the rails crash a short distance, only a little kinetic energy can be dissipated through progressive deformation and thus high deceleration could be yielded (Fang et al., 2017). They revealed that the injury-based design, which differs a lot from the energy-based design, could achieve a much safer structure (Fang et al., 2017).

2.5 Crashworthiness Goals

The ultimate goal of crashworthiness optimization is to ensure the passenger's safety.

- The body structures include progressive crush zones to absorb part of the crash K.E
- Vehicles maintain the integrity of the passenger compartment and simultaneously control the crash deceleration pulse.

Accident reconstruction and analysis of vehicle crashes provide information regarding safety performance. Currently, vehicle crashworthiness is evaluated in four distinct modes. frontal, side, rear and rollover crashes.

2.6 Crash Tests Regulatory Rules

The following are the requirements for the consumer crash tests conducted by (Babu, et al., 2012).

A. Federal Motor Vehicle Safety Standard (FMVSS)

B. Insurance Institute for Highway Safety (IIHS)

FMVSS Frontal impact requirements.

- 30 mph (48kph) into a fixed barrier
- Hybrid III in front driver and passenger seats
- Uses dummy injury measures for regulation
    - ✓ Chest G's <= 60
    - ✓ HIC <=1000
    - ✓ Femur loads <= 10KN
- Protection must be automatic
- Purpose of this test is to examine the performance of the occupant restraint systems (seatbelts, airbags, etc.)

IIHS Frontal impact requirements.

- 40% offset, 40 mph (64kph) into a deformable barrier
- Male Hybrid III dummy in front driver seat
- Good, Acceptable, Marginal and poor ratings to assess vehicle's overall crashworthiness
- Rating based on.
- Dummy injury measures
- Structural performance
- Restraint/dummy kinematics
- Evaluates the structural performance of the vehicle

FMVSS Side impact requirements.

- 33.5 mph (54kph) crabbed impact
- Impact or mass 1367.6 kg (3015lb)
- Uses SID dummy in front and rear seats
- Uses dummy injury measures for regulation

- TTI(d) <= 85g for 4 door passenger cars
- TTI(d) <= 90g for 2 door passenger cars

IIHS Side impact requirements.

- Impactor mass = 1500 Kg
- Impactor shape derived from Ford F150 front profile
- 30 mph perpendicular impact
- Driver and rear passenger dummies
- Purpose is to represent crash type that poses greatest risk to occupants (pickups/SUV as striking vehicle) promote head protection

Types of Crash Tests

All cars undergo front and side impact testing, which includes Babu, et al., 2012).

- 64kph (40mph) Front impact test. to assess car's performance in severe accident
- 50kph (30mph) Side impact test
- 29kph (18 mph) optional Pole impact test. to driver's head
- 40kph (25mph) child and adult pedestrian impact tests

2.7 Literature Summary

Passenger cars are a major mode of transport in the developed as well as in the developing countries. Therefore, the accidents caused due to passenger cars are also significantly on the rise. In all types of crash accidents, about 30 % of the total numbers of accidents are the frontal crash case. Therefore, measures to improve passenger vehicle passive safety performance in the crash to reduce injury and death of passengers during a crash to the maximum has become an important subject of research. Current car body structures and light trucks include two major categories. body-over-frame structure or unit-body structure. The body-over frame structure of a passenger car or a sport utility vehicle consists of the vehicle body, frame, and front sheet metal. Unit-body structure vehicles combine the body, frame, and front sheet metal into a single unit that is constructed from stamped sheet metal and is assembled by spot welding. Steel is the material typically used in manufacturing the structure of the vehicle. Only very few expensive cars vehicles' bodies are made from aluminum or composite materials (Joseph and Kamoji, 2015).

Joseph (2021) investigated the capability of the crashworthiness of a space frame-based vehicle, by the implementation of a modern composite reinforcement technique. The study involves using quasi-static axial compression testing, which is performed on standard Structural Square and round tubular sample elements of a space frame and specimens of the same dimensions, which have been reinforced by an exterior cladding of three and five layers of composite carbon fiber.

Upon analysis of data derived from mechanical testing, it was evident that the composite reinforcement technique played a very large role in increasing energy absorbency and specific energy absorbency of the specimen samples, the most notable being the longer sections that underwent global buckling in their plain, unreinforced state. The composite reinforcement enabled these longer sections to fail in a more desirable local buckling mode, increasing the SEA by up to 70.3%.

Joseph and Kamoji (2015) presented the Finite Element Analysis of the frontal rails of a passenger car. Front rails connect between the Front bumper and Dash Toe pan. They are one of the structural members which absorb high energies in a frontal impact so that impact energy won't transmit to driver or passengers. A rigid barrier is modeled to collide with the left frontal rail. The rail is assigned with steel material. After providing the necessary interactions and performing meshing, the whole model is run for dynamic explicit code using ABAQUS 6.11 PR3. The graph results for Artificial Strain Energy, Kinetic Energy, Internal Energy, and Total Energy are obtained and are compared with that of standard square tube. It was found that Internal Energy increased with time, Kinetic Energy decreased with time and the Total Energy of the system remained the same. Then the specific energy absorption (SEA) is calculated using the same analysis for steel and aluminum for two different velocities at 20 mph and 30 mph. As a part of the energy-absorbing criterion, the SEA of aluminum was better at both impact velocities.

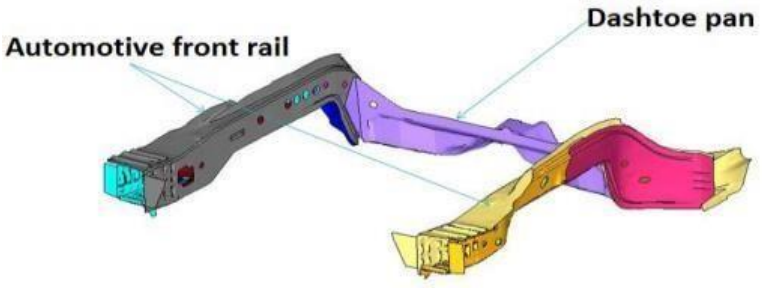

Figure 2.3. Frontal rails (Joseph and Kamoji, 2015)

The frontal rails are an integral part of the crumple zones, which form the front energy absorbing area. Front rails will connect between the Front bumper and Dash Toe pan. They are one of the structural members, which will absorb high energies in a frontal impact so that impact energy will not transmit to passengers or drivers. Figure 2.3 shows the frontal rails. The frontal rails are welded with stiffeners inside them. As the name suggests, stiffeners are required to increase the rigidity of the component just to the required level. Figure 2.4 shows the stiffeners used inside the frontal rails (Joseph and Kamoji, 2015).

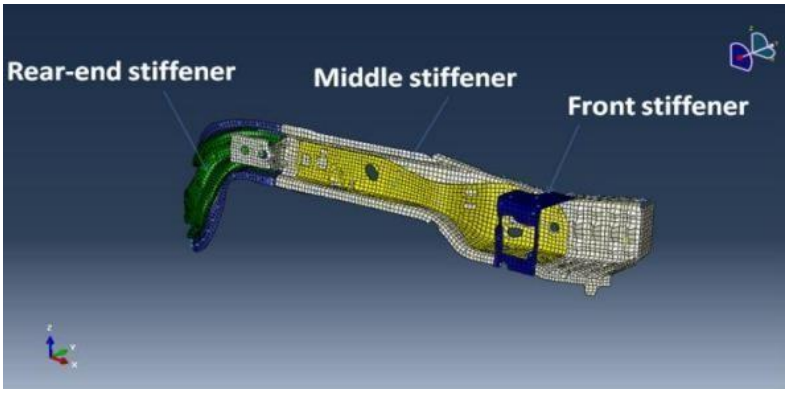

Figure 2.4. Stiffeners inside the frontal rails (Joseph and Kamoji, 2015)

2.8 Research Gap

As it is obtained from the literature review most of the time most researchers focus on improving the efficiency of the vehicle by reducing the weight of the chassis but it is necessary to balance crashworthiness and weight reduction of the chassis. In addition, since there is no crumple zone in a body on frame vehicle as that of a unibody frame, more impact energy is passed into the cabin and to the other part of the vehicle because the rails do not deform under impact. Therefore, it is necessary to optimize the body on frame chassis to solve the problem and improve the poor crashworthiness performance of the chassis.

CHAPTER THREE

MATERIALS AND METHODS

3.1 Introduction

In this chapter, the material used for this thesis listed and followed by methodology. To assess the crashworthiness of any given structure it's necessary to compare the results with well-established and acceptance criteria. The numerical result of the structure under impact should be correlated with those criteria. The required quantities should be selected based on the requirement of the study at hand and by taking previously proven results regarding the structural crash tests. Different parameters have been proven to be effective in studying structural crashes by different researchers. Some and most common parameters are implemented in the present work. The parameters to be used are Energy Absorption, Specific Energy Absorption, Peak crash force, average crash Force, crash force efficiency, crash pulse, and HIC Livermore Software Technology Corporation, 2003). This chapter gives the details about the materials used and methodology followed during this thesis work.

3.1.1 Developments of FE Models for Pickup Truck Structure

The FE Model development consists of dynamic strength analysis for frontal and side crash analyses of the chassis structure. In dynamic analysis, LS DYNA software is preferable for explicit time integration analysis than ANSYS to obtain better analysis result for a specified time. LS-DYNA is the best and most efficient for the explicit dynamic analysis because of uses a return mapping algorithm and the central difference method to avoid expensive numerical iteration and matrix inversion. This study presents the analysis of the dynamic structure strength during two loading conditions using LS DYNA R 11 by using NHTSA standard. If the initial movement direction of MPDB is positive, the initial movement direction of vehicle is negative.

3.2 Materials

The general vehicle specification and the measured values of the chassis is stated below. The Materials required for execution of this thesis work are given in Table 3.1 and 3.2. The dimensional vehicle data is given in Table 3.1 and 3.2. (Bishoftu automotive industry engineering)

Table 3.1. Specification of Bishoftu pickup vehicle

Overview	
Model	DD1022TA
Bulletin	#240
Type of vehicle	Cargo truck
Chassis	DD1022TA
Technical Specification	
Engine model	4JB1TI
Engine power	102h***p***
Performance Maximum speed capacity	120 km/hr
Rated load capacity Dimension	430 kg
Overall length	5350mm
Over all width	1725mm
Over all height	1690mm
Cargo body length	1715 mm
Cargo body width	475
Cargo body height	1455mm
Ground clearance	200mm
Undercarriage and suspension	
Wheel base	3380mm
Front track	1479mm
Rear track	1487mm
Front overhanging	785mm
Rear overhanging	1185mm

Table 3.2. Specification of chassis measured from Bishoftu Automotive industry

Measured value	
Overall length	3730 mm
Front width	1060 mm
Rear width	750 mm
Average thickness	5 mm

3.2.1 Tools

Various software's are used as a tool for designing; modeling and analysis are also given here.

- **SOLIDWORKS**

Solid Works is a modern computer aided design (CAD) program. It enables designers to create a mathematically correct solid model of an object that can be stored in a database. When the mathematical model of a part or assembly is associated with the properties of the materials used, we get a solid model that can be used to simulate and predict the behavior of the part or model with finite element and other simulation software.

- **LS DYNA**

LS-DYNA is an advanced general-purpose multi-physics simulation software package developed by the former Livermore Software Technology Corporation (LSTC), which was acquired by ANSYS in 2019. LS-DYNA is a general purpose transient dynamic finite element program capable of simulating complex real-world problems. It is optimized for shared and distributed memory UNIX, Linux, and Windows based, platforms. It is an explicit 3-D finite element program for analyzing the large deformation dynamic response of the elastic and inelastic solids and structures. The program is extensively used by many top automobile, aerospace and research organizations. A wide range of material types and interfaces enable the efficient mathematical modeling of many engineering problems (Livermore Software Technology Corporation, 2003). It contains more than one hundred and fifty material models including metallic, non-metallic and composite models which enable to define any material in the real world.

The contact capabilities such as contact between deformable bodies, between deformable and rigid bodies provided in LSDYNA can solve any contact problems which very useful in crash testing. The code's origins lie in highly nonlinear, transient dynamic finite element analysis using explicit time integration. "Nonlinear" means at least one (and sometimes all) of the following complications. Changing boundary conditions (such as contact between parts that changes over time). Large deformations (for example the crumpling of sheet metal parts). Nonlinear materials that do not exhibit ideally elastic behavior (for example thermoplastic polymers)."Transient dynamic" means analyzing high speed, short duration events where inertial forces are important. Typical uses include. Automotive crash (deformation of chassis, airbag inflation, seatbelt tensioning) Explosions (underwater Naval mine, shaped charges), manufacturing (sheet metal stamping) (Livermore Software Technology Corporation, 2003).

3.3 Methods

In order to address the general and specific objectives of this thesis work a well-designed methodology is followed. Various steps included in the methodologies are listed below and summarized in Figure 3.1. Among the procedures the modeling and analysis stage have a more detail explanation and it is stated in detail on chapter four.

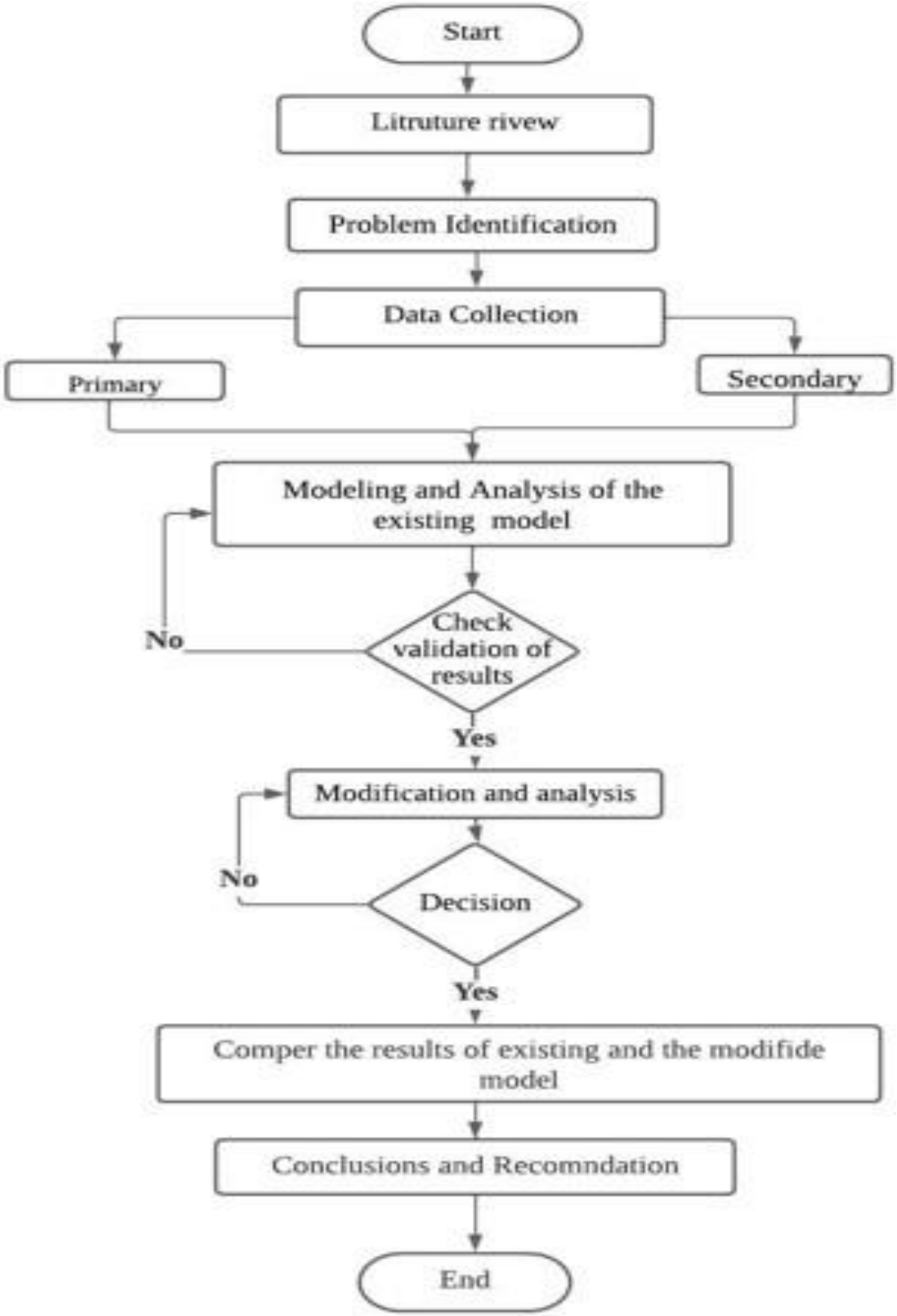

Figure 3.1. Block diagram of the methodology

Literature review and problem identification

Literature survey about chassis structural response during impact load are the key methodology of this thesis work that will help to about what others done and identified, where the limitations does exist so that this work will be based on the research gap. Latest reviews and research work in area related to development, modification, design and analysis of BPV is collected and surveyed.

Data collection

To get the details of technical specifications and necessary data of the existing Bishoftu Pickup Vehicle was collected from Bishoftu automotive engineering Industry (Bishoftu) used by primary data, and the secondary sources of data were from reference books, journals, and internet.

Concept Generation

The concept generation process results a set of productive concepts from which we make the final specification and design. A different concept towards the crashworthiness improvement of chassis structure is generated. This includes structure modification methods. The 3D modelling of chassis part is done by SOLIDWORKS 18 and after finishing the 3D modeling of the chassis then analysis of crashworthiness will be carried out by LS DYNA R11 software. After carefully observing the crashworthiness behavior of the existing chassis model, modifications and designs were made on critical parts of the vehicle. Then the modification was analyzed with the same condition as the existing. After that the numerical comparison between the existing model and modified model is done using different crashworthiness parameters such as energy absorbing ability, impact force, and deformation and so on.

Discussion

At this stage, the response of modifications is examined using engineering analysis and discussions. If the result were satisfactory the next stages of the research take place but if not, the modification is to be re-designed and repeat the steps.

Verification

Without experimental data, the appropriateness of the values obtained on a computational model accurately represented by verification process. In case LS DYNA simulation, verification can be made by checking the quantity of energy balance, deformations, kinematics,

kinetics and other quantities (Gulavani et al., 2014), the most common and logical ways are listed below.

- Energy balance
- Energy Ratio
- Ratio of Hourglass energy (HE) to Total energy (TE)

Energy Balance Curve

The energy balance of a system in an impact is governed by the law of conservation of energy. According to the law of conservation of energy, Energy can neither be created nor be destroyed, but it can be converted from one form of energy to another form. Applying the same principle to crash analysis, the amount of kinetic energy lost during impact must be converted to other forms of energy such as internal energy, sliding energy, hourglass energy and other forms of energy like heat energy.

Kinetic energy is the work input and internal energy is the work output. Internal energy is the energy absorbed by the system and is directly proportional to the product of force and deformation. It is also noted that, there may be negligible errors in calculating energy ratio because all the processes in this universe are irreversible and some losses are always included which deviates energy ratio slightly from one.

- The total applied energy should be constant throughout the simulation.
- The kinetic energy should be decreasing and internal energy should be increasing; and ideally the sum of kinetic energy and internal energy should be equal to total energy.
- The Hourglass energy should be less than 5% of total energy.

Energy ratio

The energy balance for an explicit time integration scheme is given by.

$$E_i + E_s + E_d + E_{ke} + E_h = W_{ext} + E_{i0} + E_{ke} \quad (3.1)$$

Where. $\boldsymbol{E_i}$. internal energy, $\boldsymbol{E_h}$. hourglass energies, $\boldsymbol{E_d}$. damping energy, $\boldsymbol{W_{ext}}$. work done by the external forces, $\boldsymbol{E_{ke}}$. kinetic energy, $\boldsymbol{E_S}$. interface sliding (dissipated contact energy) and the superscript $\boldsymbol{0}$ denotes the initial values.

The total sum of energies in the left-hand side of the equation represents the total energy of the system, and terms on the right-hand side of the equation represent the initial total energy plus the work done by the external forces (Wext). The ratio of the 'total energy' to the sum of 'initial total energy' and 'external work done 'is called the energy ratio. The energy ratio is also known as the 'energy balance'

$$e = \frac{Ei+Es+Ed+Eke+Eh}{Wext+Ei+Eke}$$

An energy ratio with value of equal to 1 shows more stable and reliable FEA result, but most of it is difficult to achieve such value. This is due to the modelling error which may increases or decreases the total energy (Livermore Software Technology Corporation, 2003). There are two causes which can be considered when checking the energy ratio.

- ✓ If e > 1, which mean that artificially energy is added in the model and rises the total energy values, as a results instability occur, most of the time the rises of total energy is due to a numerical instability or through initial penetration.
- ✓ If e < 1, which indicates that the total energy reduces because of artificially absorbed energy, either by excessive hour-glassing or during stabilization of an ill-conditioned contact surface.

Generally, energy ratio simply is different from unity, and then there are high probability. Since it is difficult to obtain energy ratio equal to unity so, the acceptable value of the ratio is 1.00 +/- 0.07 the discrepancies in the ratio are due to spurious energy produced in the system and simulation error.

CHAPTER FOUR

STRUCTURAL DESIGN AND IMPROVEMENT OF PICK-UP CHASSIS FRAME MODELLING OF EXISTING CHASSIS FRAME

4.1 Introduction

In this chapter, SOLIDWORKS 18 was used for geometry modeling, and LS DYNA R11was used to the Analysis of crashworthiness.

4.1.1 Geometry description

The ladder frame of the Bishoftu pick up chassis model is shown in Figure 4.1. The principal energy-absorbing component of body-on-frame cars is the ladder frame. The ladder frame is made of steel and weighs 198 kg, or around 8 % of the entire weight of the vehicle. Steel has always been used for ladder frames due to its superior energy absorption capabilities and relatively straightforward manufacturing process. Side rails, cross beams, and supports are the three constituent parts of the ladder frame.

The geometry of the designed ladder frame of the Bishoftu pick up chassis was created in SOLIDWORKS 18. The model has been done by using the overall dimensions of the ladder frame. Sketch tracer Generation is the initial stage of modeling in which the basic profile or part of the ladder frame is formed by tracing from the image. Figure 4.1 shows chassis geometry.

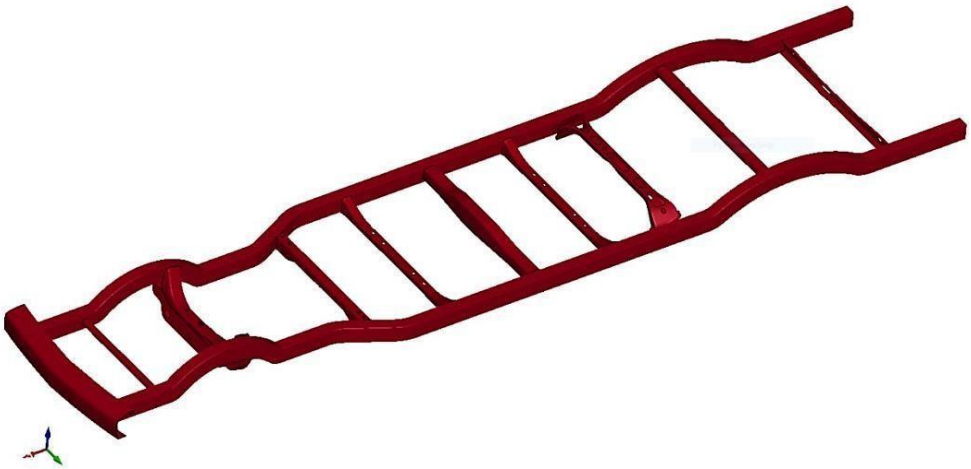

Figure 4.1. A ladder frame of the Bishoftu pick up chassis model (solid works)

After that, the surface was generated by using Surface Generation, and the corresponding extruding thickness was given for each part. Finally, the parts are assembled for checking for dimension error. The parts were named separately in SOLIDWORKS 18. Figure 4.2 shows the geometry of cross members, front-end member, rear-end member and longitudinal member.

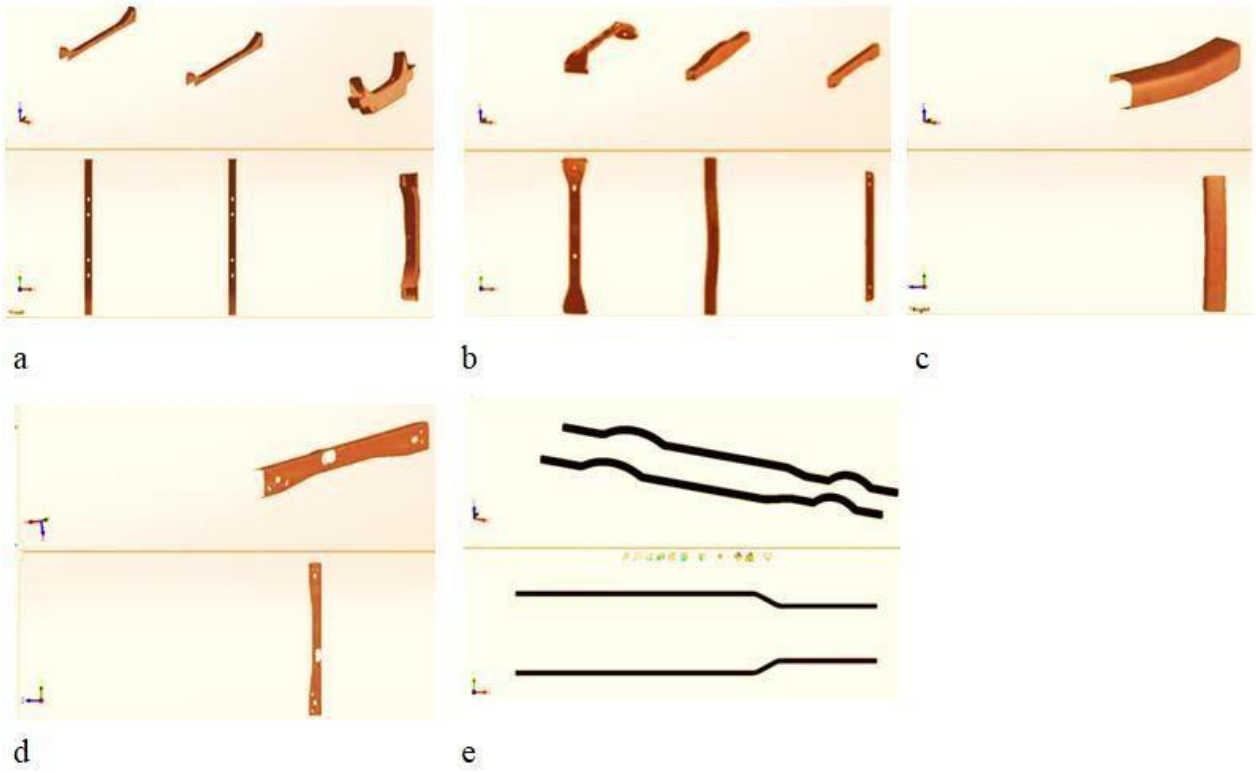

Figure 4.2. (a, b) cross members (c) front-end member (d) rear-ends member (e) longitudinal member (solid works)

4.1.2 Mesh generation for the Chassis Frame

Mesh generation includes mesh type, size and geometrical attributes. There are three different mesh types, 1D, 2D and 3D, relevant to element dimension. Mostly, chassis components were a shell element, which means that the length and width of the structure is considerably larger than its thickness. Therefore, auto mesh type was used. The pickup chassis geometry was meshed by LS DYNA software using mixing of linear quadrilateral 98.6 % and triangular elements 1.4 %. The element size for the whole model between 5 mm and 10 mm. The total number of elements for the whole meshed model was 67,847 and node 69,068. So, the whole meshed model is very complex. A fine mesh was used o as shown in Figure 4.3.

Figure 4.3. Fine mesh generated on the ladder frame (LS DYNA)

4.2 Simulation Settings

4.2.1 Material Model

Vehicle material types and properties are the most important factors, which effect significantly the accuracy of the impact simulation. Moreover, material types and properties should fulfil the automotive criteria, such as safety, environment, lightweight, fuel consumption, cost and design. Mostly, the vehicle model consists of shells, which need to identify thicknesses for every single shell besides mechanical material properties as shown in the figure 10. The keyword used for the chassis was modeled by MAT_PIECEWISE_LINEAR_PLASTICITY and Most of the chassis components thicknesses were defined by section shell with 5 mm thickness.

Table 4.1. Material mechanical properties for chassis (Gashu & Nallamothu, 2022)

Name	High- carbon steel
Phase at STP	Solid
Density	7850 kg/m^3
Ultimate Tensile Strength	685 MPa
Yield Strength	525 MPa
Young's Modulus of Elasticity	200 GPa
Brinell Hardness	200 BHN
Melting Point	1515 °C
Thermal Conductivity	50 W/mK
Heat Capacity	490J/g K

4.2.2 Constraints

After meshing the individual parts, interactions have been defined between them. These interactions are defined between the surfaces of different parts and control the transmission of forces and moments between individual members. The constraint throughout the chassis parts was given by the keyword CONSTRAINED_NODAL_RIGID_BODY in Entity creation.

4.2.3 Contact Definition

The contact between two parts is given to prevent penetration during the crash. There are a lot of contact types are available in the keyword manager. In this case, the contact is directly in within the components of the chassis parts and between the road and the tires of the impactor and between the impacting surfaces (chassis and moving barrier). In order to define the interaction between different parts of the chassis, a set of parts (PART_SET) is defined then, the keyword CONTACT_AUTOMATIC_SINGLE_SURFACE used, and for defining two different objects like the moving barrier and the ground and also the chassis and the impacting surface, then the keyword CONTACT_AUTOMATIC_SURFACE_TO_SURFACE is used. The master and slave parts are listed in Table 4.2.

Table 4.2. Master and slave parts

Contact type	Slave	Master
Automatic surface to surface	Impactor Tire	Ground
Automatic surface to surface	Chassis	moving barrier
Automatic single surface	Whole chassis	Non

4.2.4 Simulation Environment

The numerical calculation of the full-scale vehicle crash simulation has taken about 4 days on a 4-CPU, 350MHz N4000 processor. Considering the long computing time, applying the numerical optimization approach on the whole vehicle improvement is not cost-effective. Thus, to tackle this problem, the vehicle frame and frontal parts have been separated to build a sub-model for crashworthiness optimization. The detailed approach is demonstrated below. The original sub-model is composed of 15 parts and the total mass is 198 kg, consisting of 67,847 elements and 69,068 nodes. The modeling parameters for sub model are in complete agreement with those for full-scale model. Figure 4 shows the built FE sub-model.

The function of the boundary conditions is to create and define constraints and loads on finite element models. To simulate a full chassis crash, all loads and boundary conditions that occur in the actual crash event need to be modeled. Just as a chassis is subjected to gravitational loads in real life, the simulated model should have a representative gravity force applied. Friction forces between the tires and the road surface play an important role in how the chassis behaves on impact, so these have to be accounted for in the simulation.

Case 1. Frontal Impact

In front impact test, the rigid barrier is crashing with a chassis which is stationary on opposite side with the rigid barrier that has a speed of 35 mph (56 km/h) and the main purpose is to clarify the damages to chassis front. Figure 4.4 shows front impacts SET UP is in different views.

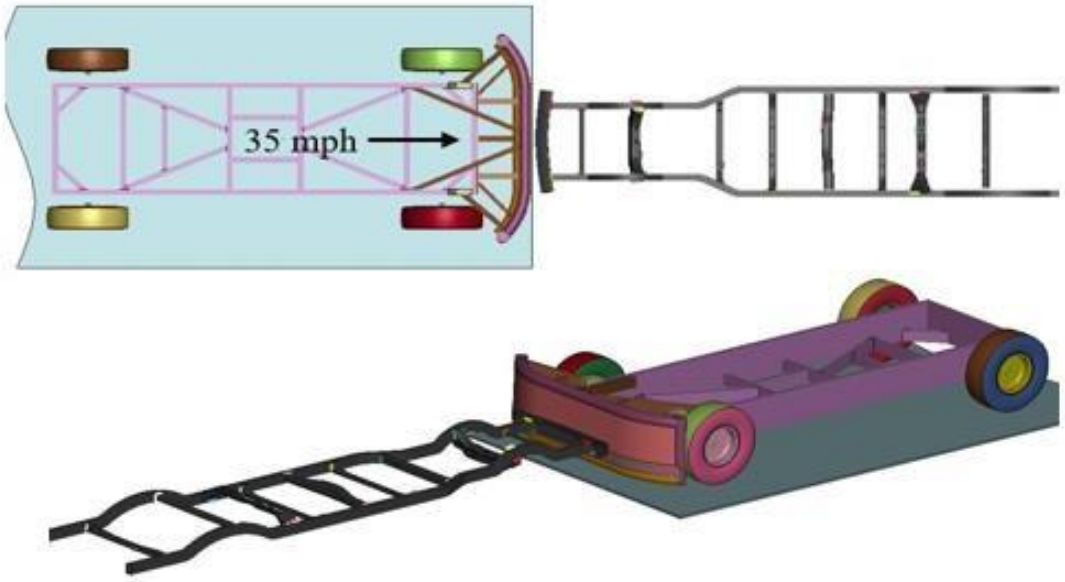

Figure 4.4. Front impacts SET UP is in different view (LS DYNA)

Case 2. Side pole impact

In side impact test, the rigid barrier is crashing with a chassis which is stationary on perpendicular with the rigid barrier that has a speed of 35 mph (56 km/h) and the main purpose is to clarify the damages to chassis side areas. Figure 4.5 shows side impacts SET UP is in different views which we will analyze in the following section.

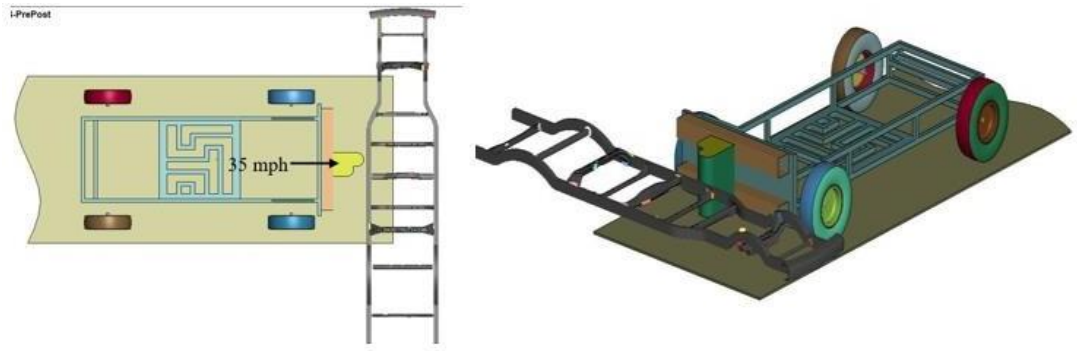

Figure 4.5. Side impacts SET UP is in different views (LS DYNA)

4.2.5 Control Simulation

Solution control has a significant influence on simulation stability and accuracy. CONTROL_TERMINATION was used to define the simulation termination time. It is used to control the time step and run time of the file. These cards are necessary to control the duration of simulation time. Run time of the key file is 100 ms (0.1 s) for frontal and 200 ms (0.2 s) for side crash the time variation is depend on the value of internal energy to become constant or maximum energy absorption. The results are plotted for the energies absorbed by the parts within 100 and 200 ms interval. DT min is the interval in which the codes are generated in processing the file in ls-dyna. It is the minimum time taken by the sound wave for travelling from one end to other of the shortest element. It is also used in plotting the graph i.e., for every 0.001s interval a point on the graph is plotted. Decreasing the value below 0.004s increases the smoothness of the curve but at the same time increases run time.

4.2.6 Database Options

Database options are given to obtain the output i.e., to generate results and to interpret plots. Database was used to define the expected results using American Standard Code for Information Interchange (ASCII) to define specific functions such as NODOUT, JNFORC, JSTIFR and DEFORC (Kunle et al., 2019). Generally, they are used to analyze the energy absorption characteristics that are discussed in next chapter on result and discussions. Some of the database plots used are.

- D3PLOT (database for complete output states and some default results)
- D3DUMP (complete database for restart when interruption occurs on running due to power or other)
- ASCII options (absorption energies (GLSTAT), material energies (MATSUM), wall force (RWFORC), Resultant contact forces (RCFORC) and so on.

4.3 Finite Element Models for Collision Dynamics Analysis

The finite element method analysis of the chassis part model makes the initial indication of the assembly deformation by force-crush behavior. Figure 4.6 shows, a methodology for enabling efficient and effective procedures for chassis structural dynamic behavior analysis under impact and improving its crash worthiness has been proposed as follows.

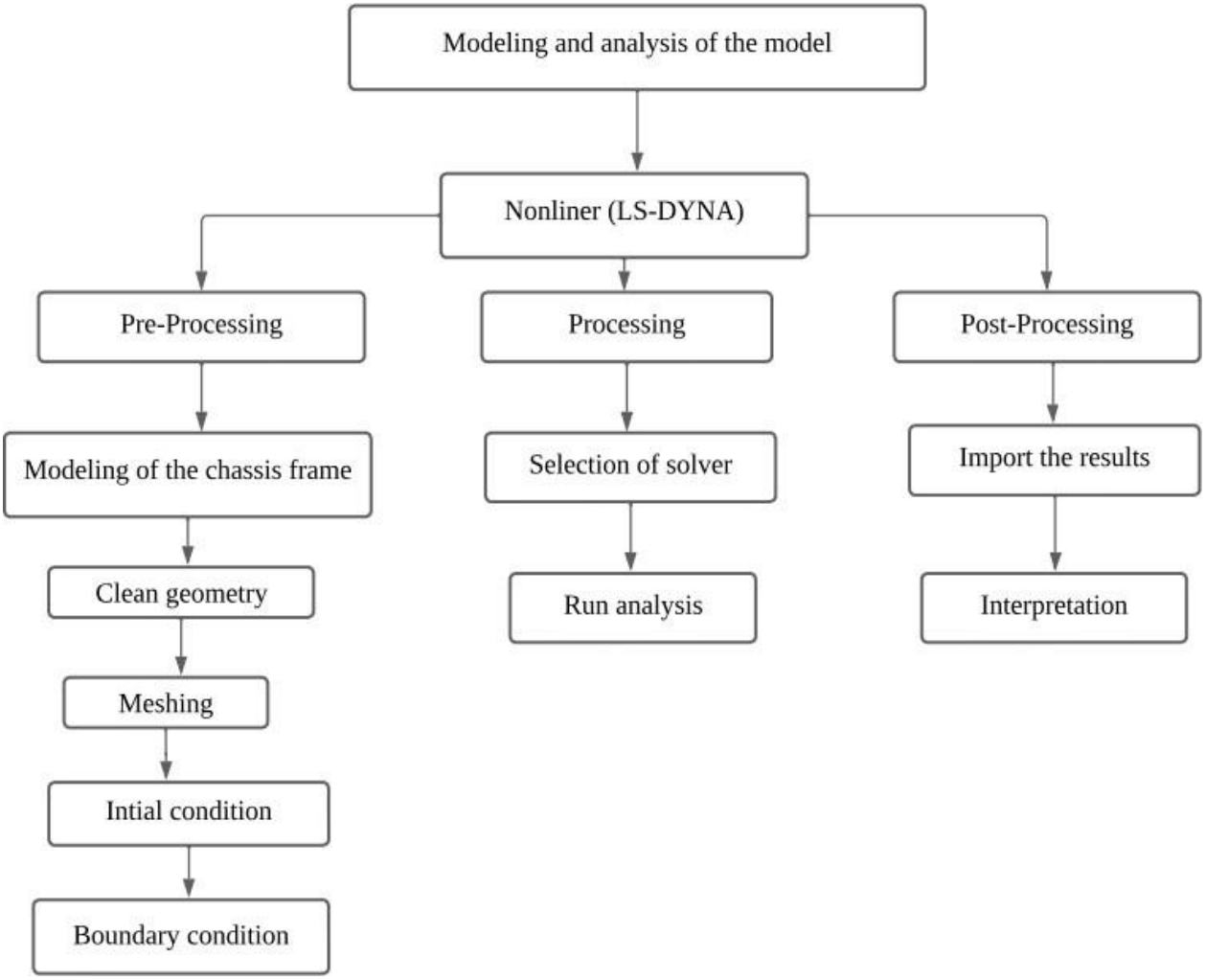

Figure 4.6. Procedures for chassis structural dynamic

4.4 Chassis Reinforcement

Chassis reinforcement is a method of increasing the stiffness of the chassis frame by shifting the natural frequency to considerable extent. This is done by placing additional stiffening members to the side rails of the chassis frame. The geometrical stiffness can be increased to different levels with respect to the position and length of the reinforcement plates added to the frame (Venkatesh, K., Kannan, M., & Kuberan, 2014).

Figure 4.7 shows the frontal and side Chassis reinforcement

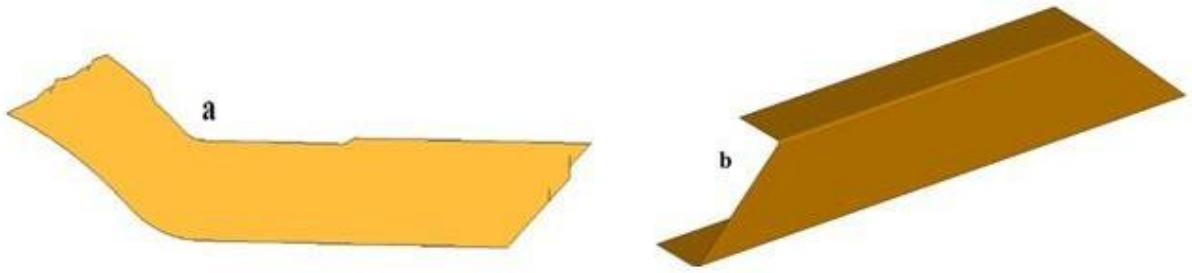

Figure 4.7. (a) Frontal (b) Side Chassis reinforcement (Venkatesh, K., Kannan, M., & Kuberan, 2014)

4.4.4 Requirement during Reinforcement

The following requirements apply to frame rail reinforcements.

- Reinforcements should not be terminated within a distance 2H from the Centre of a spring hanger (H = the frame rail depth) unless contrary practice is adopted by the vehicle manufacturer. Typical details for terminating reinforcement are shown in Figure 4.8.

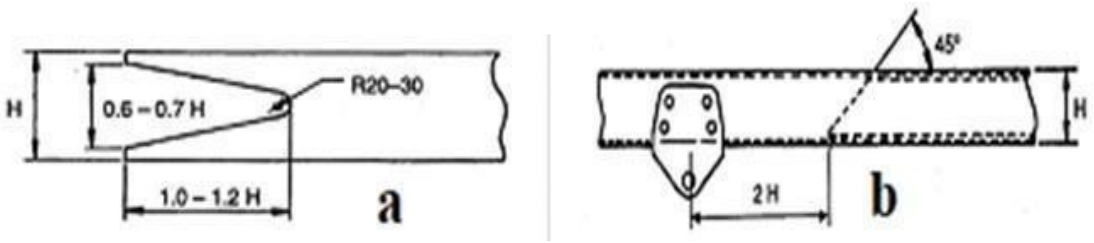

Figure 4.8. Monthly Figure. (a) Frog mouth reinforcement (b) Tapered reinforcement (S. Grzegorz, N. Paulina et al., 2014)

It is preferable that additional reinforcement should extend at least a distance of 2H forward of the rearmost front spring hanger bracket and rearward past the rearmost rear spring hanger bracket by a distance of 2H. Note. Allowance must be considered for associated components that would be displaced by the reinforcement section. Each end of reinforcement should be tapered at 45 degrees, or alternatively, a 'frog-mouth' tapering may be used. Typical frog-mouth details are shown in figure. The thickness of each reinforcement must not exceed the thickness of the main frame rail. The reinforcement section should be either angle or channel. Reinforcements may be located inside or outside the main chassis frame rail (S. Grzegorz, N. Paulina et al., 2014). All reinforcements must be securely attached to the main frame rail.

It is recommended that reinforcements be fastened by bolting. Existing bolt holes should be used where possible. Inside radius Ro of outer reinforcement curvature must be smaller than outside radius of chassis frame curvature (Outside radius of inner reinforcement curvature must

be larger than inside radius Ri of chassis frame curvature). Multi-Section Reinforcement. When a chassis is to be upgraded over its entire length, it is often difficult to fit a full-length reinforcement section due to the installation of other chassis components. A satisfactory method of overcoming these difficulties is by the use of multiple sections of reinforcement. When this method of chassis reinforcement is utilized, such reinforcements must be securely attached to each other by either overlapping or by bolting or by butt welding (S. Grzegorz, N. Paulina et al. 2014). From the literature review dimension of reinforcement should explained be as follow.

Length (mm)	Thickness(mm)	Angle tapered (degree)	Height (mm)
550	2	45	98

4.4.5 Reinforcement Material

On different surveys, it was observed that the performance of the bumper and beam at event collision is greatly depending on the material used. If it is properly selected, it produces a great impact on the vehicle performance by minimizing the weight (high fuel efficiency) without sacrificing the strength (Tie Wang & Li, 2015). So, for the chassis reinforcement closed cell Aluminum foam material are taken into consideration to achieve the required performance. The advantages of Aluminum foam for automobiles are;

- ✓ High strength and stiffness to weight ratio
- ✓ Corrosion resistance
- ✓ Withstand great damage
- ✓ Light weight
- ✓ Can be made into complex geometrical forms easily
- ✓ Extremely strong and can absorb great deal of mechanical energy

Closed-cell aluminum foam is widely used as a lightweight construction material, both in its original format, and as sandwich panels, which are valued for their low density and very high stiffness.

The main applications for this variety of foams are in the automotive industry as impact, acoustic and vibration absorbers, the aerospace industry (Aluminium Foam Properties and Applications Materials Hub, 2022). The mechanical properties directly used as the parameters in LS DYNA material options, and they are summarized in Table 4.3 below.

Table 4.3. The Material properties of aluminum foam for LS-DYNA material

Properties	Units	Value
Foam density, ρ	kg/mm^3	2.67e-6
Young's modulus, E	GPa	72
Poisson's ratio, PR	-	0.25
Yield strength (stress), YS	GPa	0.18
Ultimate tensile strength, UTS	GPa	0.32
Compressive modulus	GPa	0.5

4.4.6 Material and Section Definition

The geometric modeling of the chassis reinforcement is done by using SOLIDWORKS 18 modelling tools and mesh, boundary conditions, material properties and section properties are defined using on the Ls-pre post. Both the front and side reinforcements are uniformly meshed with 4- and 3-mm element size respectively. They are meshed with shell elements. The ends of them are constrained in all the directions. The material model or keyword used to define the material is* MAT_PIECEWISE_LINEAR_PLASTICITY*.

Since the thickness of the reinforcement which is considered is very small comparing to its all length, a shell section is used to model them. The shell elements are formulated by ELFORM=2 (Belytschko-Tsay elements). Mixed (Rectangular and triangular) cross section is used as cross section of the reinforcement. It also provides good fitting space with the existing chassis frame structure when making modification.

4.4.7 Boundary Conditions

The different boundary settings for testing after each reinforcement has been made are represented by LS-DYNA's options as follows. INITIAL_VELOCITY_GENERATION was used to define the velocity of the moving components. CONTACT_AUTOMATIC_ SURFACE_SURFACE_ID between the reinforced chassis assembly and the moving barrier. CONTROL_TERMINATION for the simulation time is set as 0.03 s for the frontal and 0.06 s for side collision case. For the output values in DATABASE_EXTENT_BINARY; D3PLOT, D3DUMP, ASCII options are selected. Figure 4.9 shows a side collision set up and front collision set up.

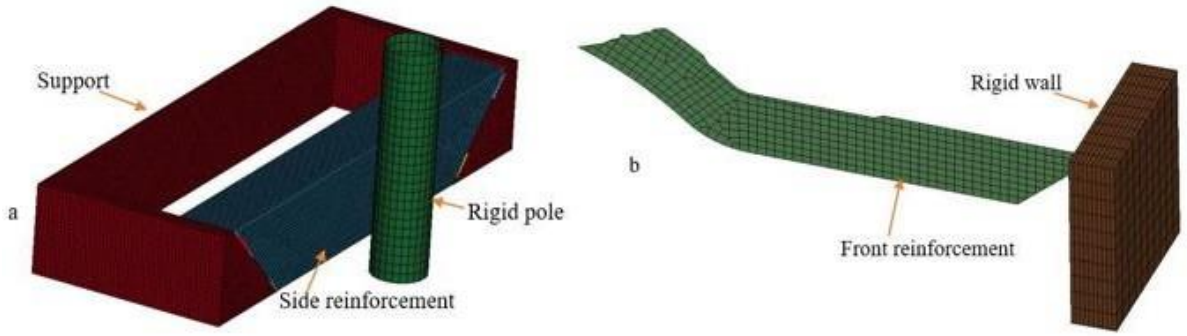

Figure 4.9. (a) Side collision set up (b) Front collision set up (LS DYNA)

4.4.8 Critical area needs reinforcement during front and side collision

During a full-frontal crash scenario in which a NHTSA barrier traveling at 35 mph collides with a stationary chassis more damaged area are shown in figure 4.10a below. From the figure below 4.10b it is necessary to reinforce the area of more damaged part of chassis as shown.

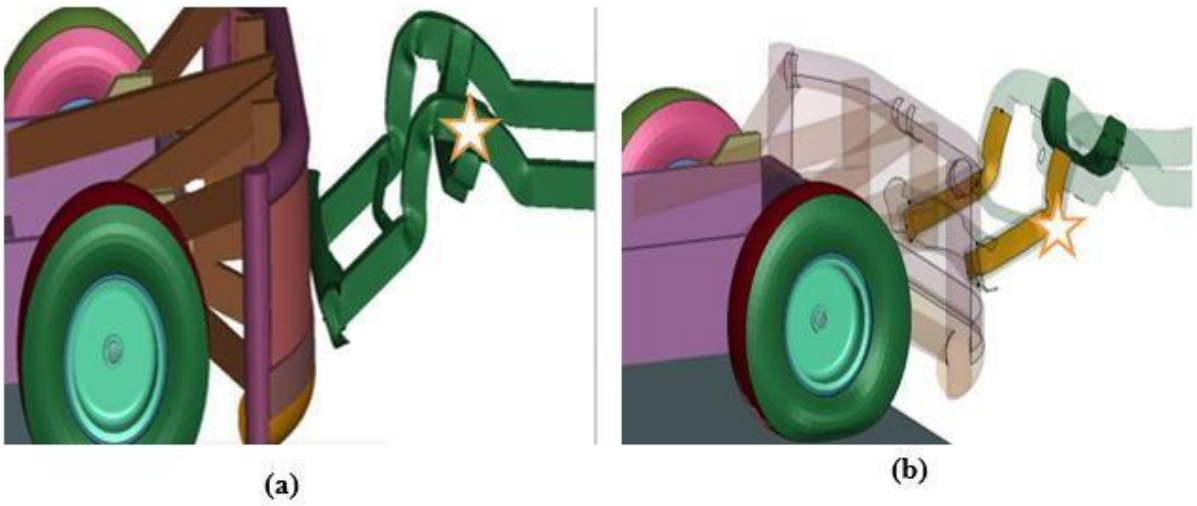

Figure 4.10. (a) Damaged part of chassis during front collision (b) reinforced part of chassis for front collision (LS DYNA)

During a side crash scenario in which a NHTSA barrier traveling at 35 mph collides with a stationary chassis more damaged area are shown in figure 4.11a below. From the figure below 4.11b it is necessary to reinforce the area of more damaged part of chassis as shown

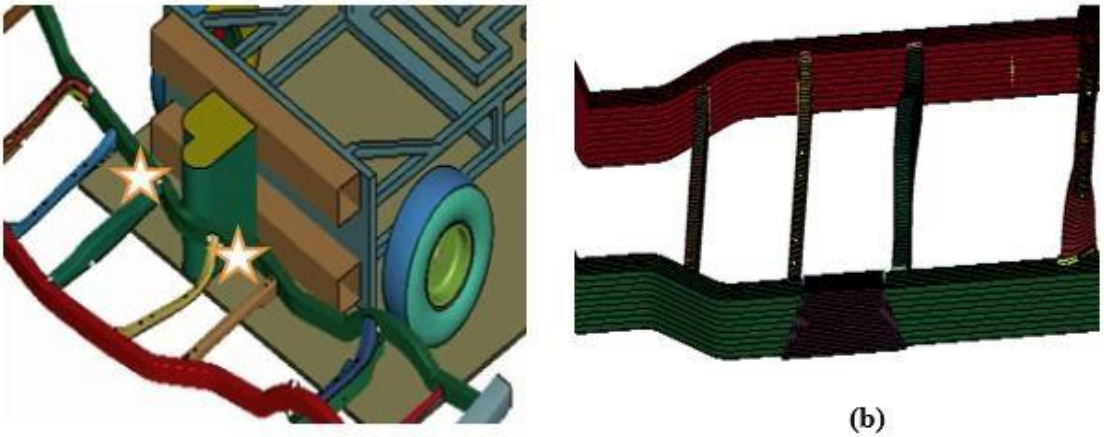

Figure 4.11. (a) Damaged part of chassis during side collision (b) reinforced part of chassis for side collision (LS DYNA)

CHAPTER FIVE
RESULTS AND DISCUSSIONS

5.1 Introduction

This chapter provided illustrations of the frontal and side impact crashworthiness study of the BISHOFTU pick up chassis. The outcomes include time history charts of several parameters, such as crash force, deformation, energy, and energy balance, energy ratio and ratio of hourglass energy (HE) to total energy (TE). For all possible impact situations, pre-processing, process and post-processing was carried out using LS DYNA. All post-processing outputs are provided at a certain moment throughout the event. The total simulation duration was divided into 50-time increments. Utilizing the shading and wireframe options, animation, contour plots, and vector plots, the findings are exhibited. Four types of crash scenarios were performed on the structure of the Pickup truck.

- Full frontal impact by using a rigid impactor
- Offset frontal impact with rigid wall
- Side perpendicular impact by impacting trolley
- Side at an angle impact by impacting trolley

5.2 Result and Discussion on Existing Model

5.2.1 Full Front Collision

The outcome of a full-frontal crash scenario in which a NHTSA barrier traveling at 35 mph collides with a stationary chassis is described. Figure 5.1 depicts the occurrence and reaction of the entire vehicle chassis throughout the course of 100 milliseconds. As seen in the image at t= 5 ms. the front part of the chassis comes into contact with the opposing stiff barrier.

At the end, the car's chassis flex and reaches its maximum absorption. As a result, the frontal portions of the chassis deform, and substantial backward movement at the chassis structure takes place.

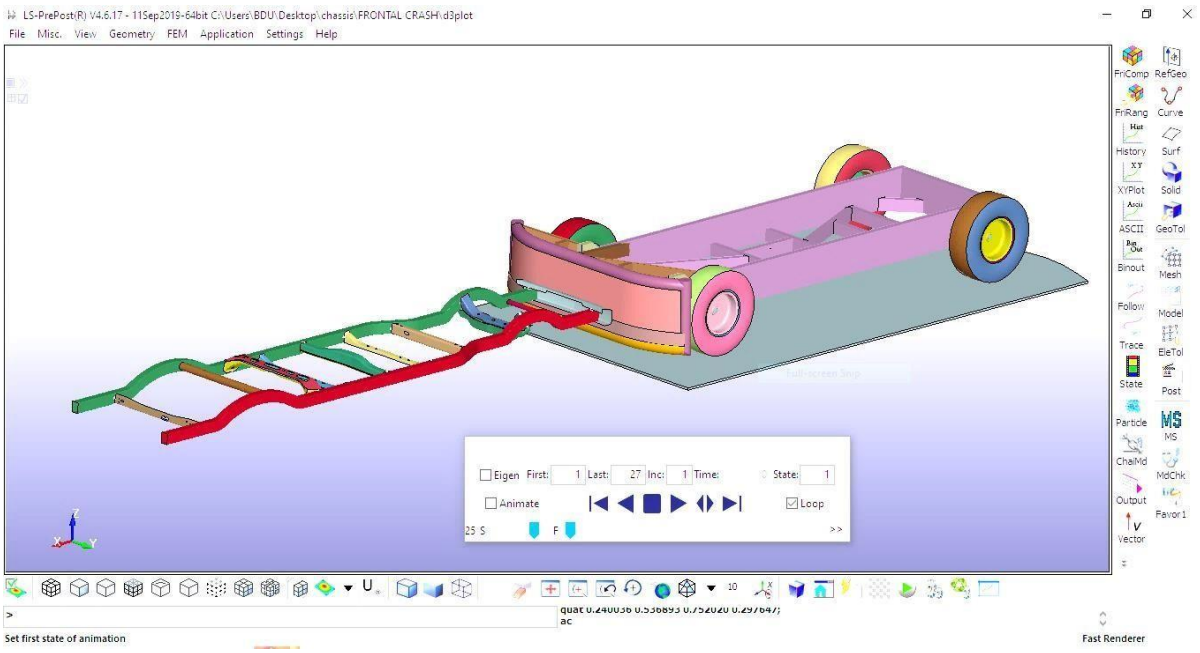

Figure 5.1. Full frontal crash (LS DYNA)

Total Deformation

As it is shown in Figure 5.2, the graph shows the behavior exhibits the similar pattern, where the deformation rises as the speed rises. Initially, up to t=0.015, there is considerable deformation until the collision comes into contact with highly stiff material, at which point the collision starts to slow down the rate of deformation, leading to plastic deformation of the structures.

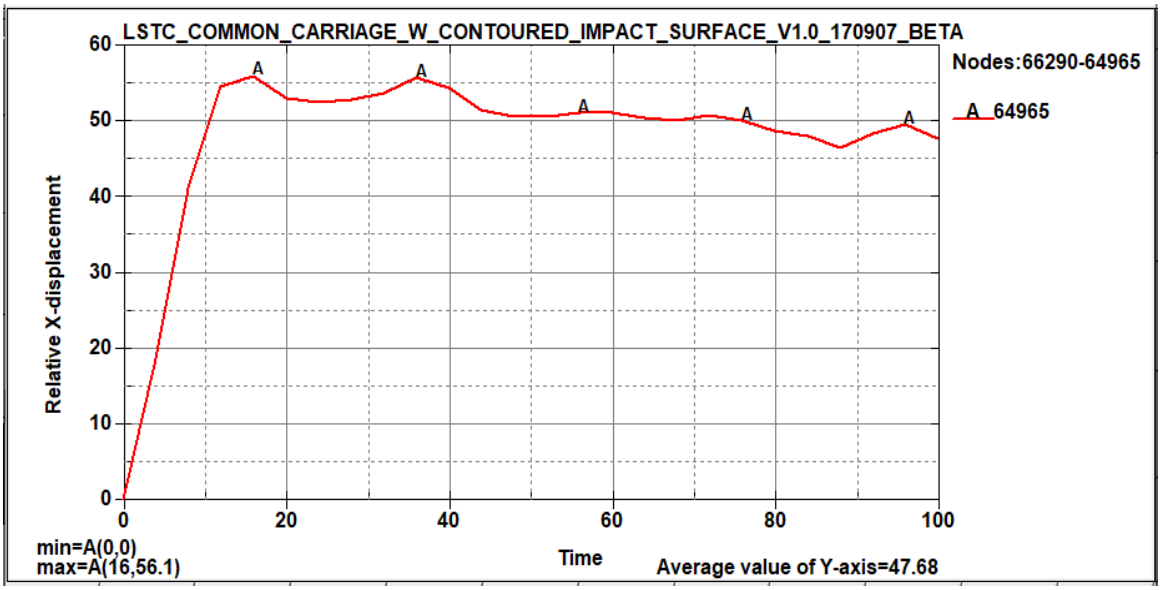

Figure 5.2. Total deformation full frontal crash (LS DYNA)

Total Energy-balance

Throughout the whole simulation, the system's total energy remains constant at 168 kN-mm, which is the same as its initial kinetic energy. As the collision process begins, the kinetic energy of the entire system starts to decline and is turned into internal energy, sliding energy and so on; which begins to increase from zero energy. The structure's deformation provides the majority of the internal energy. After 60 milliseconds, there is not much deformation seen, and as a result, the energy graphs of the K.E. and I.E become approximately flat.

The end kinetic energy is 65.9 kN-mm, which is equivalent to 39.2% of the starting kinetic energy or total energy. Therefore, we can deduce that 102.2 kN-mm, or 60.8% of the whole energy (initial K.E), is changed to different types of energy, including internal energy, hourglass energy, sliding energy, and other forms. Figure 5.3 displays the system's overall energy vs time graph.

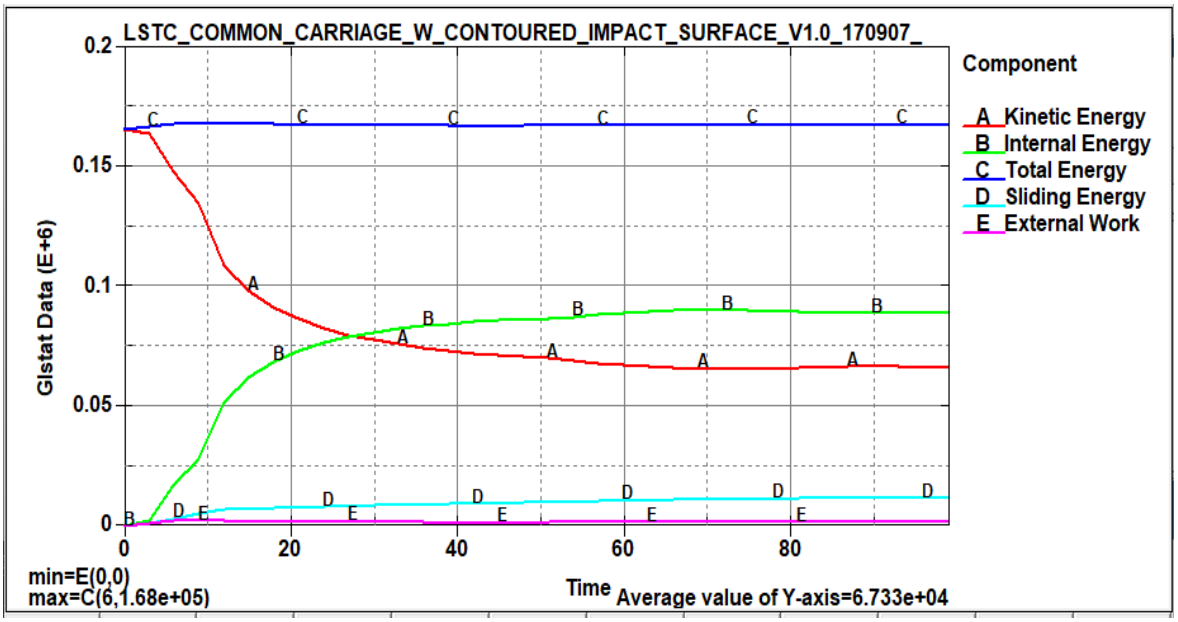

Figure 5.3. System's overall energy vs time graph of full-frontal crash (LS DYNA)

Energy Absorbed

Figure 5.4 shows the absorbed energy from the entire energy, or starting kinetic energy, the internal energy makes up 90.2 kN-mm, or 53.7% of the total energy. The remaining energies are in the form of hourglass energy, sliding energy, and other forms of energy, with values of 584 N-mm, 11.7 kN-mm, and other forms of energy, respectively.

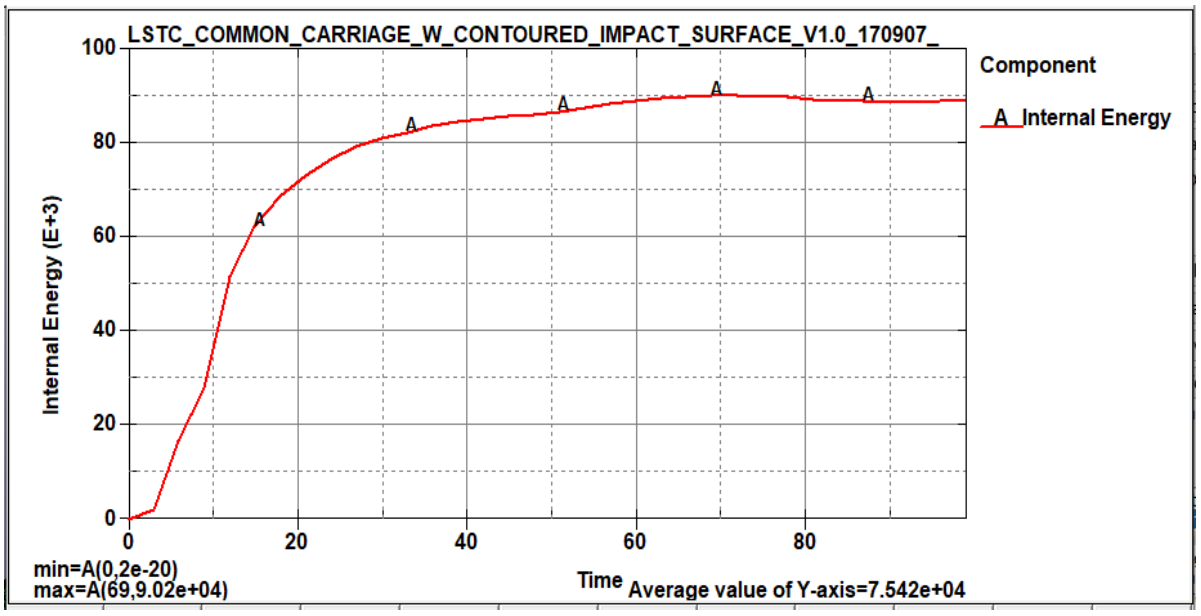

Figure 5.4. The absorbed energy of full-frontal crash (LS DYNA)

Velocity of Components

As illustrated in Figure 5.5 the form the entire graph shown, the velocity before the collision is zero this indicates that the chassis is stationary and after the barrier collides, the chassis starts to move and registers maximum velocity of 10.9 mm/ms.

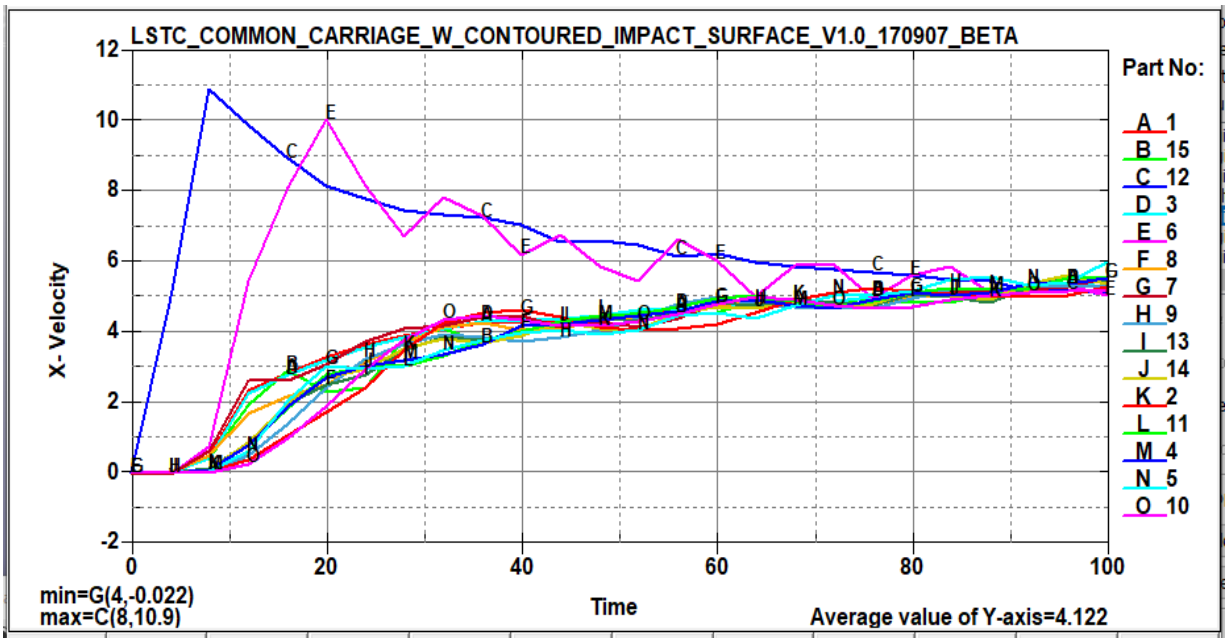

Figure 5.5. Velocity of components of full-frontal crash (LS DYNA)

Impact Force

Figure 5.6 displays the contact force between the rigid barrier and the chassis. Until the time approaches 0.002s, the first contact force is almost zero. The force then starts to grow and exhibit some oscillations. The simulation's transient (time dependent) nature is the cause of the oscillations, which is why the force on an element is not always constant. The strongest force is generated when the barrier comes into direct contact with a chassis. Stiff parts result in a greater force due to the shorter contact duration. The maximum contact force registered is 549 kN at a time of 12 ms.

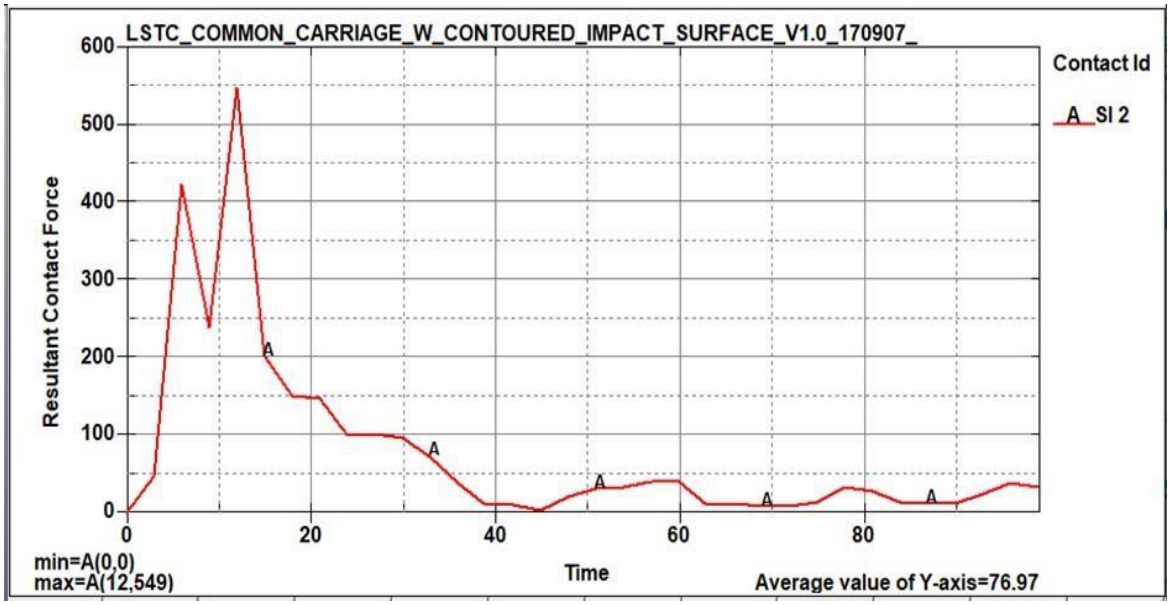

Figure 5.6. The impact force of full-frontal crash (LS DYNA)

5.2.2 Verification Parameters

Energy ratio

From the energy balance curve, it has been seen that the system energy is not fully conserved and this is due to zero energy form of some elements. So, it may be noted that, all the processes in this universe are irreversible and some losses are always included which deviates energy ratio slightly from one. This can be observed in the energy ratio graph. As it is discussed before, to be accepted the energy ratio value should be 1.00 +/- 0.07. As shown in Figure 5.7, the simulation produces maximum value of 1.0001 energy ratio, which is acceptable.

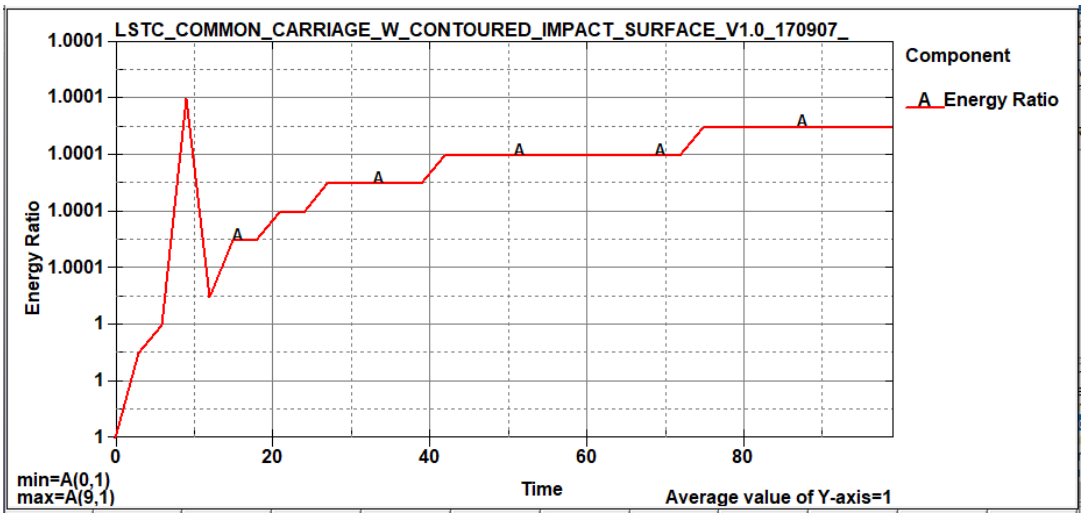

Figure 5.7. The energy ratio of full-frontal crash (LS DYNA)

Ratio of TE/HE

The ratio of total energy to hourglass energy can also be used to analyze the energy curves in order to assess whether the finite element model is correct. A model with zero energy can result from hourglass energy. The finite element model is trustworthy if the energy in the hourglass is less than 5% of the overall energy. The graphs of energy for an hourglass and total energy are displayed in the figure 5.8 below, the overall energy is equivalent to 168 kN-mm, and the hourglass's highest value is 584 N-mm, as can be seen.

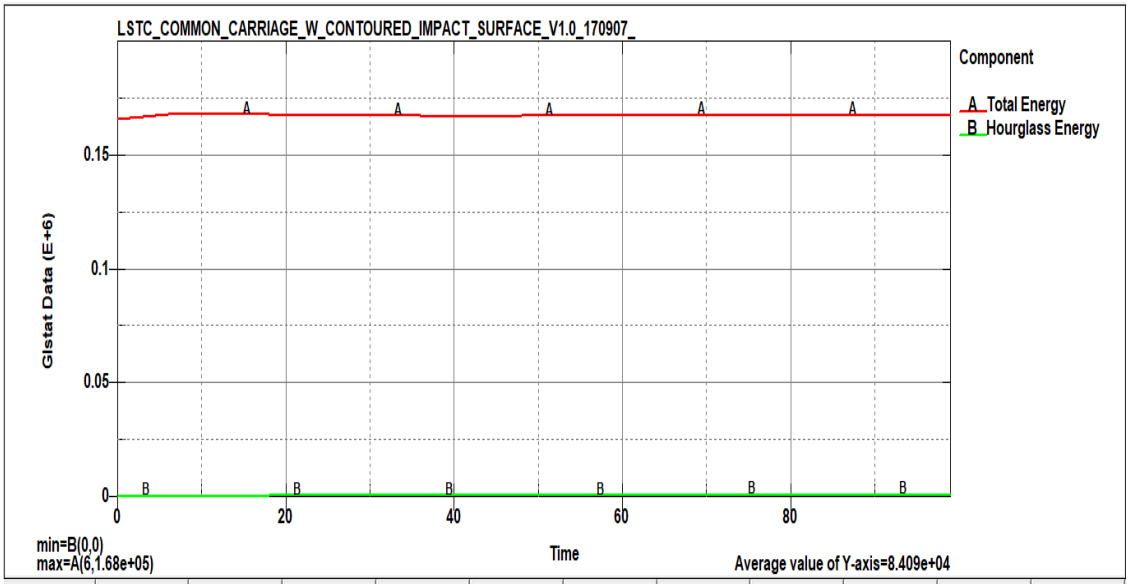

Figure 5.8. Ratio of TE/HE of full-frontal crash (LS DYNA)

If you divide these two, you get 0.004 (0.4 %). It can be inferred that the result is accurate since the hourglass energy is too low, or HG 5%.

5.2.3 Side Impact Collision

I. Structural Response

The simulation result of the chassis side crash is presented, the sequence and the appearance of the existed chassis at final state is shown on Figure 5.9. The result of side crash simulation where the barrier moving with velocity of 35 mph will collide with chassis which is stationary in opposite side of barrier. The Figure below shows the event and response of the whole chassis structure during the time 200ms.

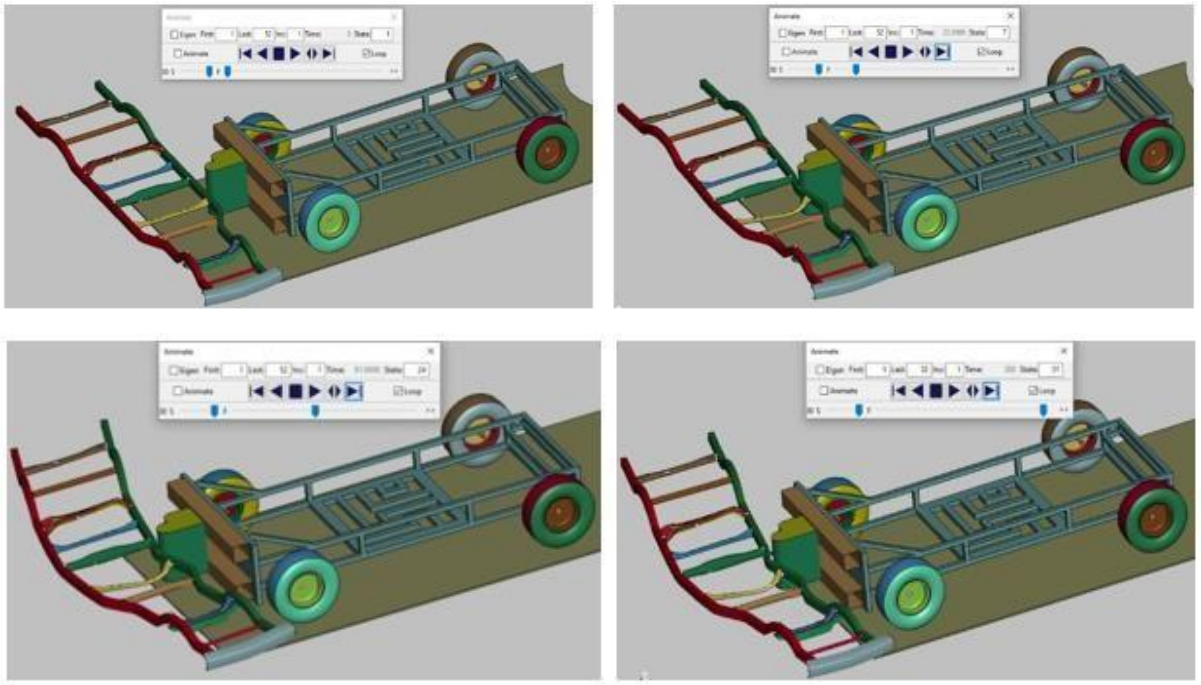

Figure 5.9. The simulation result of the chassis side crash (LS DYNA)

Total Deformation

As shown in Figure 5.10 the maximum deformation is equal with 734 mm, most of the deformation process takes place until 0.108 s and after this point only little deformation is observed. This is because the chassis reaches its maximum absorption so after that there is a little deformation is observed. After this point the force of impact is decreased as a result only less deformation is observed.

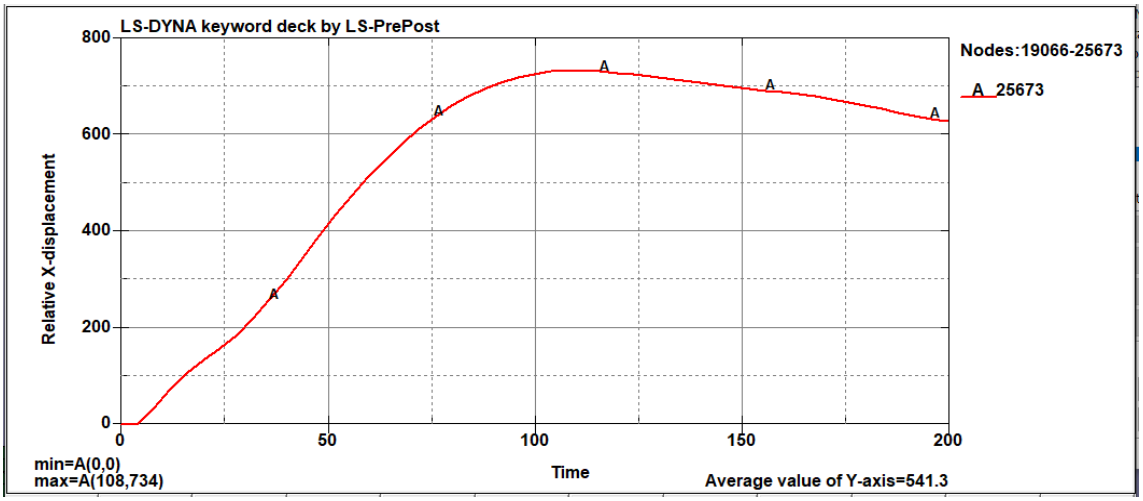

Figure 5.10. Total deformation of side crash (LS DYNA)

Total Energy-balance

The total energy of the system remains constant for the whole simulation with value equal to the initial kinetic energy which is 80.7 kN-mm. The kinetic energy of the whole system starts to decrease as the collision process starts and converted into internal energy, sliding energy and so on, which is increasing starting from zero energy as shown in the Figure 5.11.

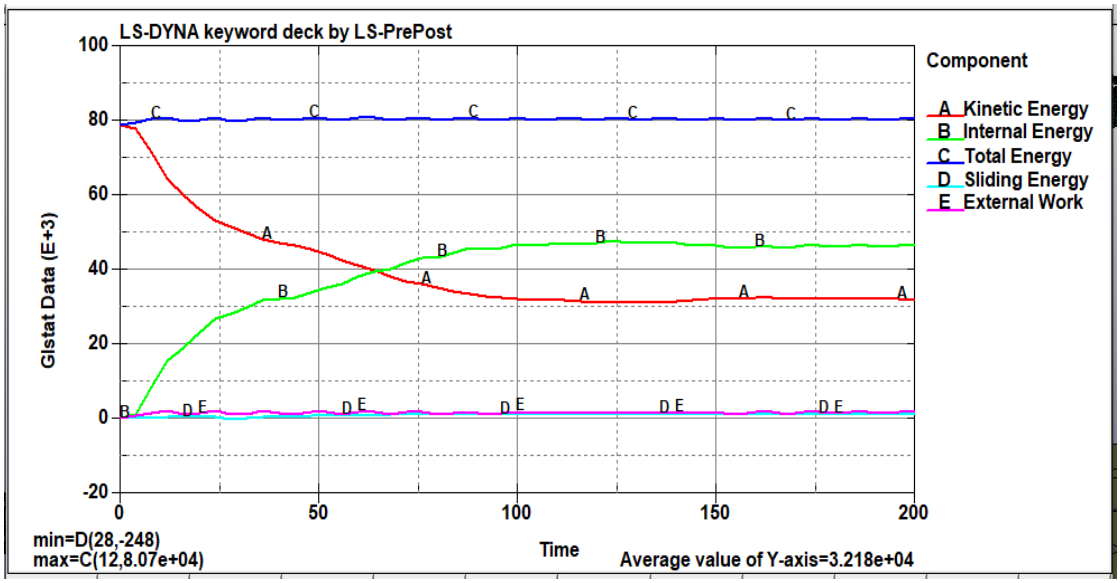

Figure 5.11. Energy balance of side crash (LS DYNA)

Energy Absorbed

From the total energy or initial kinetic energy, the internal energy is accounts for 44.5 kN-mm of energy which is 59 % the total energy and the remaining energies are in the form of hourglass energy, sliding energy and other form of energy. The total absorbed energy graph is shown on the Figure 5.12.

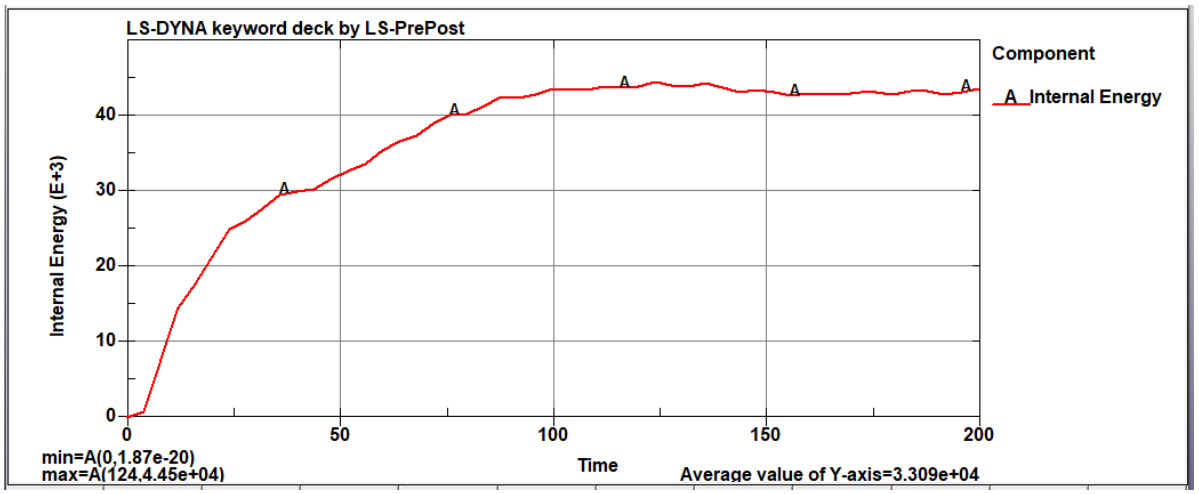

Figure 5.12. Energy absorbed of side crash (LS DYNA)

Velocity of Components

Figure 5.13 shows the velocity of components before the collision is zero this indicates that the chassis is stationary and after the barrier collides, the chassis starts to move and registers maximum velocity of 6.57 mm/ms.

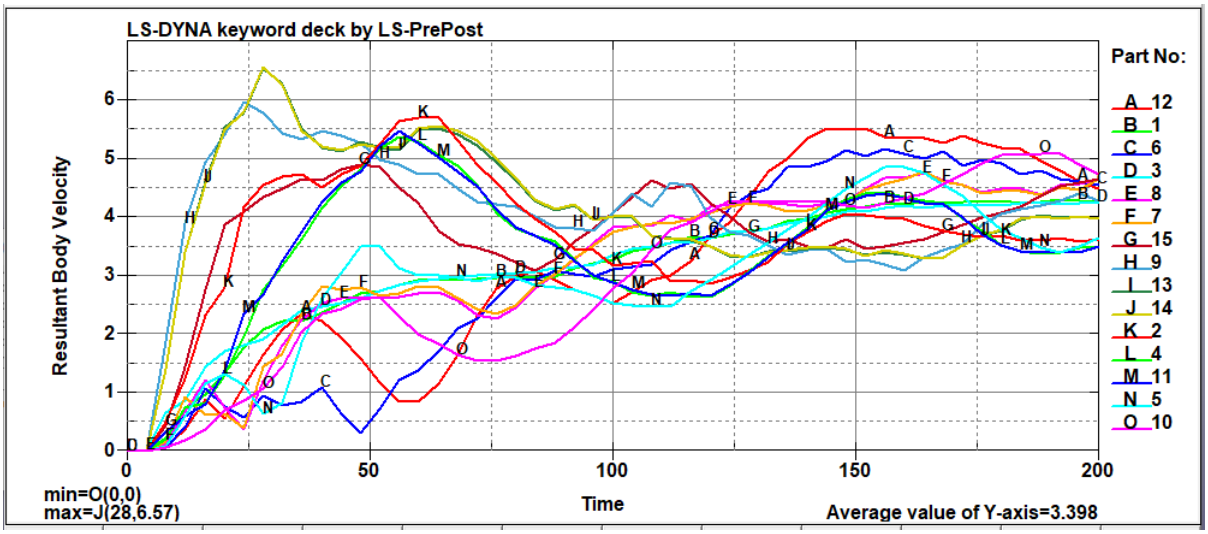

Figure 5.13. Velocity components of side crash (LS DYNA)

Impact Force

The contact force between the barrier and chassis is shown in the Figure 5.14. Initially the contact force is almost zero until the time reaches 0.003s. After this point the force starts to increase and shows some fluctuations. The fluctuations are due to the transient (time dependent) behavior of the simulation as a result the force on element is not always constant. The maximum force occurs when the simulation reaches 0.012s with a value of 281kN.

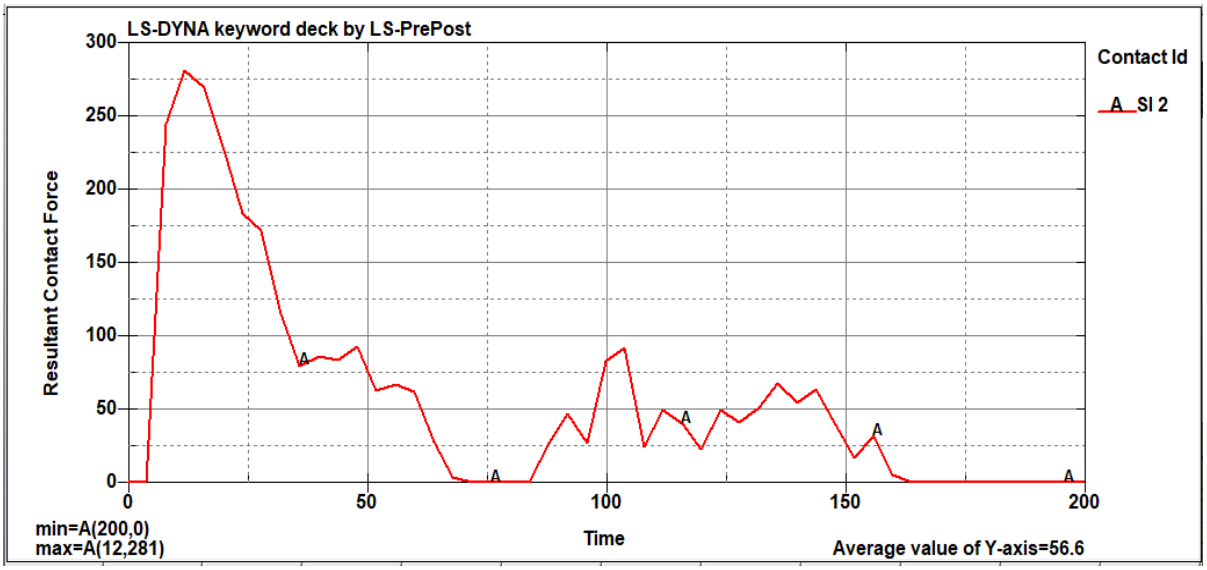

Figure 5.14. The impact force of side crash. (LS DYNA)

5.2.4 Verification Parameter

Energy ratio

As it can be seen on Figure 5.15, for the 0.2 s simulation the energy ratio value varies between 1 and 1.0002, which is within the range of acceptable value.

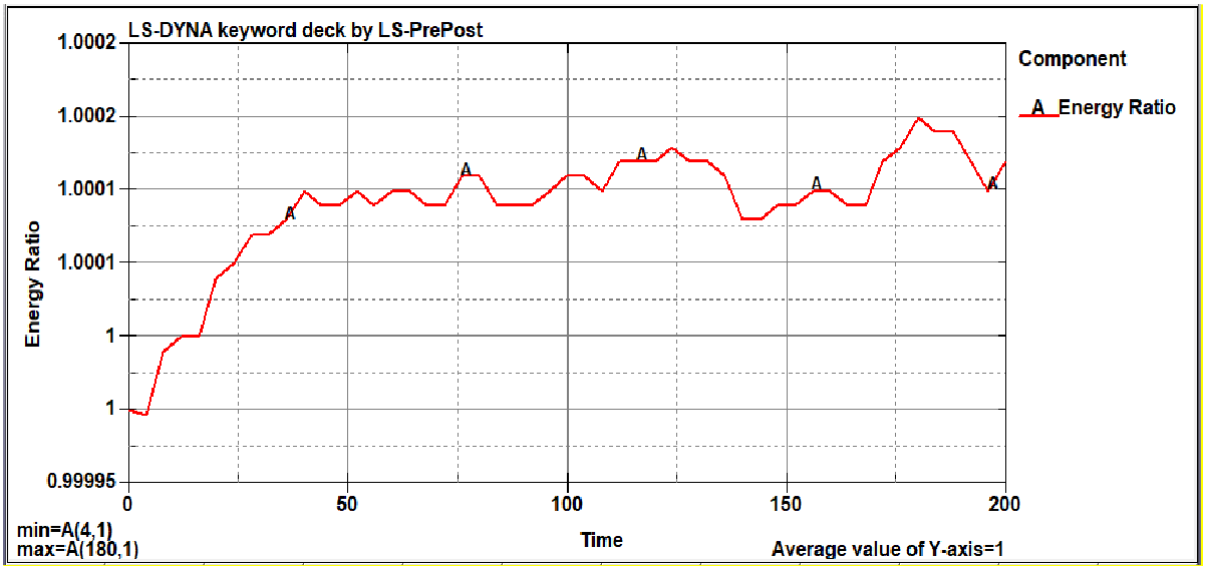

Figure 5.15. Energy ratio of side crash (LS DYNA)

Ratio of TE/HE

Through analyzing the energy curves, the verification of the finite element model can also be determined using the ratio between the total energy to hourglass energy. Hourglass energy can cause a zero-energy model.

If the hourglass Energy is less than 5% of the total energy, the finite element model is reliable. In the figure 5.16 below the hourglass energy graph is too small (0.004 or 0.4 %), i.e., HG < 5% it can be concluded that the result is reliable.

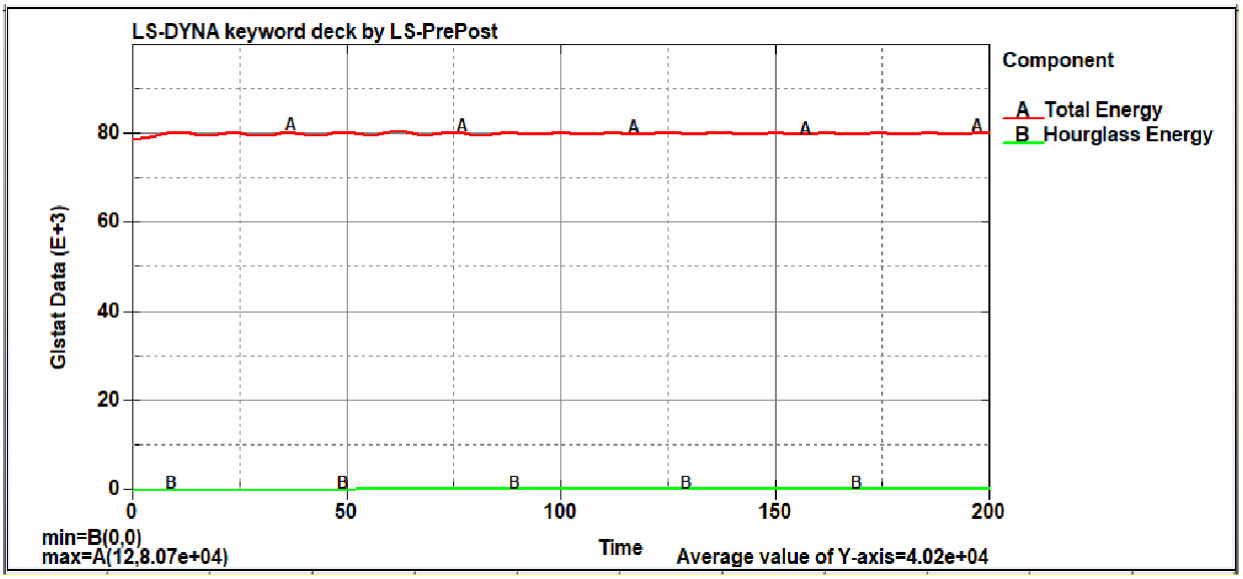

Figure 5.16. Ratio of TE/HE of side crash

5.3 Results of Reinforcement Simulation

5.3.1 Front reinforcement simulation

Under this section the impact behavior of front reinforcement under different thickness is analyzed based on parameters like impact force, displacement (deformation) and also energy absorption. On the above studies, the deformation and energy absorbed have direct relation, so it is enough to study the energy absorbed in terms deformation. The thickness considered were 1, 2, 3 and 4 mm. the result of the simulation is discussed below.

Energy absorption of the front reinforcement

As discussed on the graph, the lower thickness of the reinforcement leads to more absorption of energy during the collision. The maximum amount of energy absorbed by the front reinforcement is 398 KN-mm as shown in the Figure 5.17.

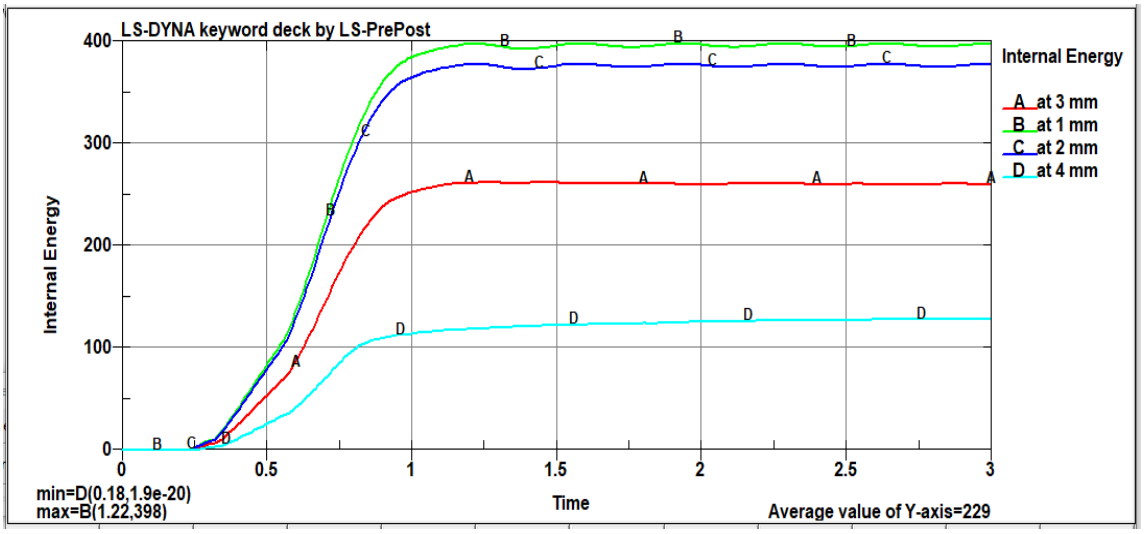

Figure 5.17. Energy absorbed by the front reinforcement (LS DYNA)

Deformation of the front reinforcement

As it is presented in graph, the behavior follows the same pattern in which the deformation increases as the thickness decreases. Initially until t=0.08 there is high deformation until it reaches its maximum deformation, then starts to decrease the rate of deformation and finally, the structures were subjected to plastic deformation is shown on Figure 5.18.

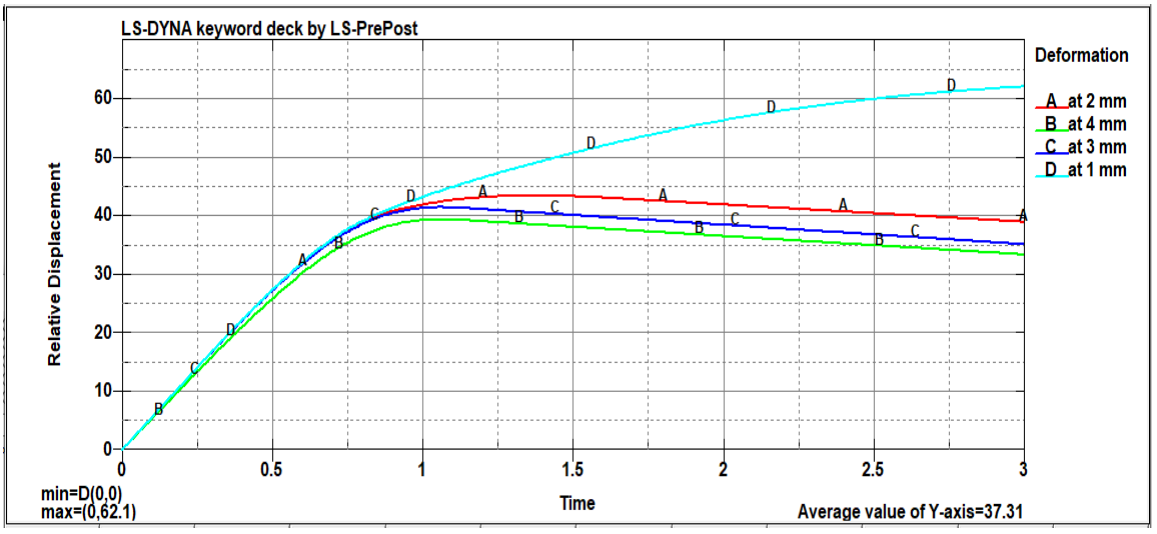

Figure 5.18. Deformation of the front reinforcement (LS DYNA)

Impact force of the front reinforcement

The fluctuation effect observed on the graph shown the compression and elongation effects occurs between the measuring nodal points of the reinforcement. From the deformation it can also concluded that the energy absorbed by reinforcement increases with more deformation and decreases with les deformation.

In another word the decrease in thickness results in more deformation and energy absorption. The contact force vs. time graph is shown in Figure 5.19. The graph reveals that as the thickness increases the force of impact increases. The maximum impact force (33 kN) occurs when the thickness is 4 mm. This behavior is obvious as the momentum increases with increase in thickness of front reinforcement. Generally looking at the above results it can have concluded that the decrease in thickness results in high deformation, high energy absorption and low contact force. So, average thickness (2 mm) is selected for the full chassis simulation in order to get low impact force, less deformation and good energy absorption.

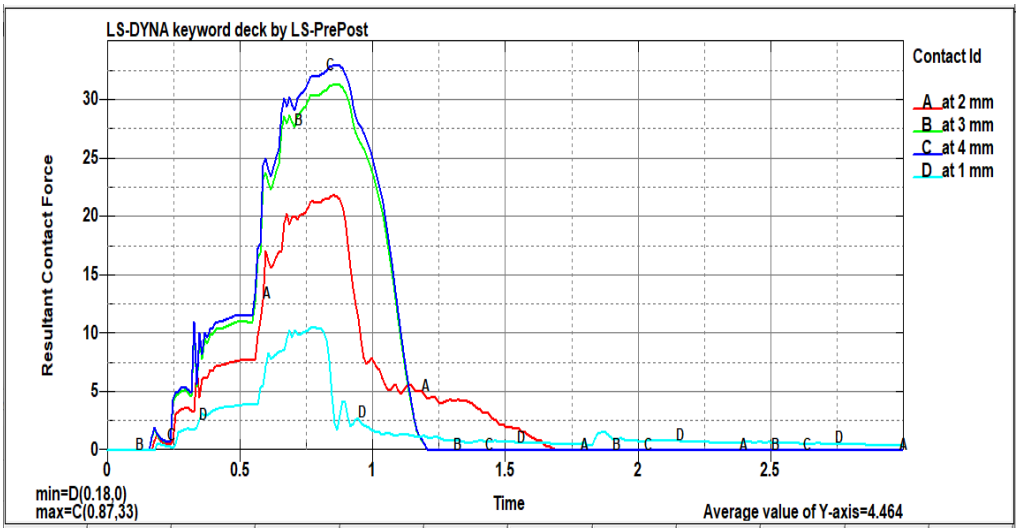

Figure 5.19. Impact force of the front reinforcement (LS DYNA)

Effective von Moises stress of front reinforcement

The effective van mosses stress of the front reinforcement is shown on Figure 5.20 the maximum stress value is equal to 0.396 GPa at element 144235. The aluminum foam material strength and failure criteria are determined based on the material's mechanical property. Since there is no dilatation of element was reported when running the simulation so based on that assumption it is safe.

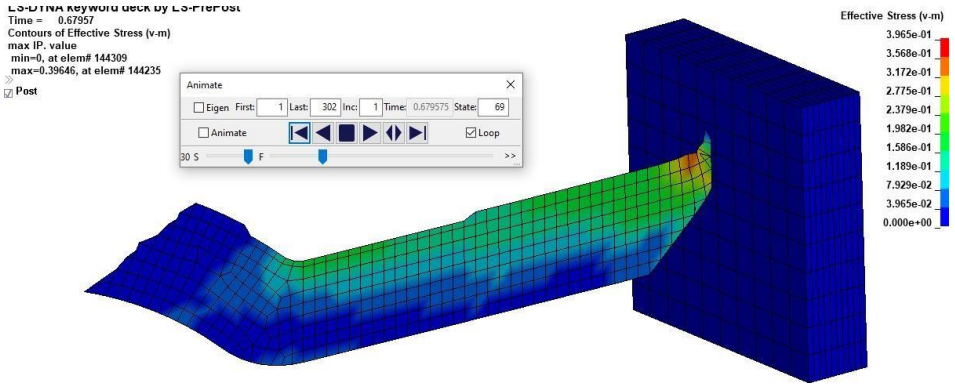

Figure 5.20. The Effective von Moises stress of front reinforcement (LS DYNA)

Resultant displacement of front reinforcement

The Resultant displacement of the front reinforcement is shown on Figure 5.21. From the contour plot it can be seen that the maximum resultant displacement (deformation) of the structure is equal to 47.1 mm at node 493648.

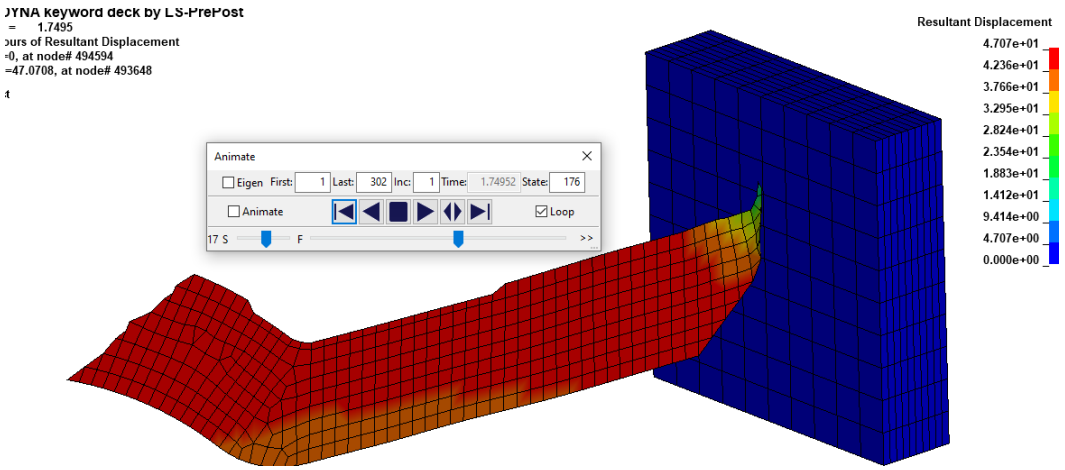

Figure 5.21. Resultant displacement of front reinforcement (LS DYNA)

5.3.2 Results of Side Reinforcement Simulation

The result for different thickness of side reinforcement is represented in graphs at regular interval of time as shown on the figure below. Judgments were going to be made by observing the impact analysis results like force, stress, deformation and energy absorption values.

Deformation of side reinforcement simulation

The deformation values are obtained by measuring the relative displacement from two nodes (one at the right or left end. With this measurement the value of deformation graph for different thickness of the beam was shown in the figure below. The thickness of the beam is 1, 2, 3 and 4 mm as shown in Figure 5.22. From the Figure shown, as the thickness of the beam increases from 1 mm to 4 mm, the maximum deformation of the beam decreases and the rate of decrease becomes also less with the increase of thickness. This does mean that abeam with less thickness is always better because more deformation means that there is probability of intrusion to the vehicle main compartments and also more energy is absorbed.

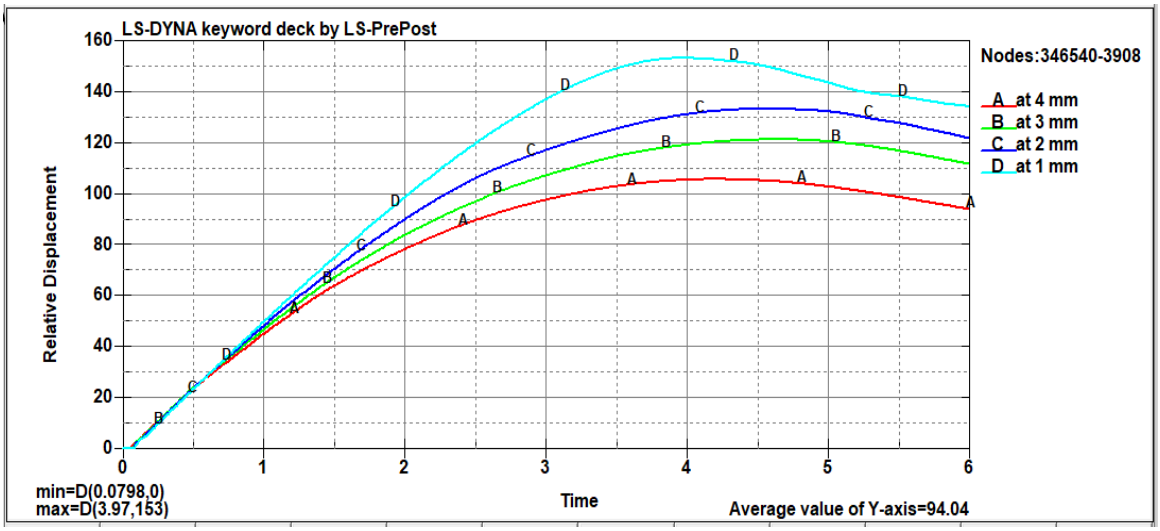

Figure 5.22. Deformation of side reinforcement simulation

Energy absorption of side reinforcement simulation

As discussed on the above, the higher deformation of the beam leads to more absorption of energy during the collision. The maximum amount of energy absorbed is reduced as the thickness become increased as shown in the Figure 5.23.

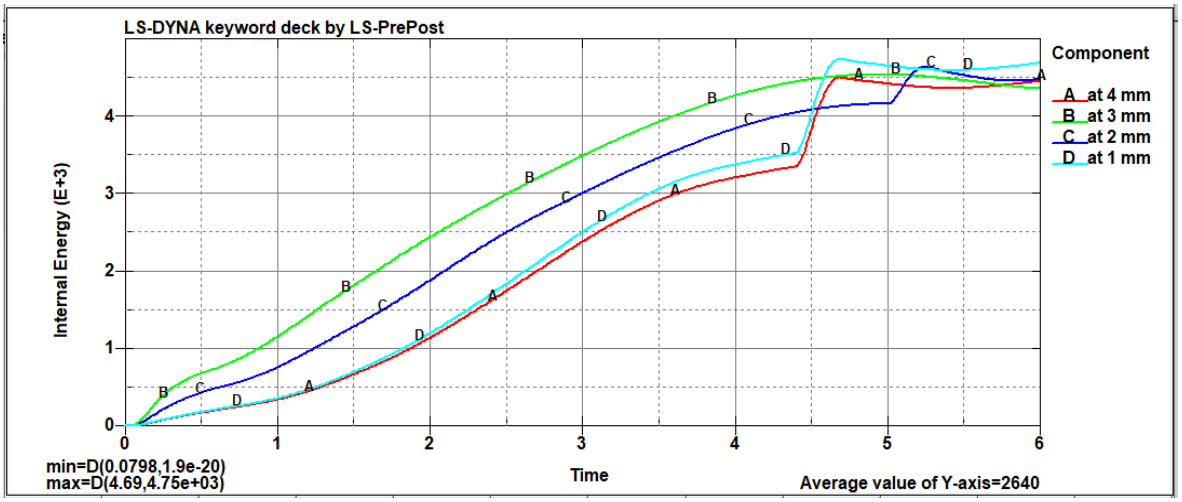

Figure 5.23. Energy absorption of side reinforcement simulation

Impact force of side reinforcement simulation

Although maximum impact force between rigid pole and side reinforcement increases with the increase of thickness. This is obvious that with increase in thickness the mass also increases as a result, high impact force is produced as shown in Figure 5.24. But that does not mean that beam with smaller thickness is better because the stress on the on the beam increases with the use of less thickness. Therefore, from the above results it can be concluded that neither abeam with less thickness nor with higher thickness is better, rather it depends on the application it is

required for. From the viewpoint of impact performance, among the listed thickness taking the average value provides improved the level of performance relative of other for the chassis. Therefore, the reinforcement with 2 mm thickness is better to be selected.

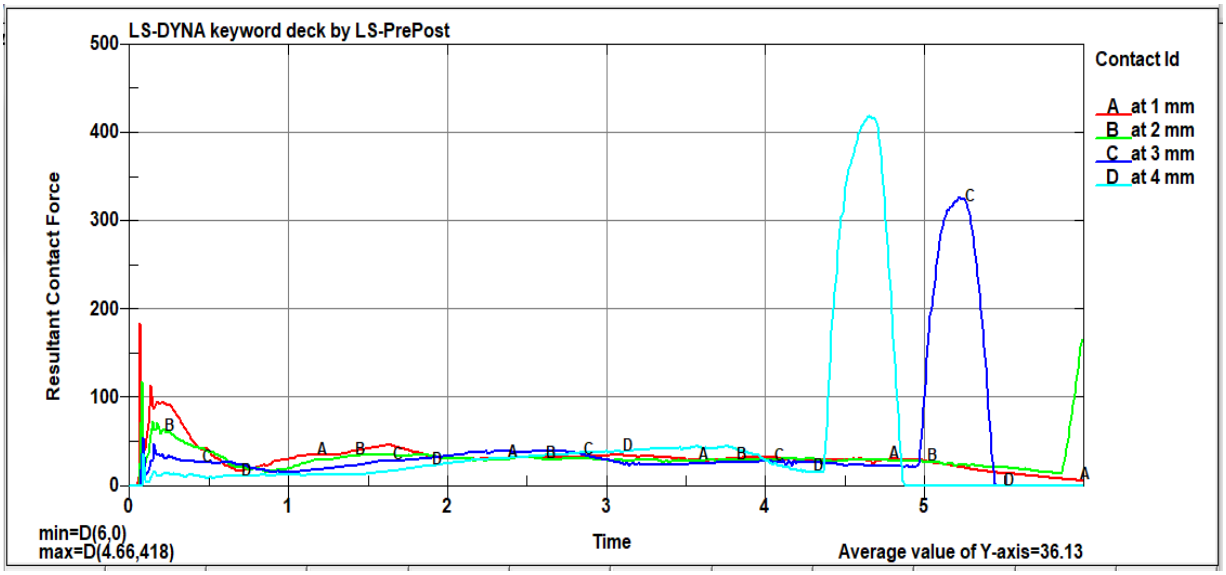

Figure 5.24. Impact force of side reinforcement simulation (LS DYNA)

Effective von Moises stress of side reinforcement simulation

The effective van mosses stress of the side reinforcement is shown on Figure 5.25 the maximum stress value is equal to 0.59 GPa at element 287188. The aluminum foam material strength and failure criteria are determined based on the material's mechanical property. Since there is no dilatation of element was reported when running the simulation so based on that assumption it is safe.

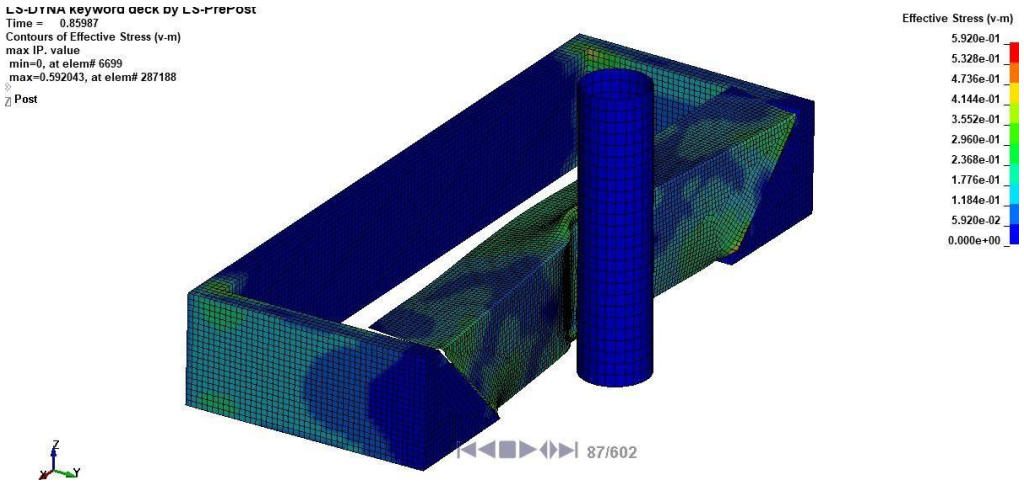

Figure 5.25. Effective von Moises stress of side reinforcement simulation (LS DYNA)

Resultant displacement of side reinforcement simulation

The Resultant displacement of the front reinforcement is shown on Figure 5.26. From the contour plot it can be seen that the maximum resultant displacement (deformation) of the structure is equal to 48.3 mm at node 379774.

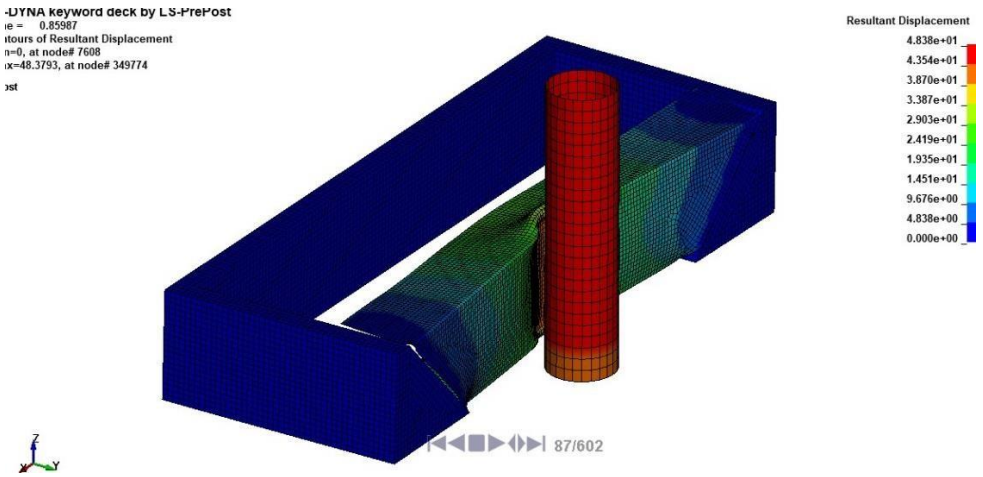

Figure 5.26. Resultant displacement of side reinforcement simulation (LS DYNA)

5.4 Result and Discussion on Modified Model

5.4.1 Structural response of Modified Model for full front collision

The result of frontal crash simulation where the car moving with velocity of 35mph will collide with rigid wall which is stationary in opposite side of car and is discussed. Figure 5.27 shows the event and response of the whole vehicle structure during the time 100 ms.

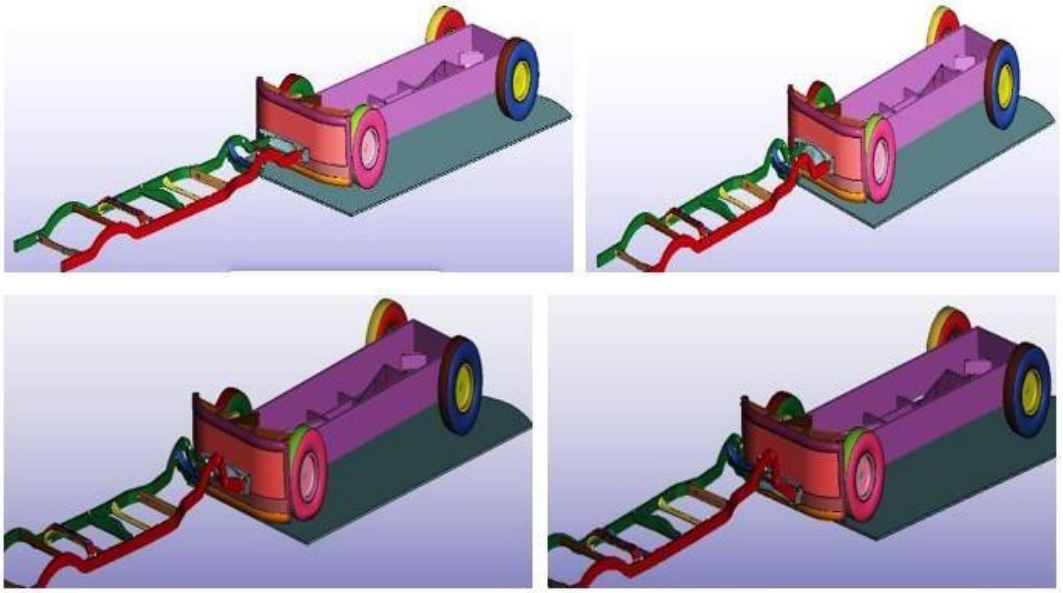

Figure 5.27. Structural response of modified model for full front collision (LS DYNA)

Total deformation of modified model for full front collision

As shown in the graph, the behavior exhibits the similar pattern, where the deformation rises as the speed rises. Initially, up to t=0.009s, there is considerable deformation until the collision comes into contact with chassis material and gets maximum deformation of 40.5 mm, at which point the collision starts to slow down the rate of deformation, leading to plastic deformation of the structures as illustrated in Figure 5.28.

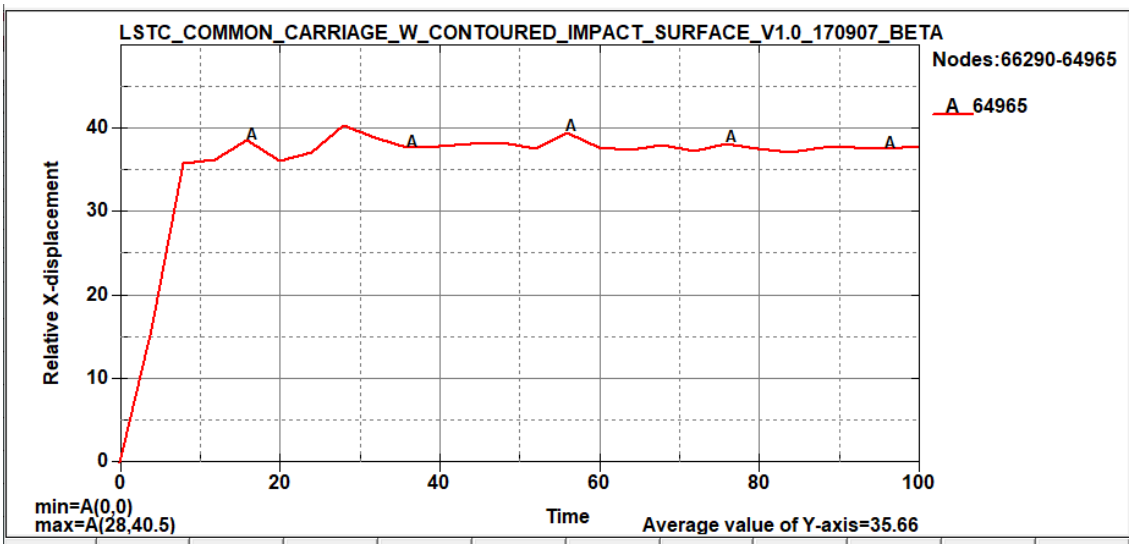

Figure 5.28. Total deformation of modified model for full front collision

Total Energy-balance for modified model for full front collision

The energy versus time graph of the total system is shown in Figure 5.29. As it is shown through the simulation the Conservation of energy principle is obeyed in which the amount of kinetic energy lost during impact is converted to other forms of energy such as internal energy, sliding energy and hour glass energy. The total energy graph remains approximately constant. Initially the kinetic energy is equal with total energy with value equal to 168 kN-mm but as the vehicles starts motion the KE value decrease and get converted into internal energy and other forms. As a result of final state, it reaches energy value equal to 43.7 kN-mm this indicate that 74 % of kinetic energy is lost and converted in to other forms of energy.

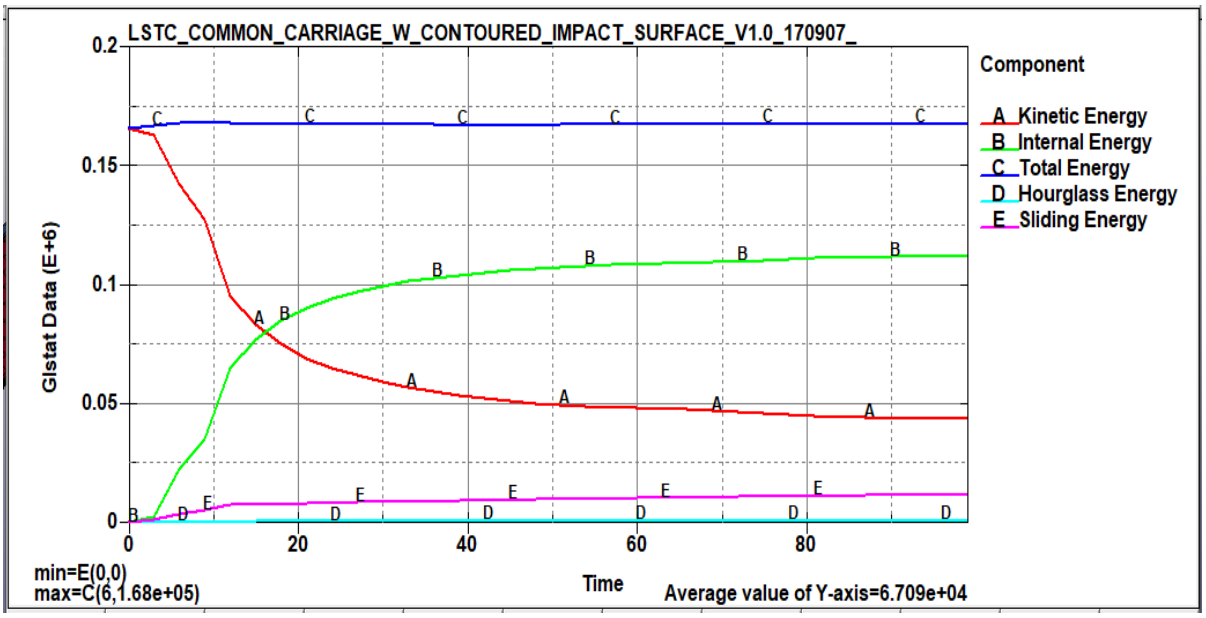

Figure 5.29. Total Energy-balance of modified model for full front collision

Energy Absorbed

As shown in the below Figure 5.30 from the entire energy, or starting kinetic energy, the internal energy makes up 112 kN-mm, or 66.67 % of the total energy. The remaining energies are in the form of hourglass energy, sliding energy, and other forms of energy, with values of 736 N-mm, 11.4 kN-mm, and other forms of energy, respectively.

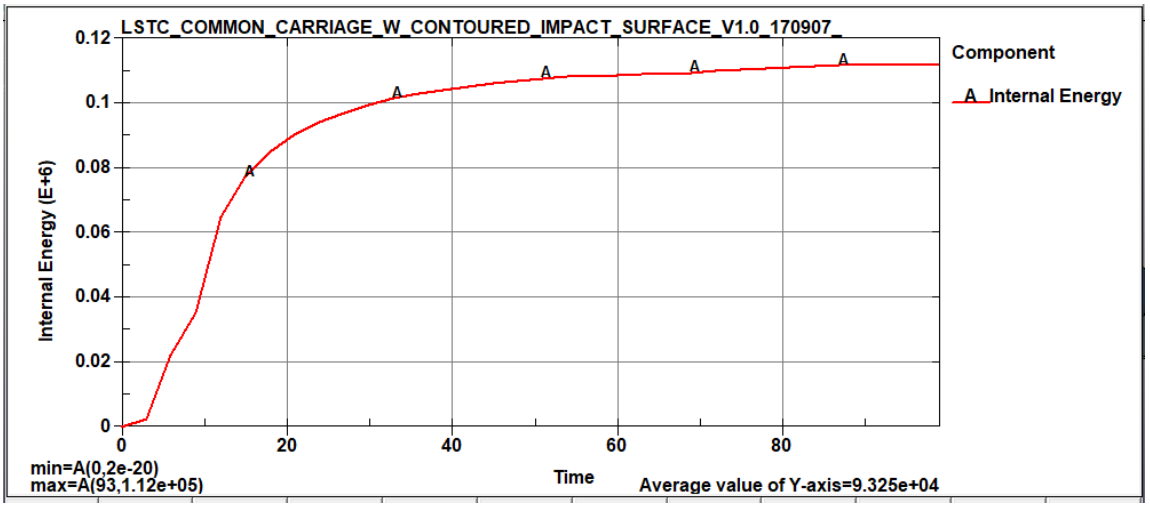

Figure 5.30. Energy absorption of modified model for full front collision

Velocity of components

The entire graph shown in Figure 5.31 below, the velocity before the collision is zero this indicates that the chassis is stationary and after the barrier collides, the chassis starts to move and registers maximum velocity of 10.6 mm/ms.

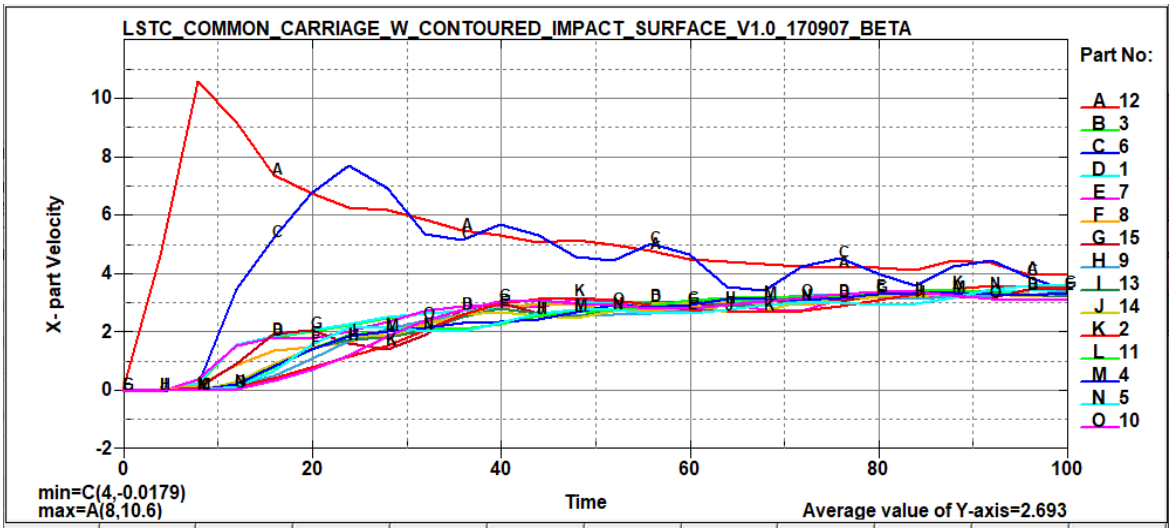

Figure 5.31. Velocity of components of modified model for full front collision

Impact Force

The contact force between the modified chassis and the rigid barrier is shown on Figure 5.32. As shown the Contact force pulse data shows maximum force at 0.012s. This maximum force is equal to 770kN.

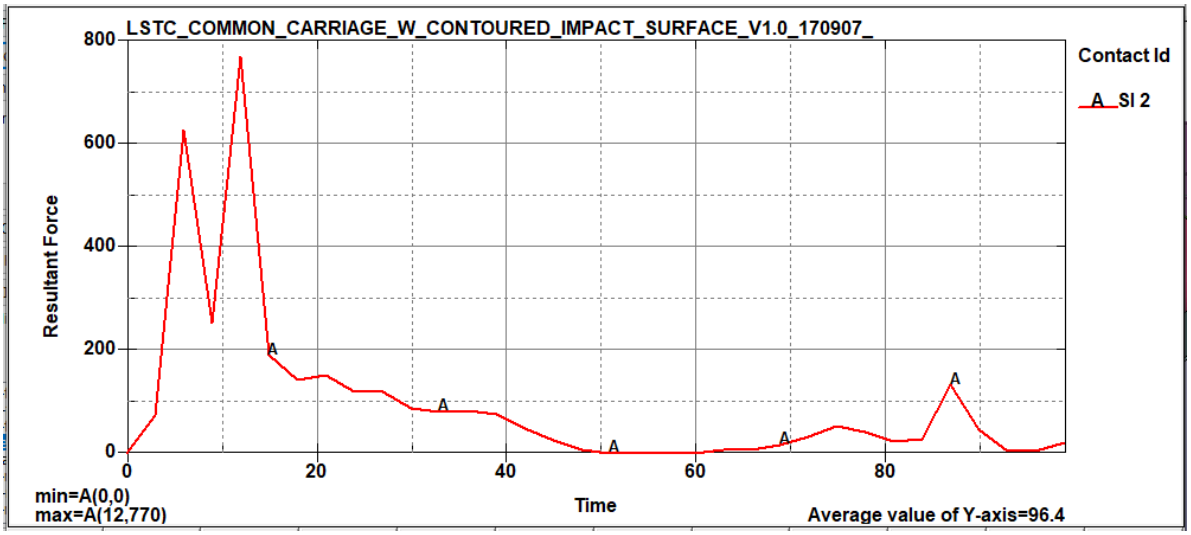

Figure 5.32. Impact force of modified model for full front collision

5.4.2 Verification Parameters

Energy Ratio

The energy ratio of the whole system is presented on Figure 5.33, the energy ratio value varies between 1 and 1.0001. This value in the range stated above is acceptable.

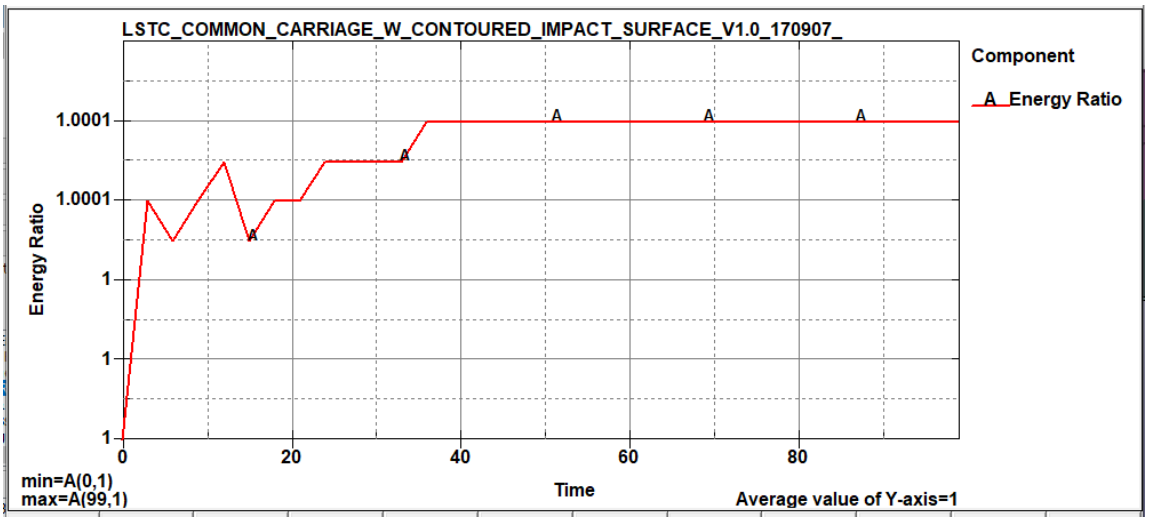

Figure 5.33. Energy ratio of modified model for full front collision

Ratio of TE/HE

As it can be easily seen from Figure 5.34, the value of hourglass energy is very less as compared to the total energy. The ratio resulted in 0.0226 or 2.26%. Since the energy ratio is less than 5% so the results are acceptable.

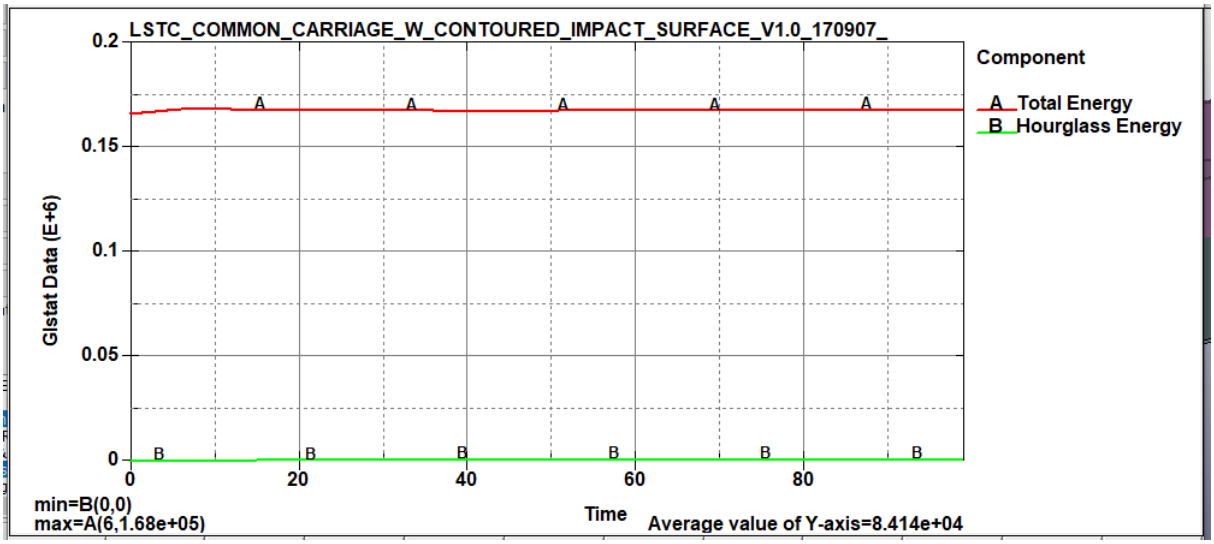

Figure 5.34. Ratio of TE/HE of modified model for full front collision

5.4.3 Side Impact Collision

Total Deformation

The resultant displacement of the modified model in lateral direction is shown on Figure 5.35. From the graph, the maximum displacement is equal with 558 mm. The maximum deformation occurs at 0.12 s and after this point the deformation decrease. Although after this point the force of impact is decreased as a result only less deformation is observed.

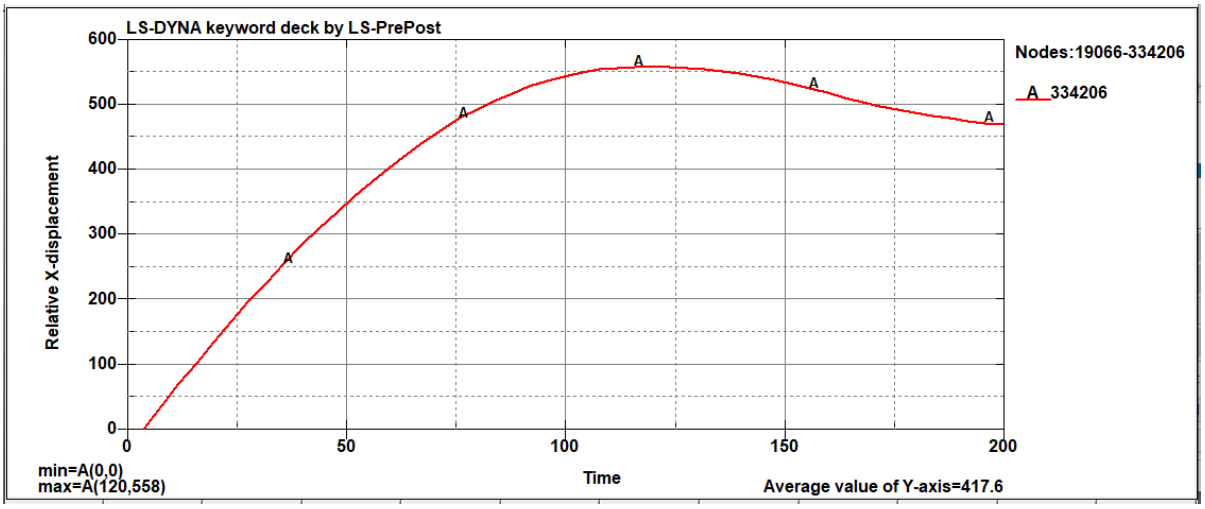

Figure 5.35. Total deformation of modified model for Side impact collision

Total Energy-balance

The energy versus time plot of the total system is shown in Figure 5.36. As it is shown the total energy of the system remain almost constant for the whole 0.2s simulation with value equal to the initial kinetic energy which is 80.8 kN-mm. On the other hand, the kinetic energy of the whole system starts to decrease as the collision process starts and converted into internal energy, hourglass energy, sliding energy or other forms of energy.

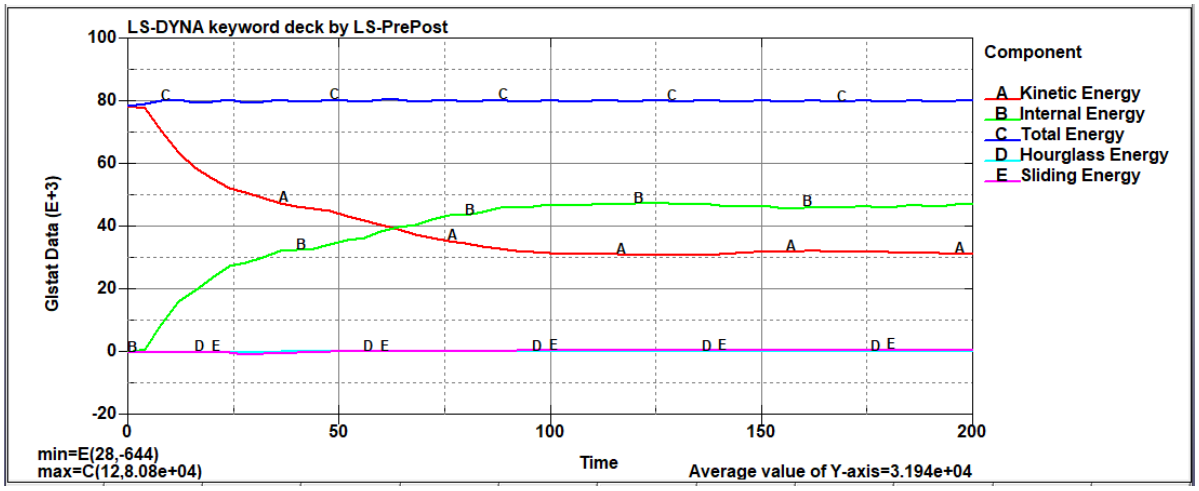

Figure 5.36. Total Energy-balance of modified model for Side impact collision

Energy Absorbed

From the total energy or initial kinetic energy 48 kN-mm of energy is in the form of internal energy as shown on Figure 5.37. This mean that internal energy takes 60 % of the dissipated or lost KE. The remaining 32.5 kN-mm of energy is in the form of hourglass, sliding energy and other form of energy.

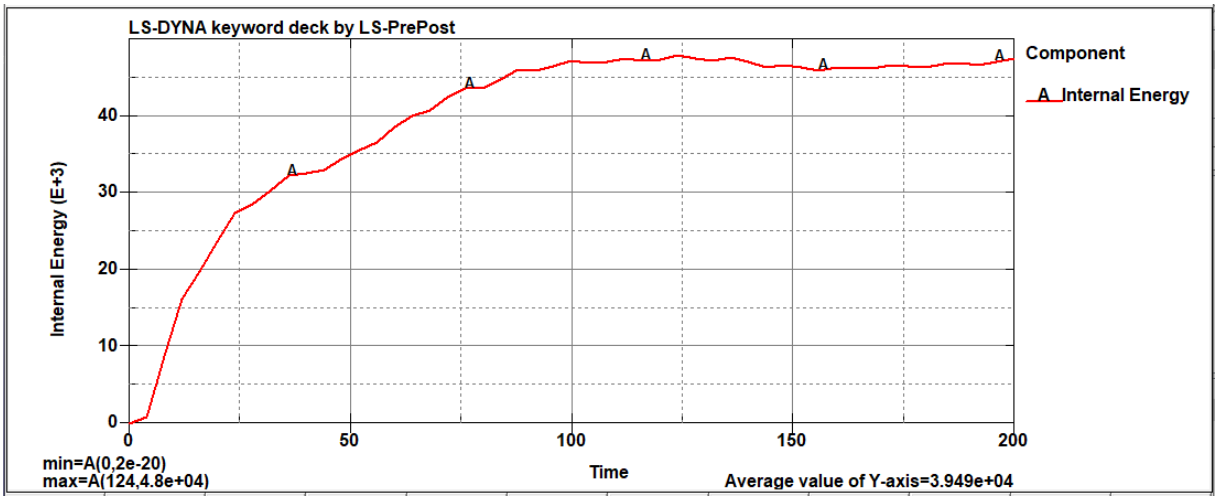

Figure 5.37. Energy absorbed of modified model for Side impact collision

Velocity of Components

As shown in Figure 5.38, the velocity before the collision is zero this indicates that the chassis is stationary and after the barrier collides, the chassis starts to move and registers maximum velocity of 7.54 mm/ms.

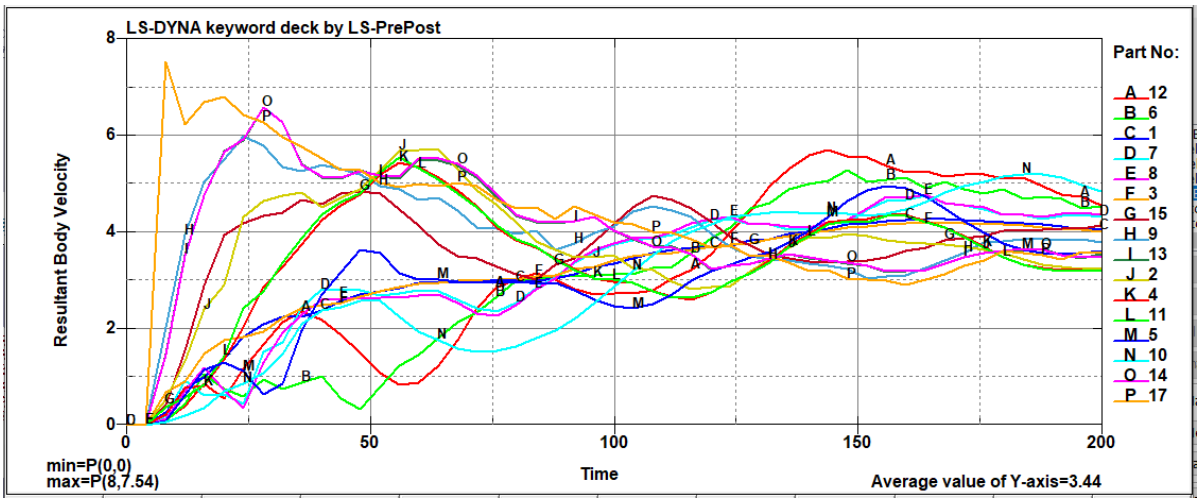

Figure 5.38. Velocity of components of modified model for Side impact collision

Impact Force

The impact force between the movable barrier and the chassis is shown in the Figure 5.39. Until the time reaches 0.004 s it is minimum. After this point the force starts to increase and shows some fluctuations. As mentioned before the fluctuations are due to the transient (time dependent) behavior of the simulation. The maximum resultant force occurs at t=0.012 s with value equal to 288kN.

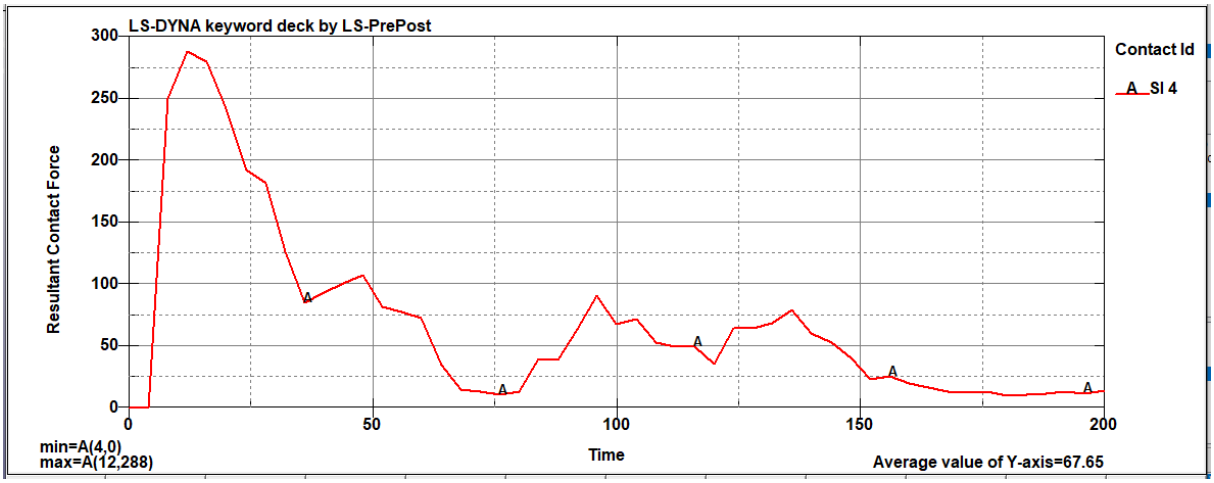

Figure 5.39. Impact force of modified model for Side impact collision

5.4.4 Verification parameters

Energy ratio

As it can be seen on Figure 5.40, for the 0.2 s simulation the energy ratio value varies between 1 and 1.00025 which is within the range of acceptable value.

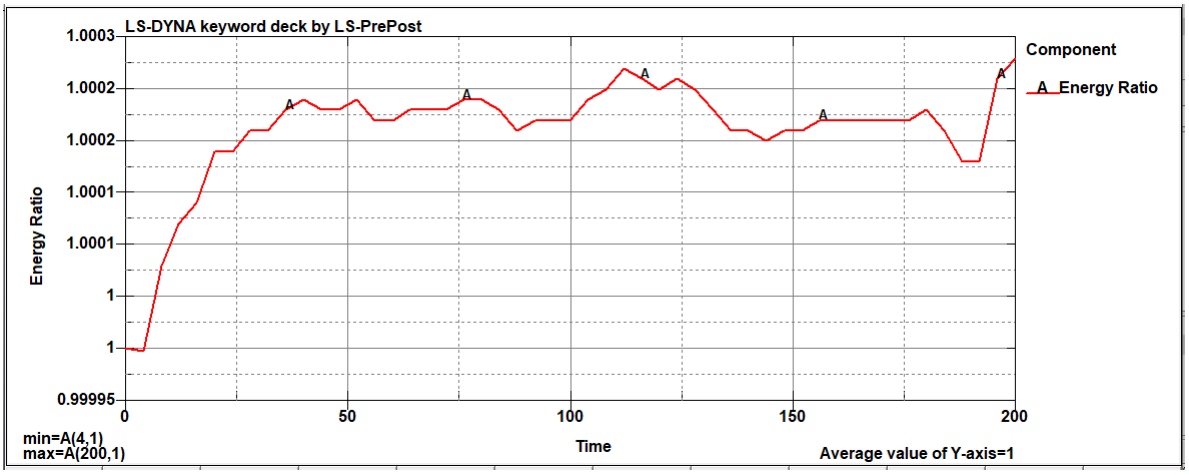

Figure 5.40. Energy ratio of modified model for Side impact collision

Ratio of TE/HE

Another means for validating the FEA result is the ratio between the total energy to hourglass energy. Figure 5.41 indicated on the maximum hourglass energy is equal with 0.356 kN-mm and the total energy is 80.8 kN-mm. The ratio between this value (HE/TE) is less than 5%. If the hourglass Energy is less than 5% of the total energy, the finite element model is reliable.

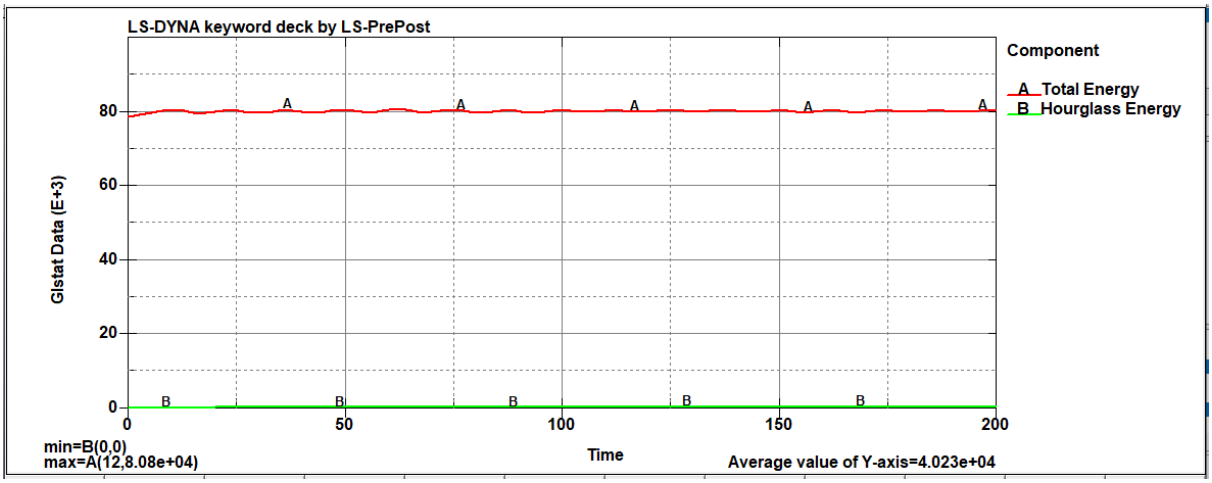

Figure 5.41. Ratio of TE/HE of modified model for Side impact collision

5.5 Comparisons of Existing and Modified Model

5.5.1 Frontal Impact

Total Deformation

The total deformation by the existing and modified model is shown on Figure 5.42. As it can be seen the maximum amount of deformation is occurred during the Existed model. This is due to the reinforced material properties used for the modification, as a result these may deformed less. Their difference in deformation is 15.6 mm (27.8 % improvement in deformation).

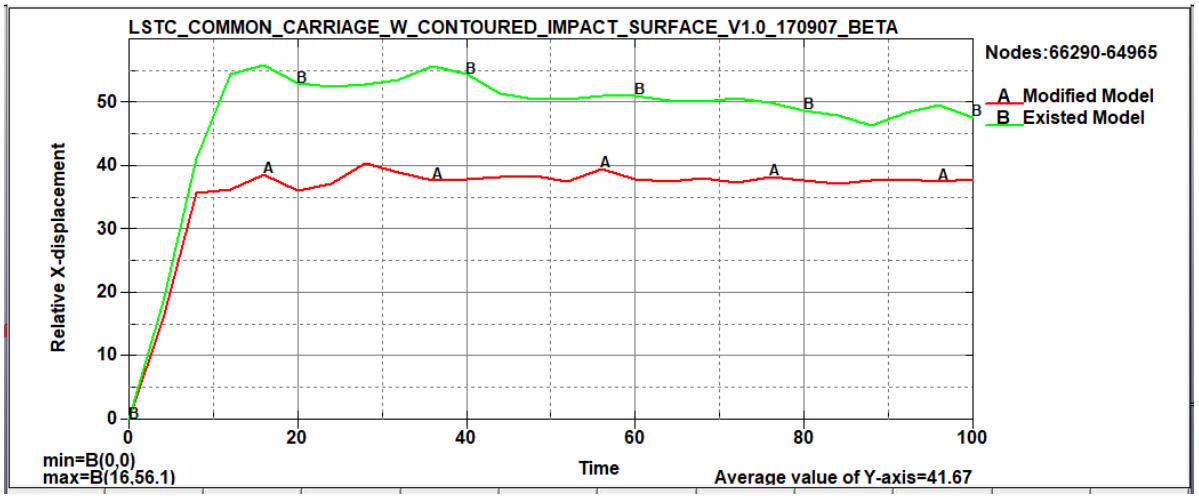

Figure 5.42. Total deformation of existing and modified model for Frontal Impact collision

Structural Response

Figure 5.43 shows the structural response of the existing (a) and modified (b) chassis for 0.1S simulation. From the Figure, the structural deformation of the existing chassis looks more as compared to the modified.

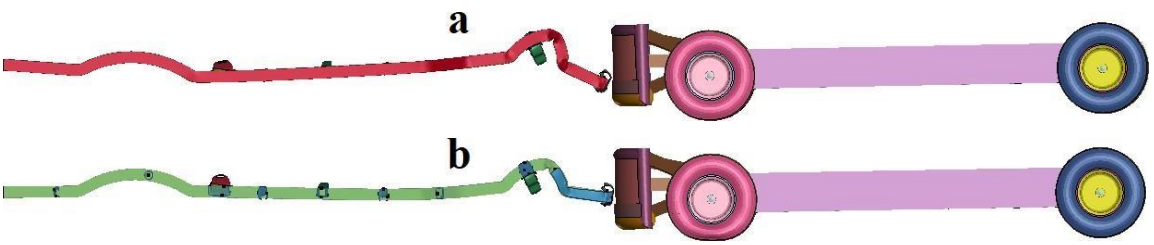

Figure 5.43. Structural response of the existing (a) and modified (b) for 0.1S simulation (LS DYNA)

Energy Absorbed

The total energy absorbed by the existing and modified model is shown on Figure 5.44. As it can be seen the maximum amount of energy is absorbed during the modified model. This is due to the reinforced material properties used for the modification, as a result these may deformed less and produces more absorption. Their difference in absorption is 21.8 kN-mm (19.5 % improvement in energy absorption).

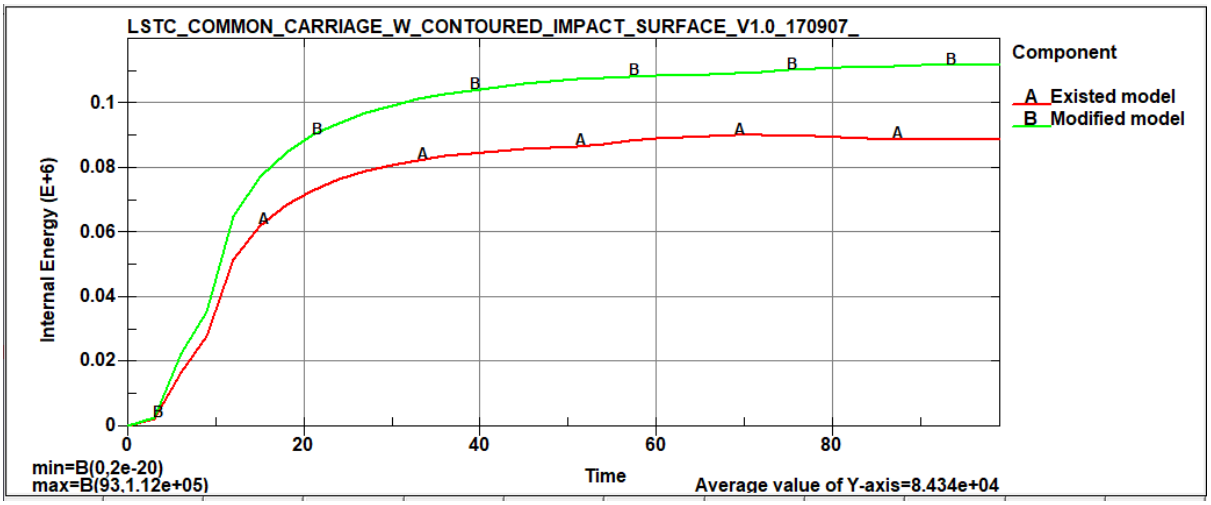

Figure 5.44. Energy absorbed of existing and modified model for Frontal Impact collision

Impact Force

The force of impact for the Existing model is better as shown on Figure 5.45. The maximum impact force occur on the existing model is equal to 549 kN, whereas the modified produced 770 kN, the difference is 221 KN. This is due to the reinforcement of the modified model which increases the overall thickness of the chassis.

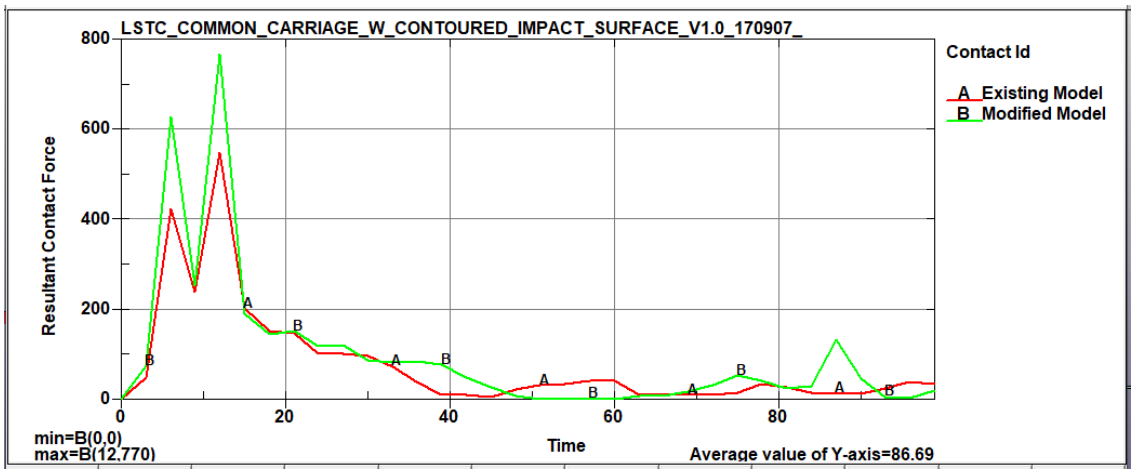

Figure 5.45. Impact force of existing and modified model for Frontal Impact collision

5.5.2 Side Impact

Total deformation

The deformation results on the existing and modified models are shown on Figure 5.46. The red line shows the relative displacement of the modified chassis model and the green line indicate the existed model. The maximum deformation for existing model and modified model is equal to 734 mm and 558 mm respectively. It is clear that the maximum deformation occurs on the existing model.

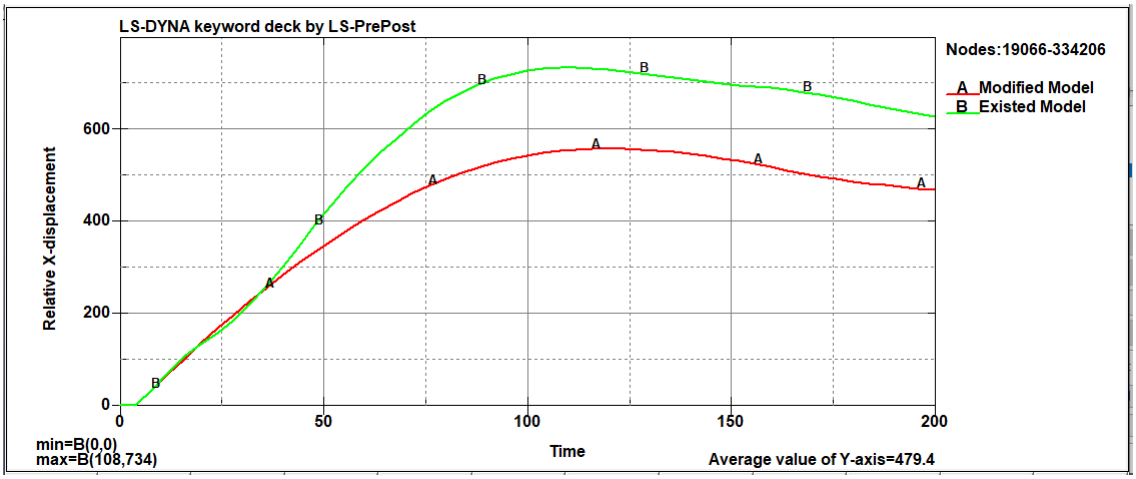

Figure 5.46. Total deformation of existing and modified model for Side Impact collision

Energy Absorbed

The absorption energy of the modified and existing model is shown in Figure 5.47. Since the same conditions are applied in the simulation of both models so, the energy absorption capacity of the models is determined by using the total internal energy graph. The models' internal energies are shown with red (modified) and green lines (existing).

As it is indicated on the graph among them maximum amount of kinetic energy is absorbed in case of modified model with value equal to 48 kN-mm of internal energy where as for the existing model remain with 44.6 kJ. This show that for the same condition, the modified model have the ability to absorb more kinetic energy with less deformation.

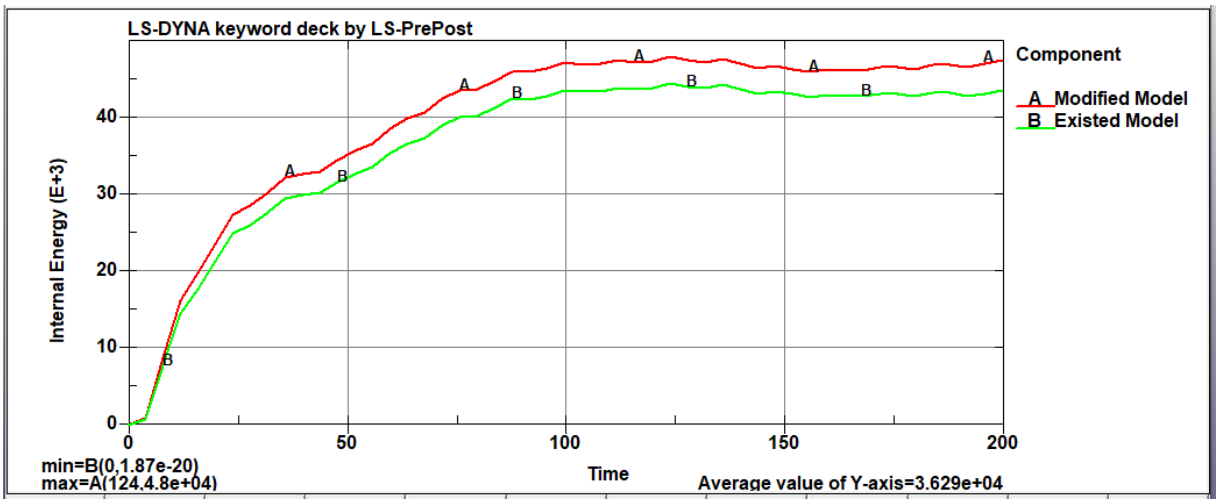

Figure 5.47. Energy absorbed of existing and modified model for Side Impact collision

Impact Force

The contact force between the BPV and the rigid pole for existing and modified model is shown in the Figure 5.48. The green line indicates existing model and the red one shows the modified model force of impact. From the figure below, the maximum impact force occurs at the existing model with value 281 KN whereas the force on the modified model is equal to 288 KN. so, their difference equals 7 KN this is due to the reinforcement that increase in thickness.

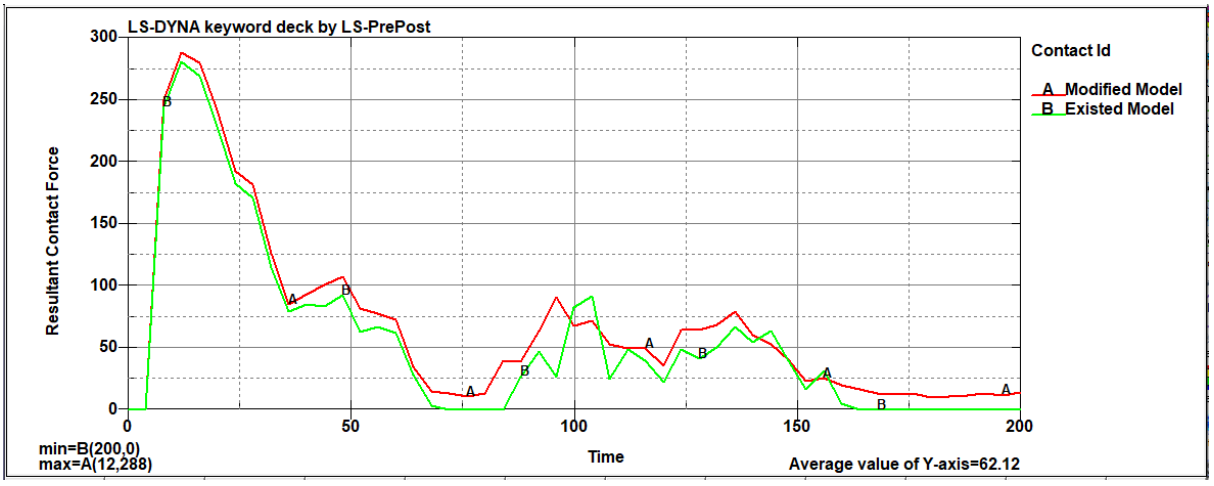

Figure 5.48. Impact force of existing and modified model for Side Impact

5.6 Results of Material Selection Simulation

Under this section the impact behavior of reinforcement under different materials are analyzed based on parameters like impact force, resultant displacement (deformation) and also energy absorption. On the above studies, there are many materials used for the chassis reinforcement, some of them are grey cast iron, AISI 4130 alloy steel, high strength Structural Steel and also aluminum foam. The results of the simulation are discussed below.

a. Total deformation

The deformation values are obtained by measuring the relative displacement from two nodes (one at the right or left end. With this measurement the value of deformation graph for different material of the reinforcement was shown in the Figure 5.50 below. From the Figure shown, the deformation values for AISI 4130 alloy steel, Aluminum foam, grey cast iron, High strength Structural Steel are 64mm, 106mm, 92.9mm and 91.3mm respectively. So, the maximum deformation of the reinforcement is registered on the aluminum foam. This does mean that the material with high deformation is always better because more deformation means that there is probability of more energy is absorbed.

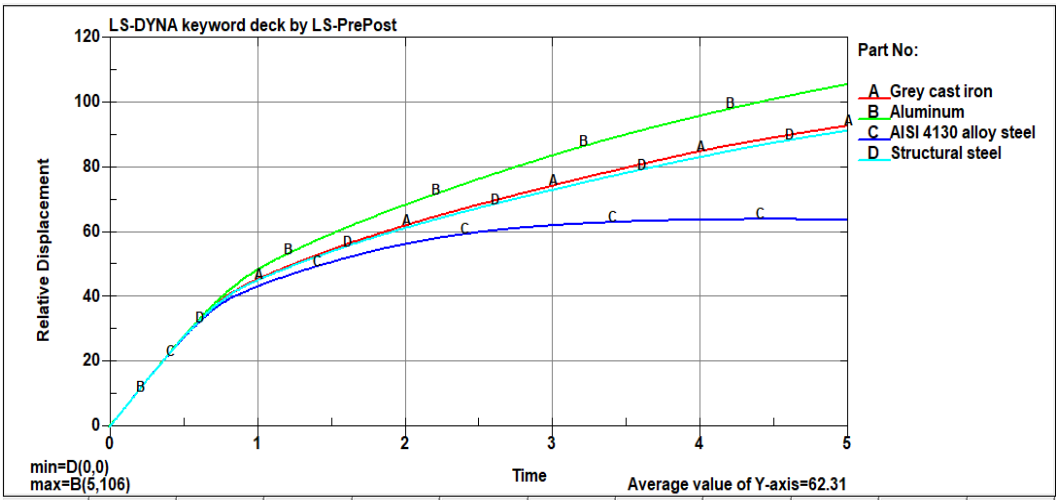

Figure 5.49. Deformation graph for different material of the reinforcement at frontal impact collision

b. Impact Force

The fluctuation effect observed on the graph shown the compression and elongation effects occurs between the measuring nodal points of the reinforcement. From the deformation it can also concluded that the energy absorbed by reinforcement increases with more deformation and decreases with les deformation as shown in Figure 5.51.

The graph reveals that, the impact force for AISI 4130 alloy steel, Aluminum foam, grey cast iron and High strength Structural Steel is 26kN, 10.6kN, 17.8kN, 26kN. The minimum impact force (10.6kN) on Aluminum foam.

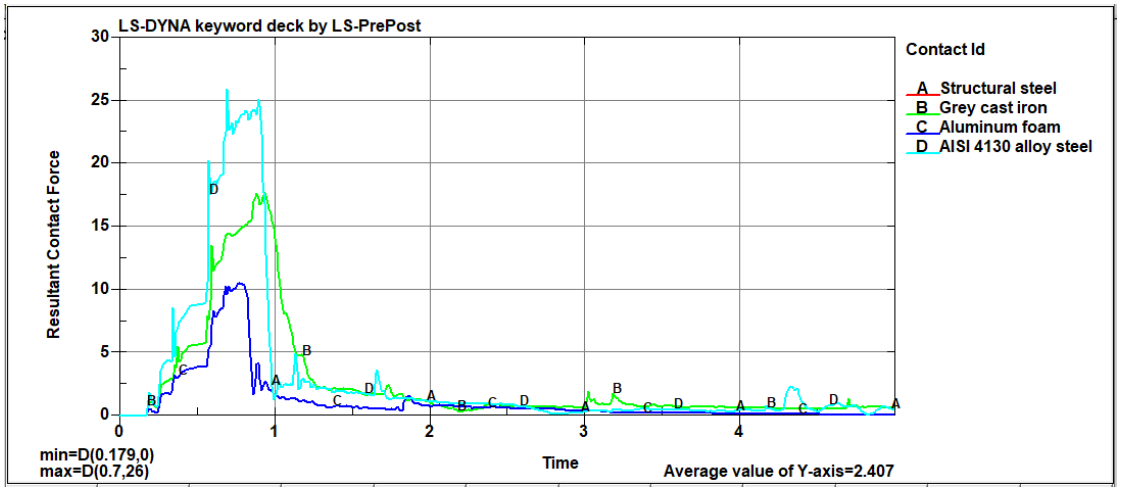

Figure 5.50. Impact force for different material of the reinforcement at frontal impact collision

c. Internal energy

As discussed on the graph, the more deformation of the reinforcement leads to more absorption of energy during the collision. The internal energy for AISI 4130 alloy steel, Aluminum foam, grey cast iron and High strength Structural Steel is 128 N-mm, 375 N-mm, 354 N-mm and 354 N-mm. The maximum amount of energy absorbed by the reinforcement is 375 N-mm which is Aluminum foam as shown in the Figure 5.52.

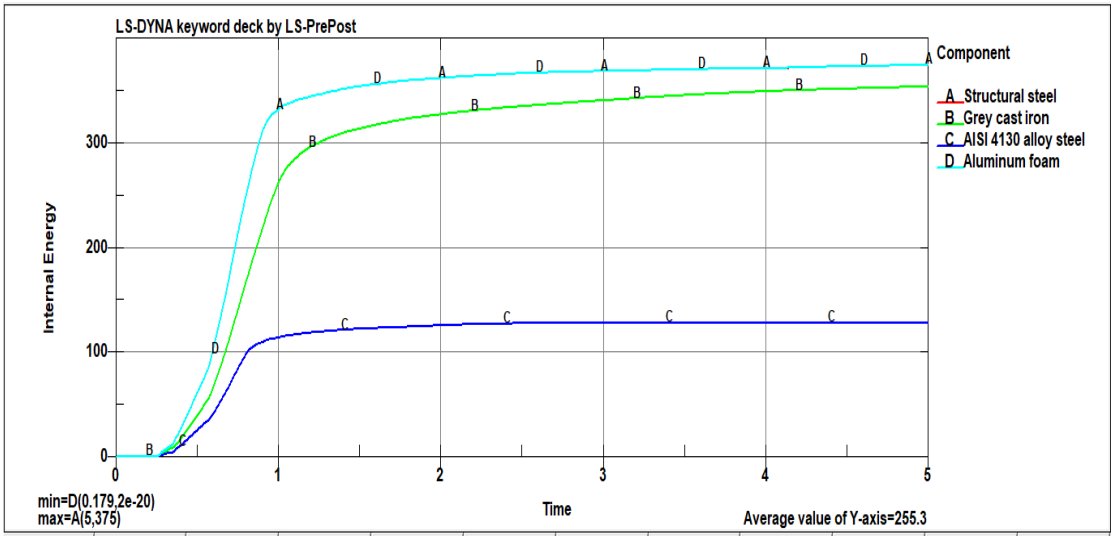

Figure 5.51. Internal energy for different material of the reinforcement at frontal impact collision

Generally looking at the above results it can conclude that the decrease in deformation results in high impact energy, low energy absorption and vice-versa. As this is reinforcement, the material with high energy absorber will increase the performance of chassis during collision. So, Aluminum foam material is selected for the full chassis reinforcement simulation in order to get low impact force with good energy absorption.

d. Structural response for the materials during side crash

The result of the simulation where the test material moving with velocity of 40 mph will collide with rigid pole which is stationary in opposite side of the reinforcement and is discussed. Figure 5.53 shows the event and response of the materials throughout the simulation time.

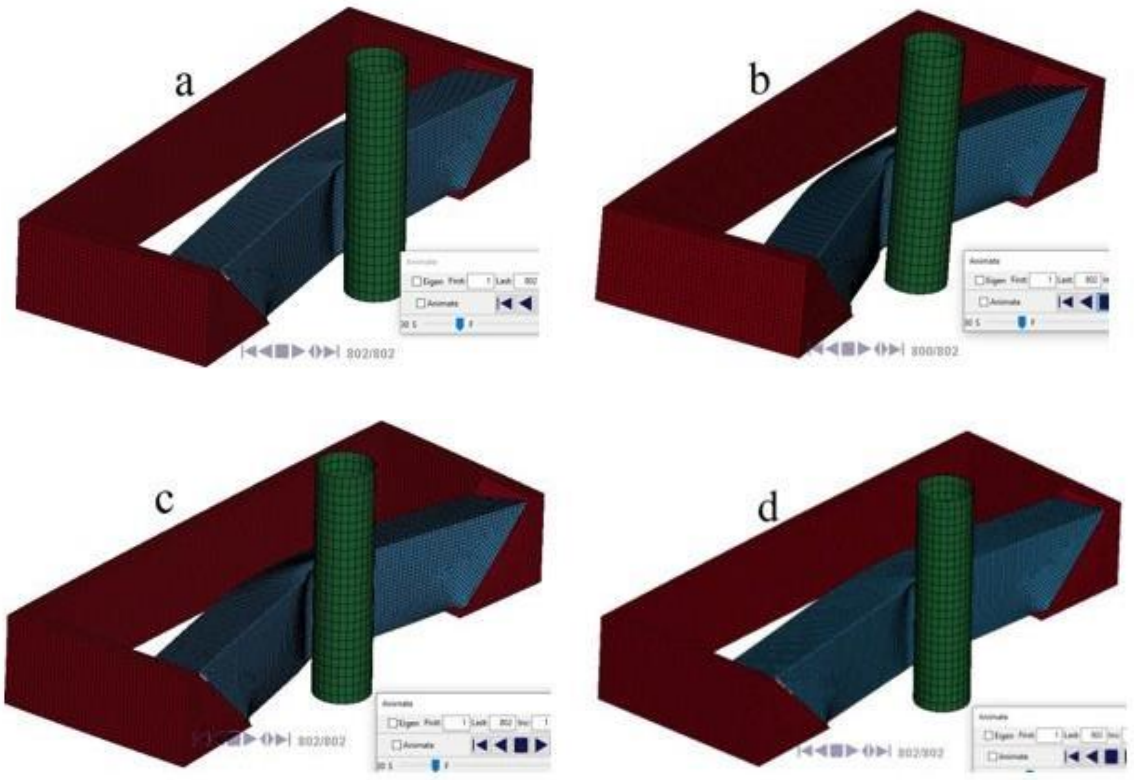

Figure 5.52. Structural response of (a) AISI 4130 alloy steel (b) Aluminum foam (c) Grey cast iron (d) High strength Structural Steel (LS DYNA)

e. Total deformation

The deformation values are obtained by measuring the relative displacement from two nodes (one at the right or left end. With this measurement the value of deformation graph for different material of the reinforcement was shown in the Figure 5.54 below. From the Figure shown, the deformation values for AISI 4130 alloy steel, Aluminum foam, grey cast iron, High strength Structural Steel are 20.5mm, 36.9mm, 33.1mm and 21.4mm respectively. So, the maximum

deformation of the reinforcement is registered on the aluminum foam. This does mean that the material with high deformation is always better because more deformation means that there is probability of more energy is absorbed.

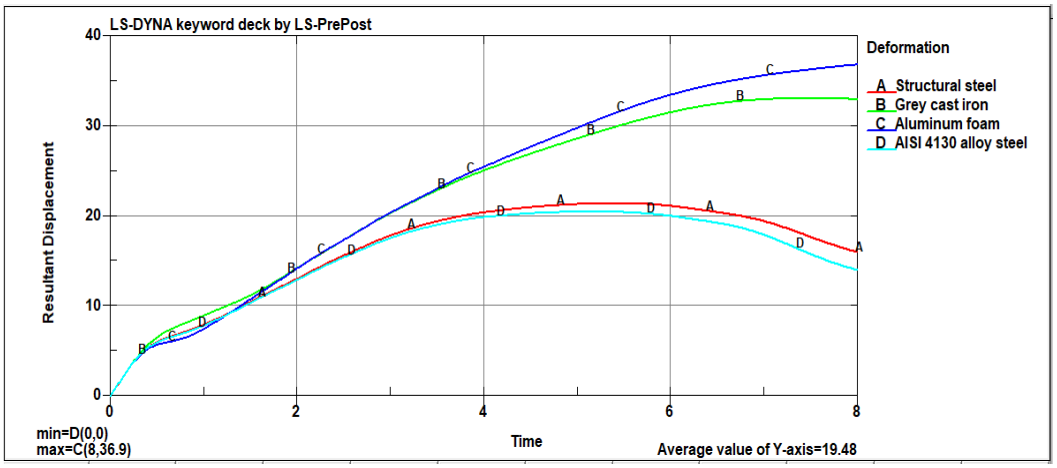

Figure 5.53. Deformation graph for different material of the reinforcement for side impact collision

f. Structural response for the materials during frontal crash

The result of the simulation where the test material moving with velocity of 40 mph will collide with rigid pole which is stationary in opposite side of the reinforcement and is discussed. Figure 5.49 shows the event and response of the materials throughout the simulation time.

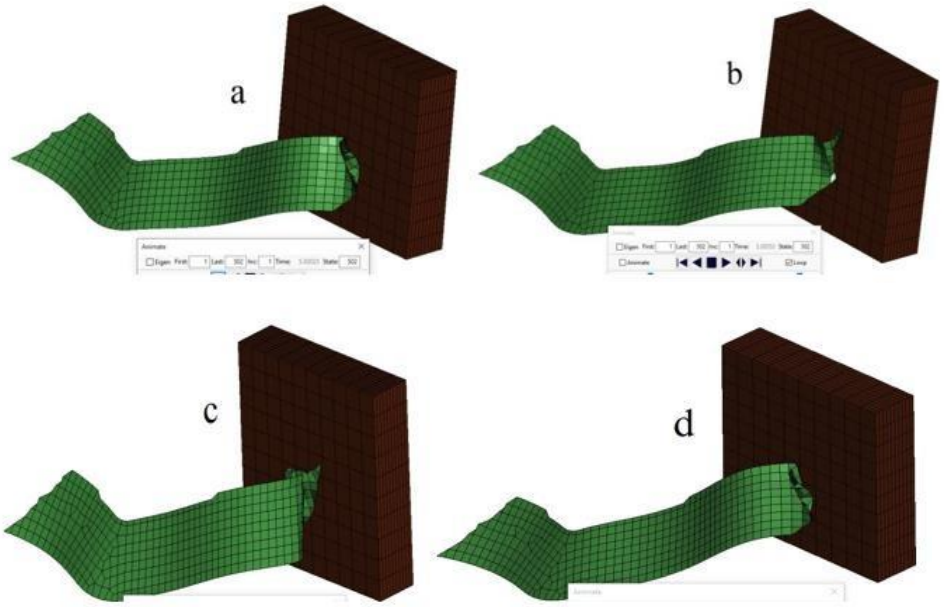

Figure 5.54. Structural response of (a) AISI 4130 alloy steel (b) Aluminum foam (c) Grey cast iron (d) High strength Structural Steel frontal impact collision (LS DYNA)

g. Impact Force

The fluctuation effect observed on the graph shown the compression and elongation effects occurs between the measuring nodal points of the reinforcement. From the deformation it can also concluded that the energy absorbed by reinforcement increases with more deformation and decreases with les deformation. In another word the more deformed material will register less impact force with the same thickness as shown in Figure 5.55 The graph reveals that, the impact force for AISI 4130 alloy steel, Aluminum foam, grey cast iron and High strength Structural Steel is 207kN, 68.2kN, 166kN, 209kN. The maximum impact force (209 kN) occurs with High strength Structural Steel and the minimum (68.2kN) on Aluminum foam. This behavior is obvious as the momentum increases with increase in impact force of the reinforcement.

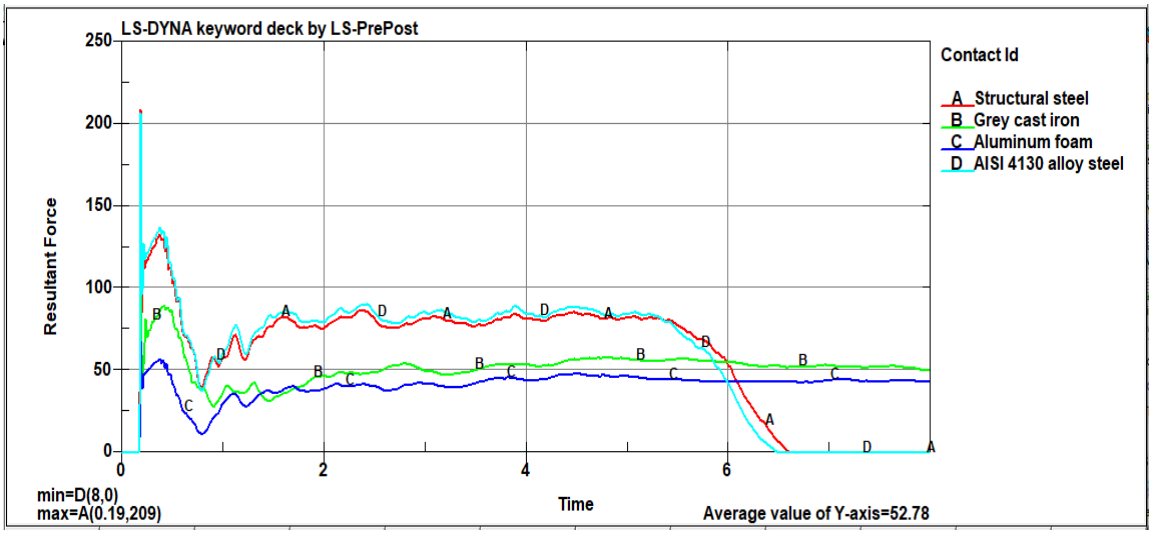

Figure 5.55. Impact force for different material of the reinforcement at side impact collision

h. Internal energy

As discussed on the graph, the more deformation of the reinforcement leads to more absorption of energy during the collision. The internal energy for AISI 4130 alloy steel, Aluminum foam, grey cast iron and High strength Structural Steel is 2.99kN-mm, 3.11kN-mm, 3.03kN-mm and 3.02kN-mm. The maximum amount of energy absorbed by the reinforcement is 3.11 KN-mm which is Aluminum foam as shown in the Figure 5.56.

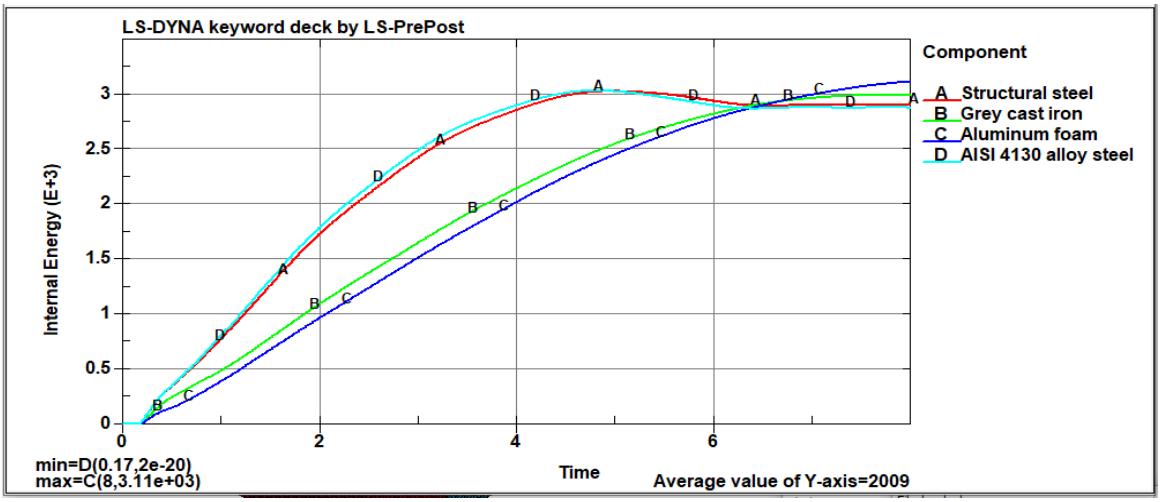

Figure 5.56. Internal energy for different material of the reinforcement at side impact collision

Generally looking at the above results it can conclude that the decrease in deformation results in high impact energy, low energy absorption and vice-versa. As this is reinforcement, the material with high energy absorber will increase the performance of chassis during collision. So, Aluminum foam material is selected for the full chassis reinforcement simulation in order to get low impact force with good energy absorption.

CHAPTER SIX
CONCLUSIONS AND RECOMMENDATIONS

6.1 Conclusion

This study uses numerical methods to facilitate a Bishoftu pickup chassis structure's frontal and side dynamic analysis (LS-DYNA R11). Moreover, this research also develops an alternative design solution of reinforcement design with numerical optimization for all FE analyses. Furthermore, the preferable welding types on the original structural connections via dynamic simulation.

The main output parameters include total deformation, energy absorption, impact force and structural response estimates in the dynamic strength analysis according to the frontal and side collision cases. Moreover, the shell thickness as a design parameter (variable) is defined in optimization tasks to reduce the structure's weight within better stiffed and also, during reinforcement design, the design cross-section and layout of the frame with the addition of reinforcement are considered as design inputs for baseline structure. Consequently, the dynamic strength analysis and optimization obtained results can be summarized as follows.

The modified model shows better protection by deforming less as compared to the existing model during frontal collision, it gives protection to the occupant compartment after collision.

- ✓ Among the initial kinetic energy, 102.2 kN-mm of kinetic energy which is 60.8 % is lost in the existing model where as for the modified model, the loss of kinetic energy is 124.3 kN-mm which is 74 % of the total energy or the initial kinetic energy during frontal collision.
- ✓ The total deformation by the existing is 56.1 mm and modified model is 40.5 mm. As it can be seen the maximum amount of deformation is occurred during the Existed model. This is due to the reinforced material properties used for the modification, as a result these may deformed less. Their difference in deformation is 15.6 mm (27.8 % improvement in deformation).
- ✓ The total energy absorbed by the modified model is more as compared to the existing model. This is due to the reinforced material properties used for the modification, as a result these may deformed less and produces more absorption. Their difference in absorption is 21.8 kN-mm (19.5 % improvement in energy absorption).

- ✓ The force of impact for the Existing model is better. The maximum impact force occur on the existing model is equal to 549 kN, whereas the modified produced 770 kN, the difference is 221 KN this is due to the reinforcement which increases the overall thickness of the chassis.

6.2 Recommendations

Based on the studies done on this thesis work the following points are recommended.

- ✓ It can be observed that with little modification the safety of the current chassis can be improved, so that the owners and manufacturers shall implement some of the safety developments concepts discussed on this thesis work to improve the crash worthiness.
- ✓ As the study shows even with average speed the chassis has causing more sever damages, so it is better if the government and concerning bodies implement the crash and safety regulation and also quality evaluation for pickups which are play avital role on the economy of our country.

6.3 Recommendations for Future Work

Considering the review of the existing research limitations and results the motivations for future research are suggested as follows.

- ✓ The present work evaluated the crash behavior of existing Bishoftu pickup chassis by considering the response of the structure and this work can be extended to evaluating the response of other major parts that are exposed to collision.
- ✓ This work does not include rear impact. So, it does not include the effect on rear parts of the chassis, so it can be studied in the future

REFERENCES

A. Mamalis, D. Manolakos, G. Demosthenous and M. Ioannidis (1998). *Crashworthiness of Composite Thin-Walled Structural Components*. Boca Raton. CRC Press LLC. Advances in Mechanical Engineering, 10(5), 1–12. https.//doi.org/10.1177/168 7814018778480

Aluminum Foam, Properties and applications Materials Hub. (2022). https.//www.materialshub.com/material/aluminium-foam/

Babu, T., Praveen, D., & Venkateswarao, M. (2012). *Crash analysis of car chassis frame using finite element method*. International Journal of Engineering Research & Technology, 1(8), 1-8.

B. O'Neill (2009). *Preventing passenger vehicle occupant injuries by vehicle design a historical perspective from IIHS.* Traffic Injury Prevent 10.113–126

D. Liao, J. Wang, X. Zuo and H. Feng (2006). *Application of Finite Element Analysis of Heavy Vehicle Frames*. Vehicle & Power Technology, no. 2, pp. 63-74

E. Joseph (2021). *Improving the crashworthiness of space frame-based vehicles using composites*. The Plymouth Student Scientist, 14, (1), 310-340

Georgiou, G., & Zeguer, T. (2018). *On the assessment of the macro-element methodology for full vehicle crashworthiness analysis*. International Journal of Crashworthiness, 23(3), 336–353. https.//doi.org/10.1080/13588265.2017.1328723

Gashu, A., & Nallamothu, R. B. (2022). *Analysis of crashworthiness of Bishoftu pickup vehicle structure during side Pole crash*. Journal of Engineering, 2022(1), 8386877.

Gulavani, O., Hughes, K., & Vignjevic, R. (2014). *Explicit dynamic formulation to demonstrate compliance against quasi-static aircraft seat certification loads (CS25.561) -Part I. Influence of time and mass scaling.* Proceedings of the Institution of Mechanical Engineers, Part G. Journal of Aerospace Engineering, 228(11), 1982–1995. https.//doi.org/10.1177/0954410013506333

Hershman, L. L. (2001). The US new car assessment program (NCAP). Past, present and future.

H. Basavaraju (2005). *Design and Analysis of a Composite Beam for Side Impact*. December

H. Jeong and B. Han (2011). *A study on the body structure crashworthiness for small overlap crash*. KSAE Annual Conf. Proc., Korean Society of Automotive Engineers, no. 6, pp. 2032–2038

H. Ren, L. Zhong and Y. Wang (2005). *Finite element analysis of HFC6100KY Pickup Truck chassis frame*. Journal of Hefei, no. 8, pp. 34-45

J. Fang, G. Sun, N. Qiu, H. Kim and Q. Li (2017). *On design optimization for structural crashworthiness and its state of the art*. Springer, DOI 10.1007/s00158-016-1579

J. Marsolek, H. Reimerdes (2004). *Energy absorption of metallic cylindrical shells with induced non-axisymmetric folding patterns*. International Journal Impact Eng. 30.1209–1223

K. Daniel, C. Kumar, P. Babu and J. Kumar (2018). *Design & Analysis of Ladder Frame I Section Chassis*. International Journal for Research in Applied Science & Engineering Technology, ISSN. 2321-9653, Volume. 6, Issue. IV

K. Bradsher (2002). *High and Mighty. SUVs the World's Most Dangerous Vehicles*. Public Affairs, New York

Kotari, S., & Gopinath, V. (2012). *Static and dynamic analysis on tatra chassis*. International Journal of Modern Engineering Research (IJMER), 2(1), 086-094.)

Koora, R., Suman, R., & Quadri, S. A. P. (2016). *Design Optimization of Crush Beams of SUV Chassis for Crashworthiness*. International. Journal of Science and Research, 5.

Kunle, M. A., Farah, M. J., Ahmed, A. Hakim, & Mohamed. (2019). *Auto Rickshaw Impacts with Pedestrians - A Computational Analysis of Post- Collision Kinematics and Injury Mechanics*. A Thesis Submitted to Cardiff University for the Degree of Doctor of Philosophy By. September.

Livermore Software Technology Corporation. (2003). *LS-DYNA User's Manual*, Version 970. Vol. I (Issue May).

M. Ossiander, D. Koepsell and B. McKnight (2014). *Crash fatality risk and unibody versus body on frame structure in SUVs*. Accident Analysis and Prevention 70 (2014) 267–272

Patil, S. B., & Joshi, D. G. (2015). *Structural Analysis of Chassis. A Review*. International Journal of Research in Engineering and Technology, 4(4), 293-295.

Prakash, V. R. (2009). *Assessing the structural crashworthiness of a three-wheeler passenger vehicle*. In ICORD 09. Proceedings of the 2nd International Conference on Research into Design, Bangalore, India 07.-09.01. 2009 (pp. 152-159).

P. Babu and V. Narasimha (2016). *Design and Analysis of Automobile Frame*. International Journal of Scientific Engineering and Technology Research, ISSN 2319-8885, Vol.05, Issue. 51

P. Baskar, P. Gandhi, A. Kulkarni and S. Gauri (2014). *Finite Element Analysis of Fire Truck Chassis for Steel and Carbon Fiber Materials.* Journal of Engineering Research and Applications, No.4, pp.69-74.

Predictive Engineering Goods Consumer (2020). *The Advanced Simulation Tool for Nonlinear, Linear, Dynamic, and Static Analysis LS-DYNA*. 1–16

R. Joseph and M. Kamoji (2015). *Crash Analysis for Energy Absorption of Frontal Rails of a Passenger Car*. International Research Journal of Engineering and Technology, Volume. 02 Issue. 03

S. Grzegorz, N. Paulina et al. (2014). *Some basic tips in vehicle chassis and frame design*. Journal of Measurements in Engineering, no. 2, pp. 208-214

The Aluminum Automotive Manual (2013). *Car body structures*. European Aluminum Association

Vijayakumar, M. D., Kannan, C. R., Manivannan, S., Vairamuthu, J., Tilahun, S., & Ram, P. B. (2020, December). *Finite element analysis of automotive truck chassis.* In IOP Conference Series. Materials Science and Engineering (Vol. 988, No. 1, p. 012114). IOP Publishing.

Wang, Tao, Wang, L., Wang, C., & Zou, X. (2018). *Crashworthiness analysis and multi-objective optimization of a commercial vehicle frame. A mixed meta-modeling-based method.*

Wang, Tie, & Li, Y. (2015). *Design and analysis of automotive carbon fiber composite bumper beam based on finite element analysis*. Advances in Mechanical Engineering, 7(6), 1–12. https.//doi.org/10.1177/1687814015589561

X. Ma et al. (2002). *Application of FEM to the Inverse Design of the Body Structure.* Pickup Truck Technology and Research, no. 2, pp. 23-35

APPENDICES

Results on existing frontal impact

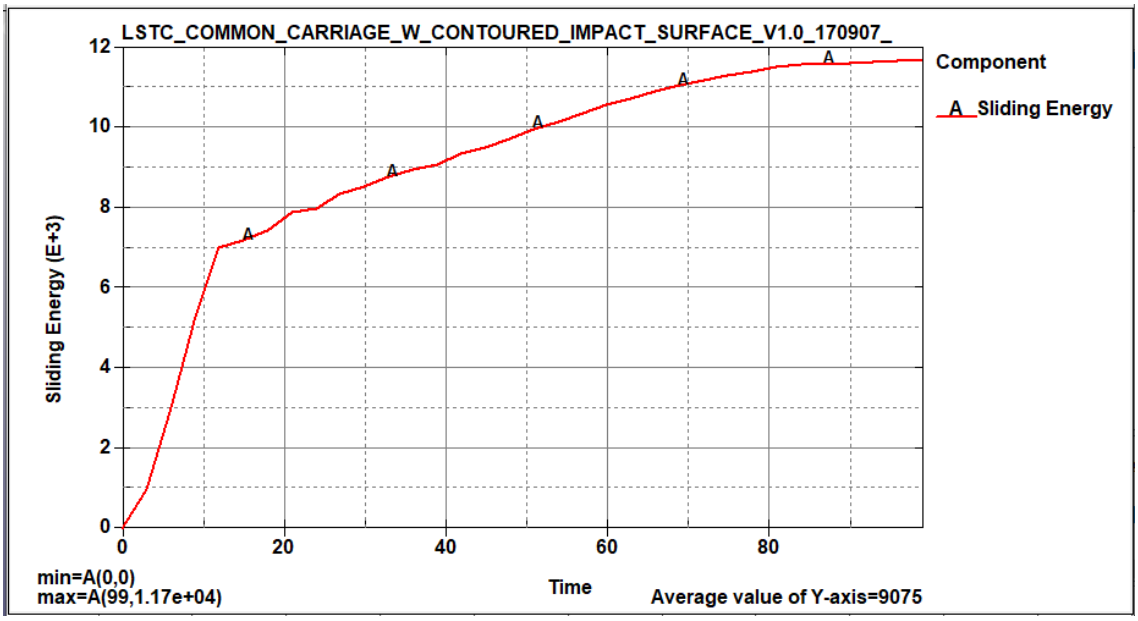

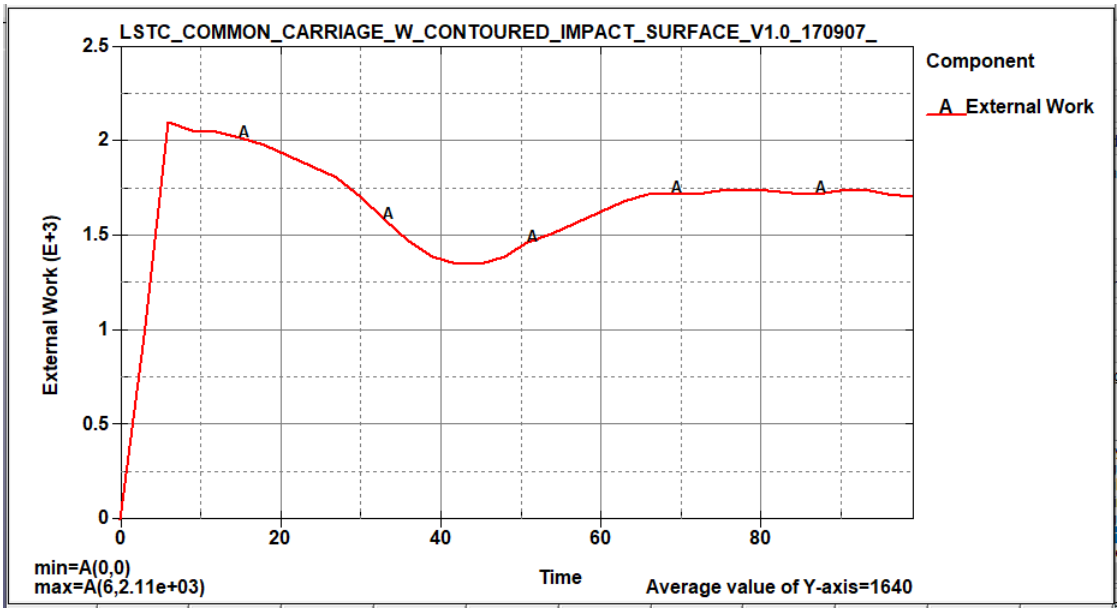

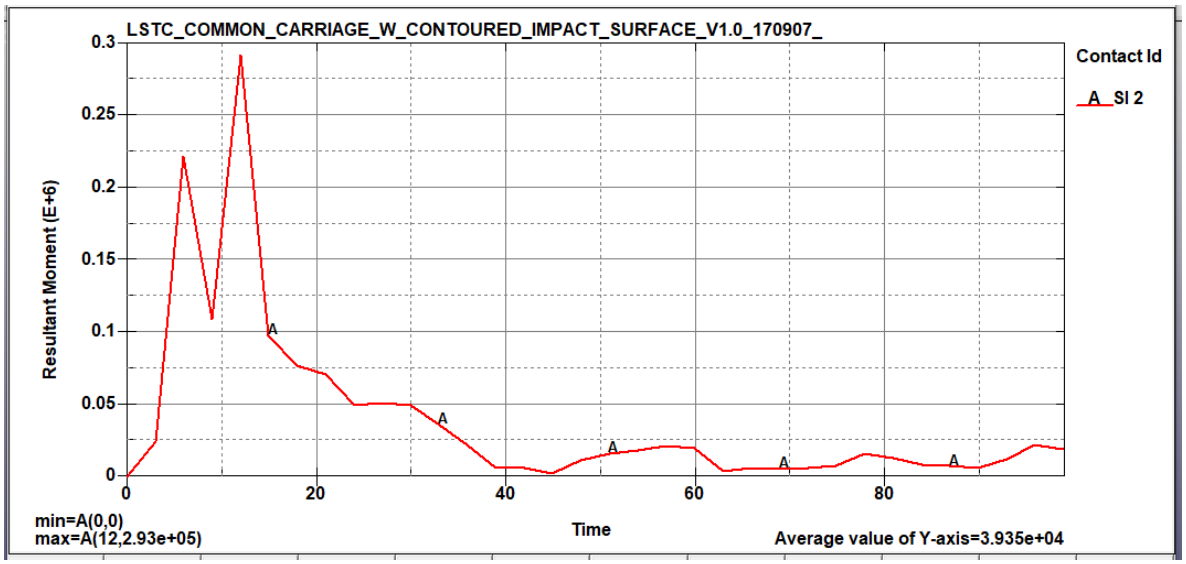
LSTC_COMMON_CARRIAGE_W_CONTOURED_IMPACT_SURFACE_V1.0_170907_
Contact Id
A SI 2
Resultant Moment (E+6)
0.3
0.25
0.2
0.15
0.1
0.05
0
0
20
40
60
80
Time
min=A(0,0)
max=A(12,2.93e+05)
Average value of Y-axis=3.935e+04

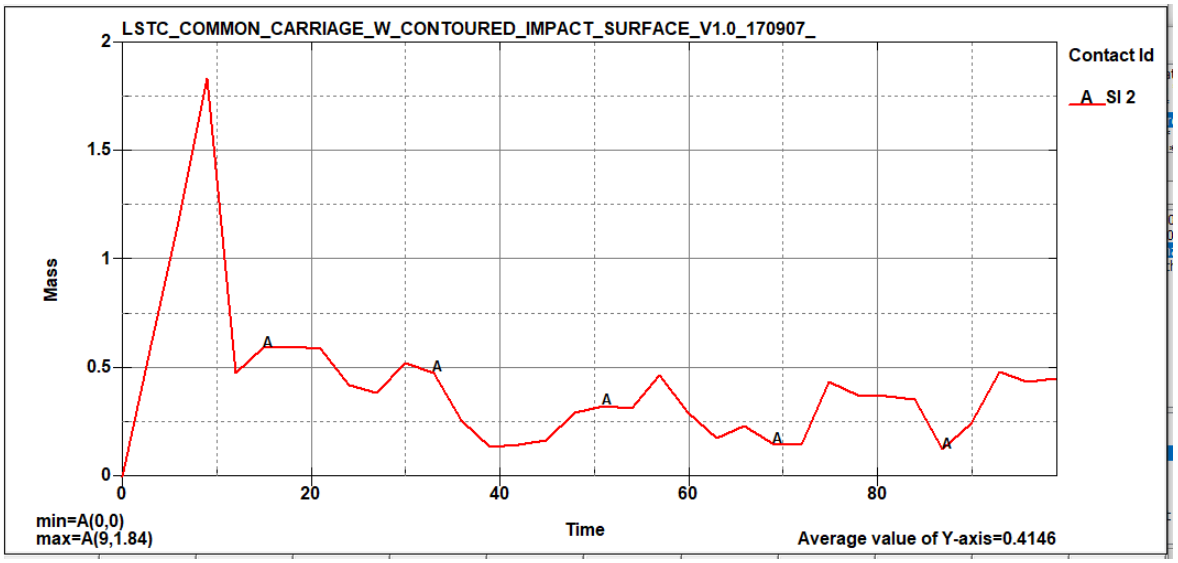
LSTC_COMMON_CARRIAGE_W_CONTOURED_IMPACT_SURFACE_V1.0_170907_
Contact Id
A SI 2
Mass
2
1.5
1
0.5
0
0
20
40
60
80
Time
min=A(0,0)
max=A(9,1.84)
Average value of Y-axis=0.4146

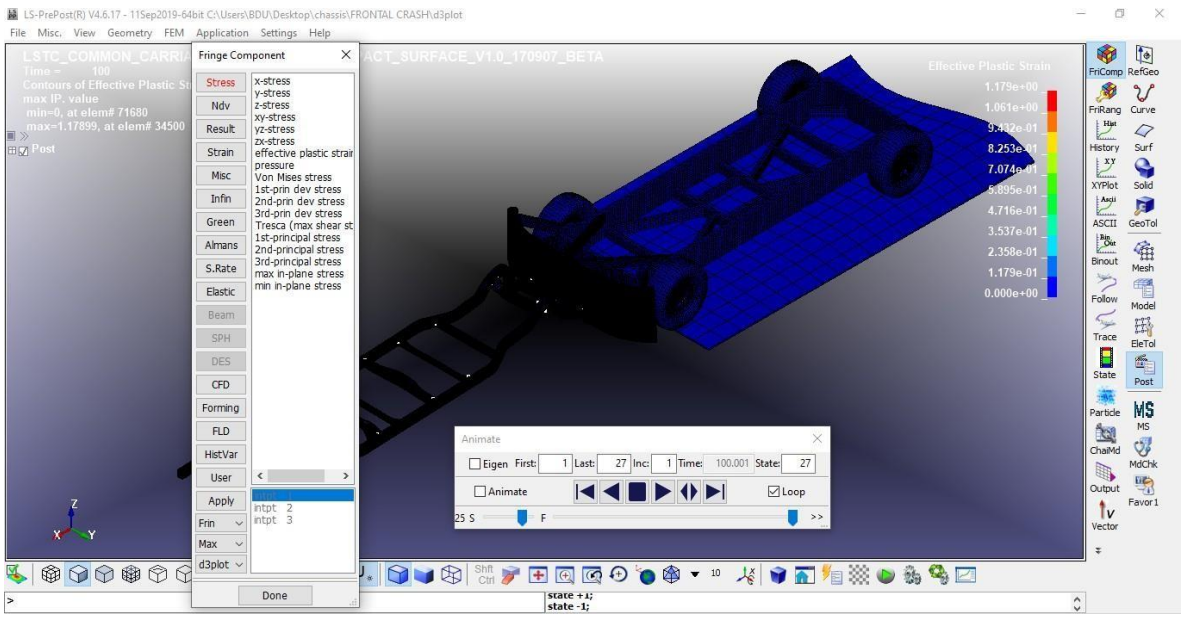
Fringe Component
Stress
Ndv
Result
Strain
Misc
Infin
Green
Almans
S.Rate
Elastic
Beam
SPH
DES
CFD
Forming
FLD
HistVar
User
Apply
Frin
Max
d3plot
Done
Animate
Eigen
Animate
Loop
Effective Plastic Strain

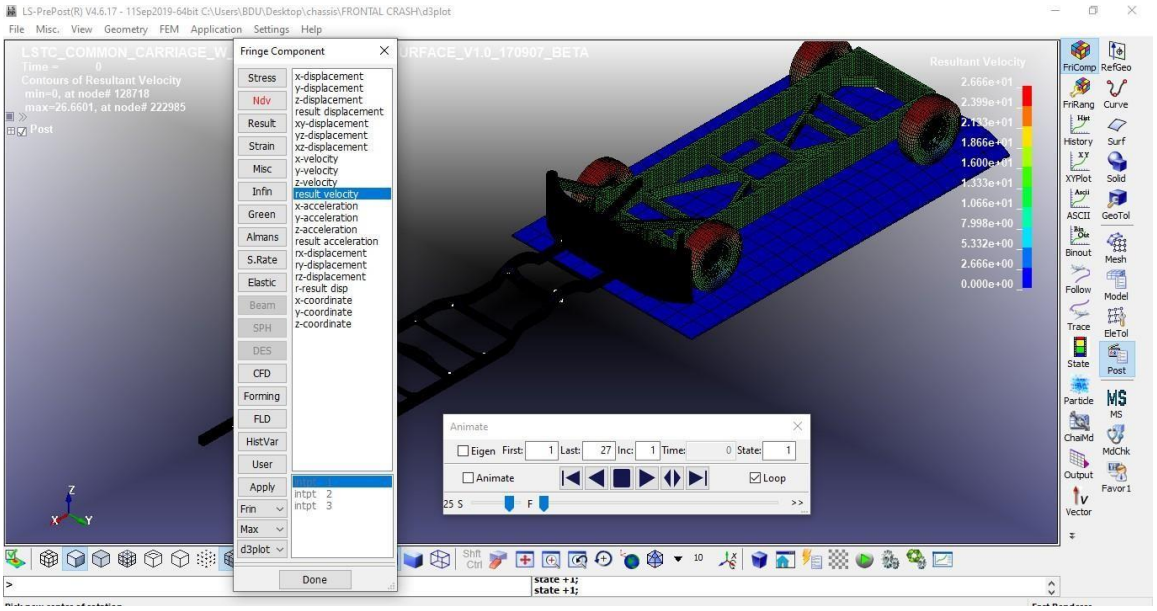

Results on existing side impact

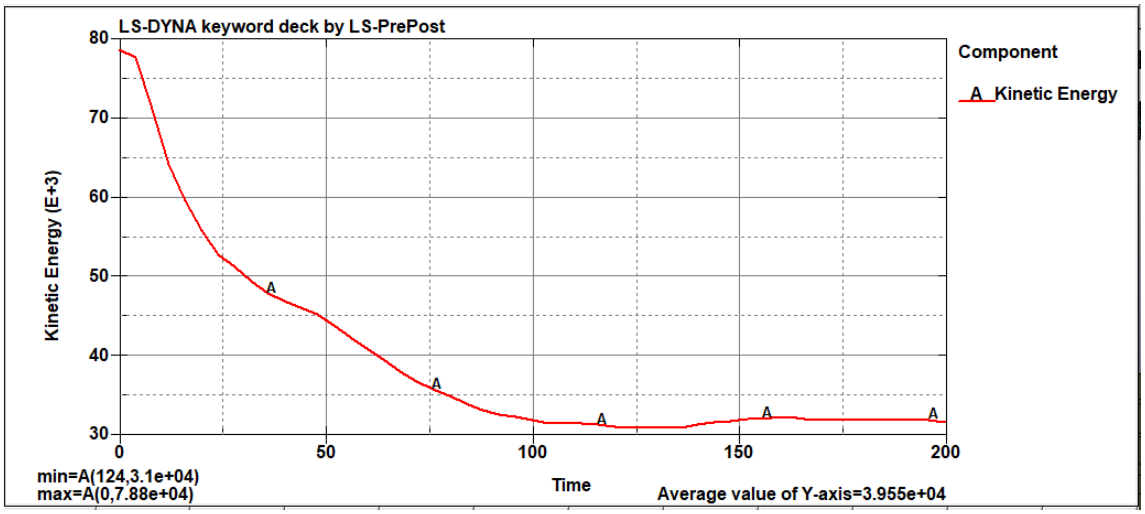

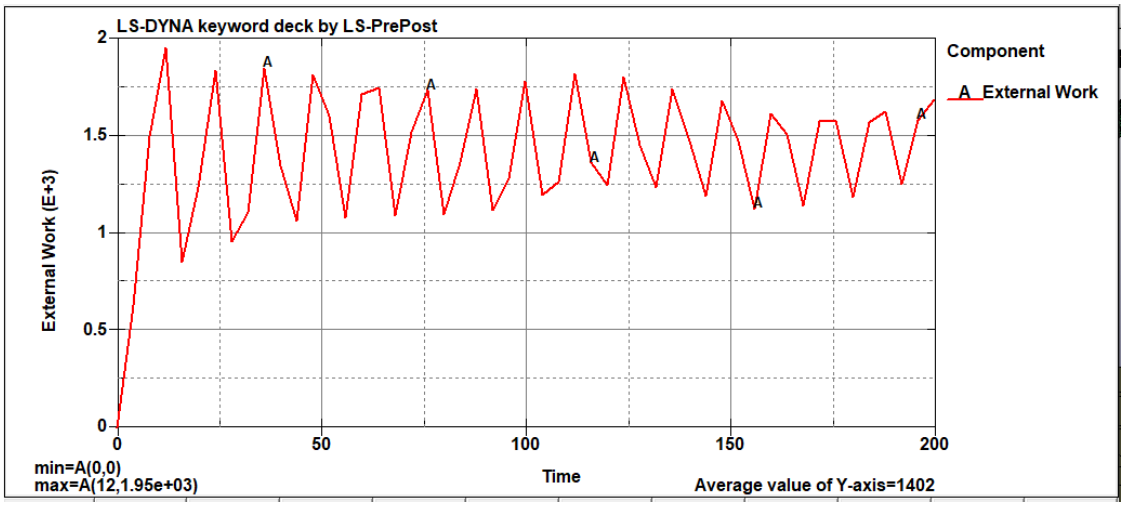

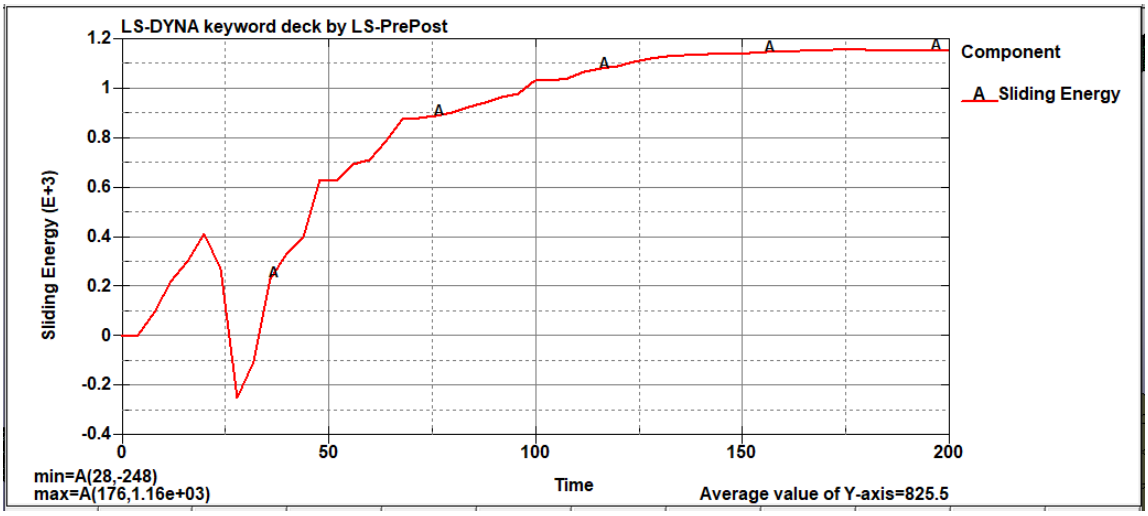
LS-DYNA keyword deck by LS-PrePost
Sliding Energy (E+3)
1.2
1
0.8
0.6
0.4
0.2
0
-0.2
-0.4
0
50
100
150
200
Time
Component
A Sliding Energy
min=A(28,-248)
max=A(176,1.16e+03)
Average value of Y-axis=825.5

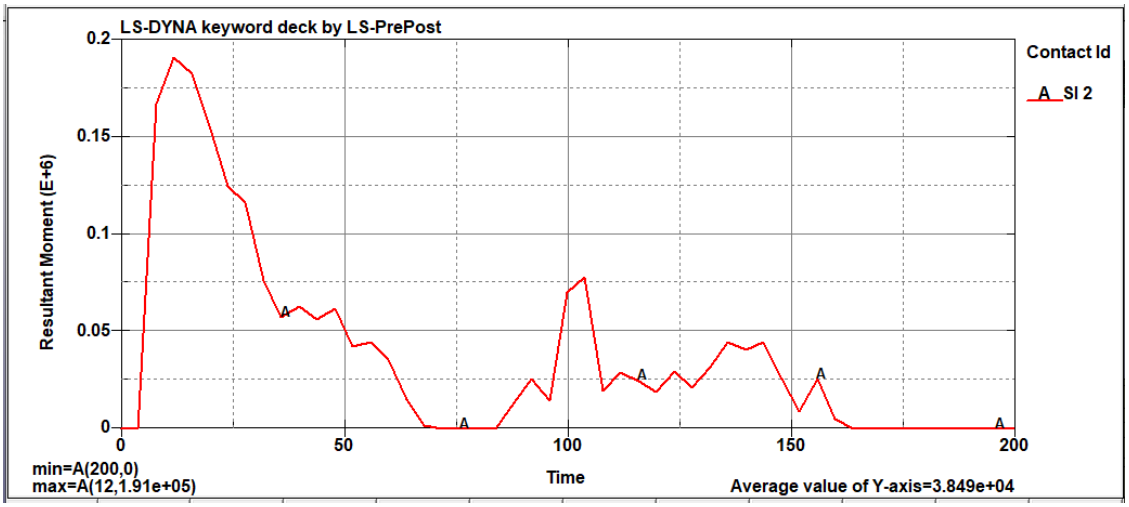
LS-DYNA keyword deck by LS-PrePost
Resultant Moment (E+6)
0.2
0.15
0.1
0.05
0
0
50
100
150
200
Time
Contact Id
A SI 2
min=A(200,0)
max=A(12,1.91e+05)
Average value of Y-axis=3.849e+04

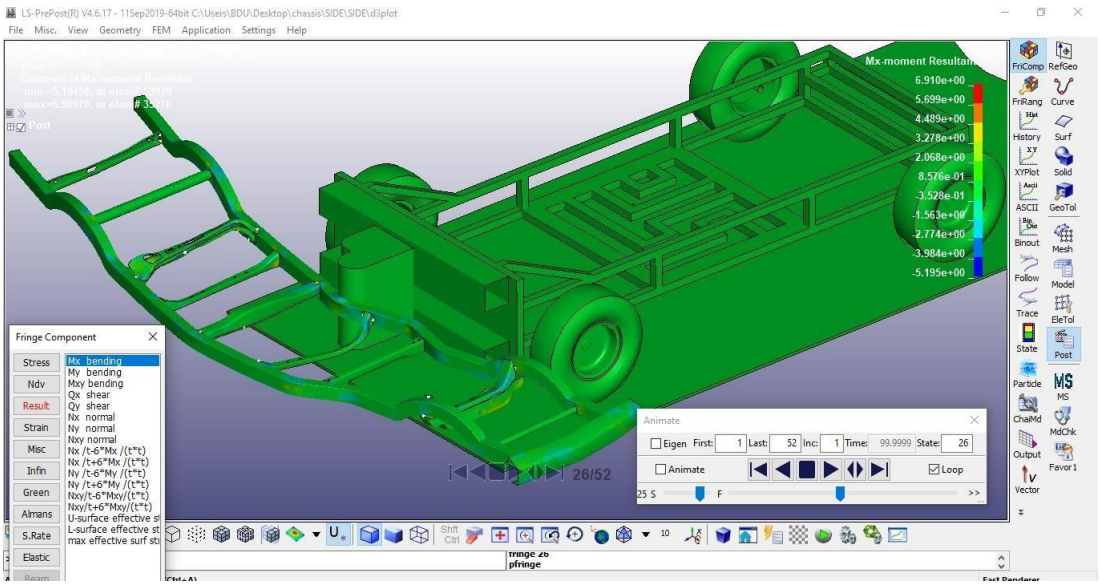
Mx-moment Resultant
6.910e+00
5.699e+00
4.489e+00
3.278e+00
2.068e+00
8.576e-01
-3.528e-01
-1.563e+00
-2.774e+00
-3.984e+00
-5.195e+00
Fringe Component
Stress
Ndv
Result
Strain
Misc
Infln
Green
Almans
S.Rate
Elastic
Mx bending
My bending
Mxy bending
Qx shear
Qy shear
Nx normal
Ny normal
Nxy normal
Animate
Eigen
Animate
Loop
26/52

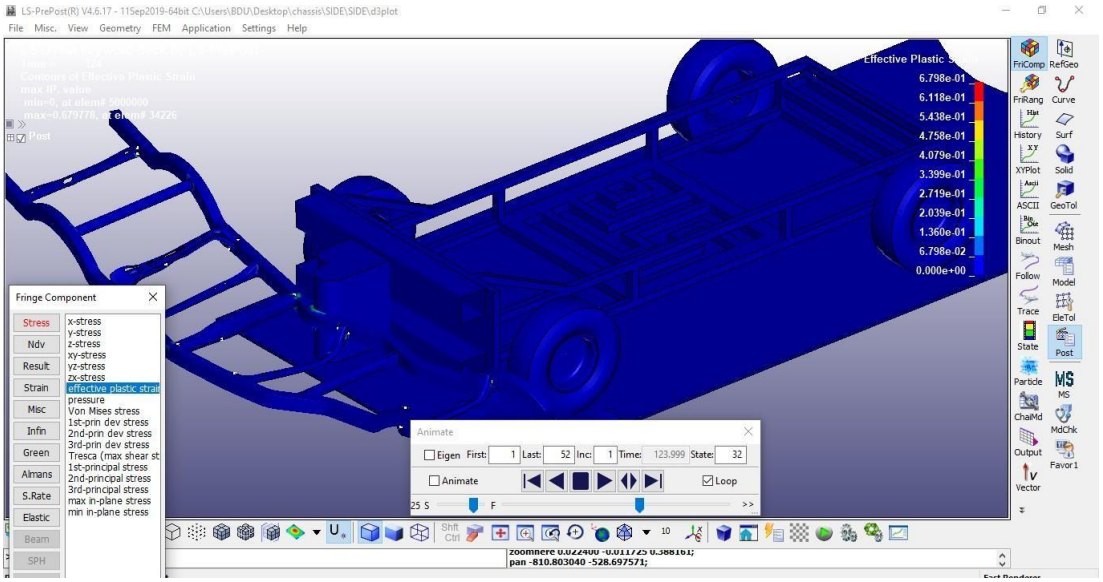
Effective Plastic S
6.798e-01
6.118e-01
5.438e-01
4.758e-01
4.079e-01
3.399e-01
2.719e-01
2.039e-01
1.360e-01
6.798e-02
0.000e+00
Fringe Component
Stress
Ndv
Result
Strain
Misc
Infin
Green
Almans
S.Rate
Elastic
Beam
SPH
x-stress
y-stress
z-stress
xy-stress
yz-stress
zx-stress
effective plastic strai
pressure
Von Mises stress
1st-prin dev stress
2nd-prin dev stress
3rd-prin dev stress
Tresca (max shear st
1st-principal stress
2nd-principal stress
3rd-principal stress
max in-plane stress
min in-plane stress
Animate
Eigen First: 1 Last: 52 Inc: 1 Time: 123.999 State: 32
Animate
Loop

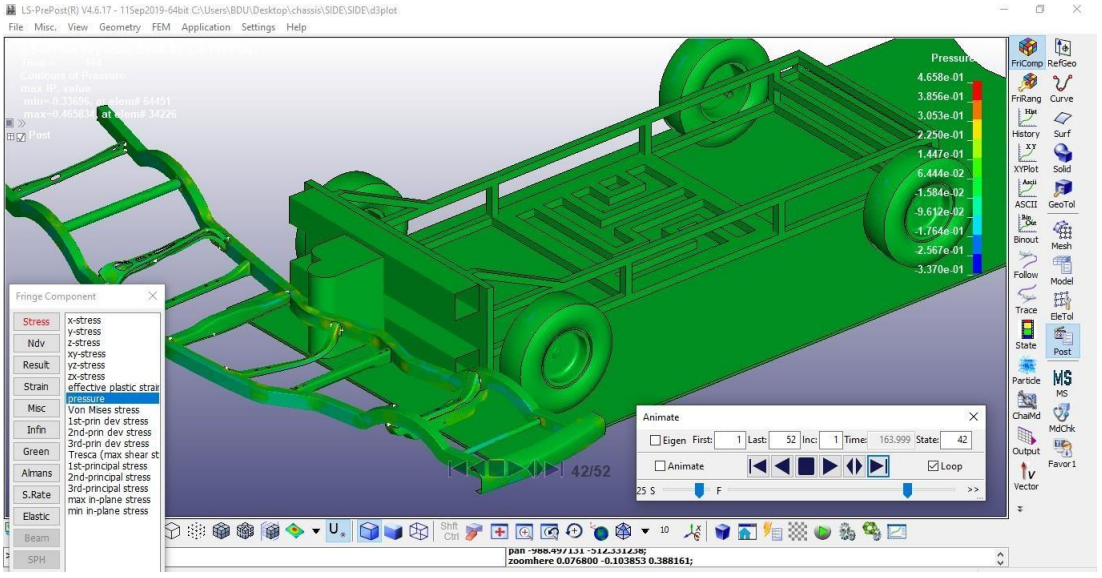
Pressure
4.658e-01
3.856e-01
3.053e-01
2.250e-01
1.447e-01
6.444e-02
-1.584e-02
-9.612e-02
-1.764e-01
-2.567e-01
-3.370e-01
Fringe Component
Stress
pressure
Animate
Eigen First: 1 Last: 52 Inc: 1 Time: 163.999 State: 42
Animate
Loop
42/52

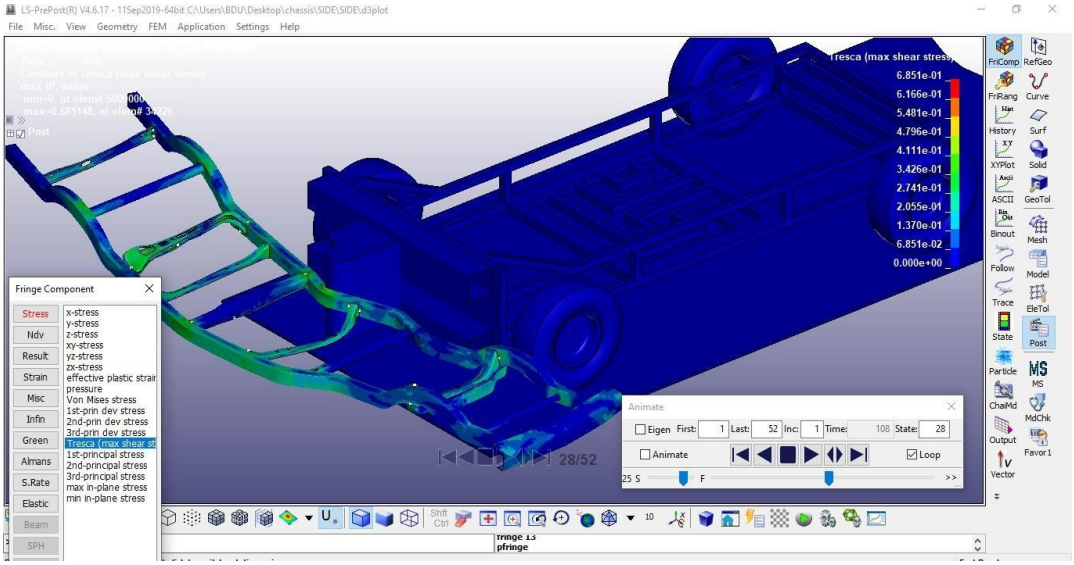
Tresca (max shear stress)
6.851e-01
6.166e-01
5.481e-01
4.796e-01
4.111e-01
3.426e-01
2.741e-01
2.055e-01
1.370e-01
6.851e-02
0.000e+00
Fringe Component
Stress
Tresca (max shear st
Animate
Eigen First: 1 Last: 52 Inc: 1 Time: 108 State: 28
Animate
Loop
28/52

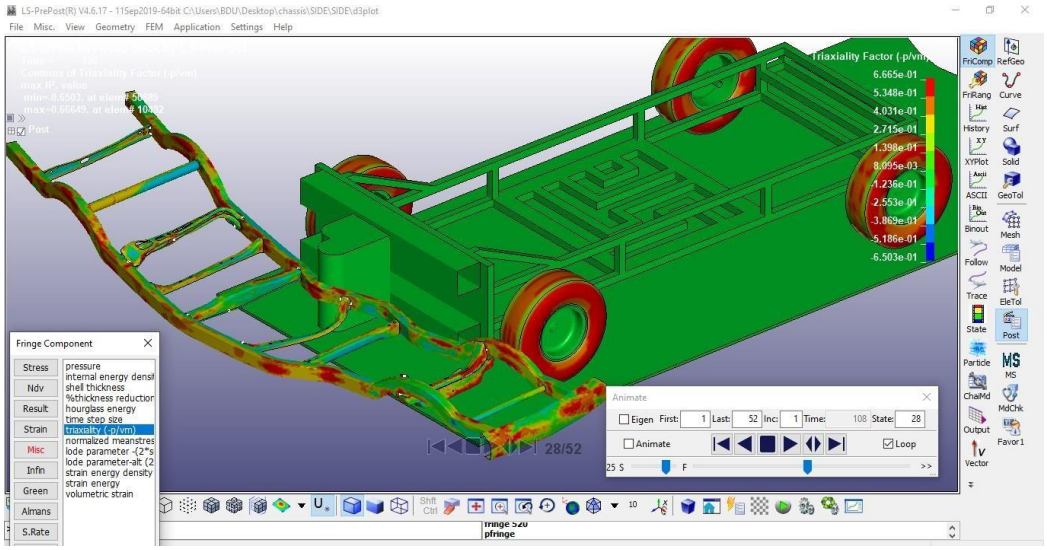

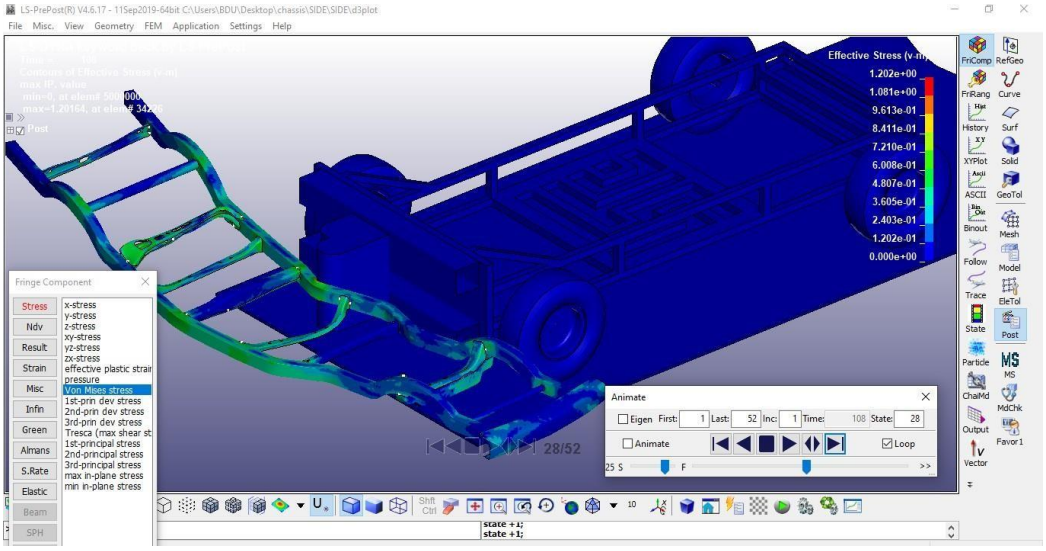

Results on modified frontal impact

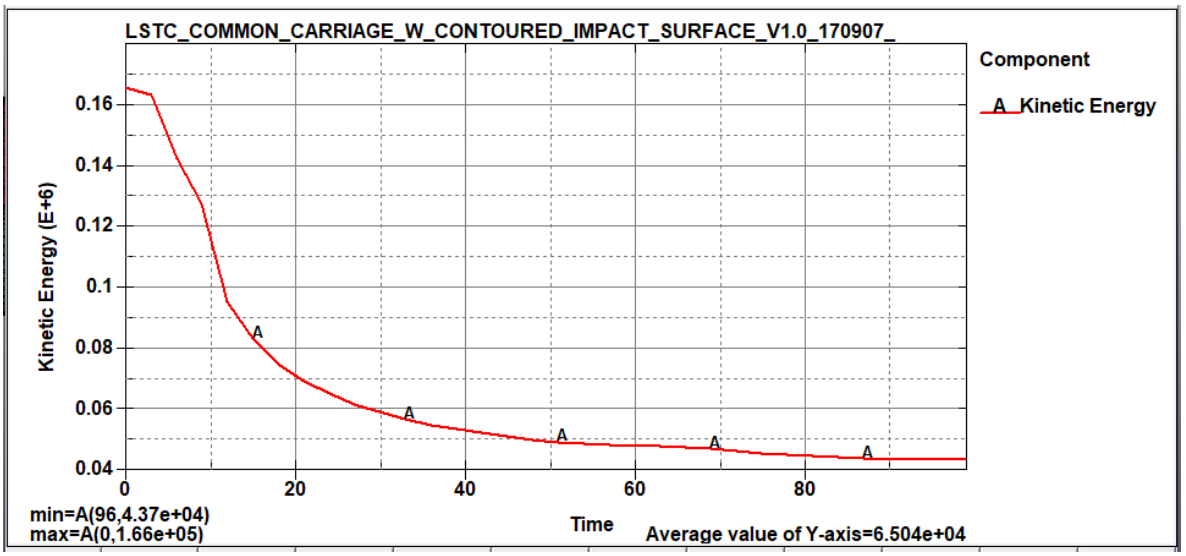

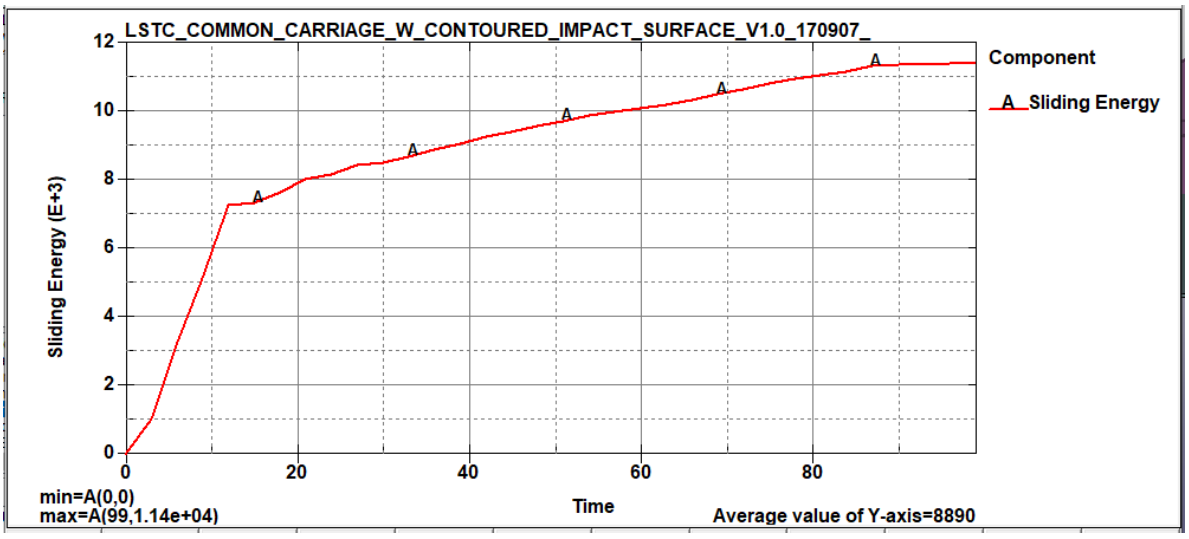
LSTC_COMMON_CARRIAGE_W_CONTOURED_IMPACT_SURFACE_V1.0_170907_
Component
A Sliding Energy
Sliding Energy (E+3)
Time
min=A(0,0)
max=A(99,1.14e+04)
Average value of Y-axis=8890

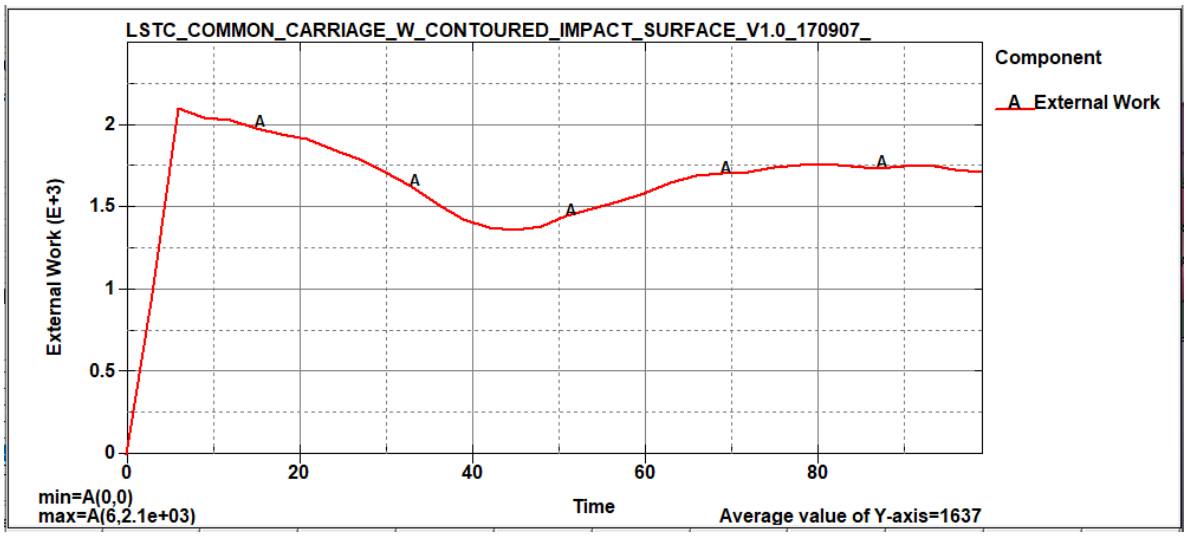
LSTC_COMMON_CARRIAGE_W_CONTOURED_IMPACT_SURFACE_V1.0_170907_
Component
A External Work
External Work (E+3)
Time
min=A(0,0)
max=A(6,2.1e+03)
Average value of Y-axis=1637

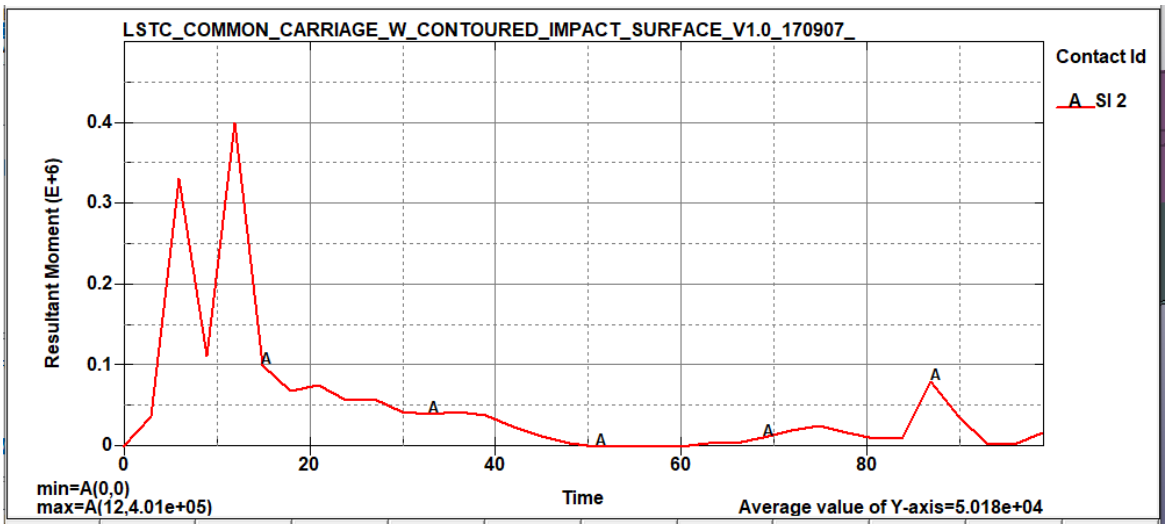
LSTC_COMMON_CARRIAGE_W_CONTOURED_IMPACT_SURFACE_V1.0_170907_
Contact Id
A SI 2
Resultant Moment (E+6)
Time
min=A(0,0)
max=A(12,4.01e+05)
Average value of Y-axis=5.018e+04

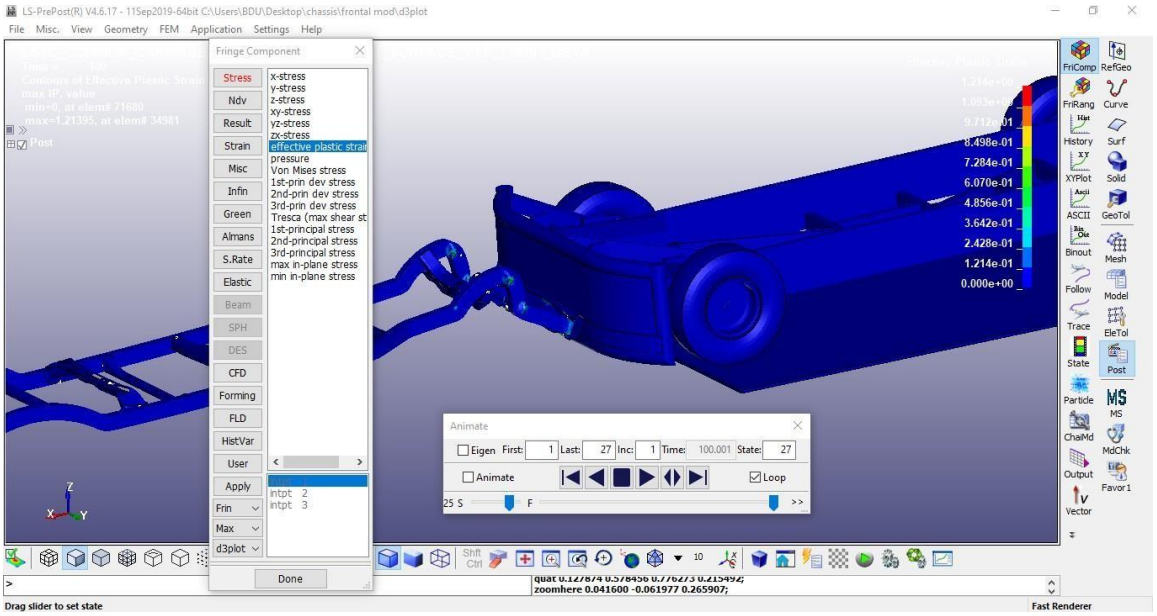
LS-PrePost(R) V4.6.17 - 11Sep2019-64bit C:\Users\BDU\Desktop\chassis\frontal mod\d3plot
File Misc. View Geometry FEM Application Settings Help
Fringe Component
Stress
Ndv
Result
Strain
Misc
Infin
Green
Almans
S.Rate
Elastic
Beam
SPH
DES
CFD
Forming
FLD
HistVar
User
Apply
Frin
Max
d3plot
x-stress
y-stress
z-stress
xy-stress
yz-stress
zx-stress
effective plastic strain
pressure
Von Mises stress
1st-prin dev stress
2nd-prin dev stress
3rd-prin dev stress
Tresca (max shear st
1st-principal stress
2nd-principal stress
3rd-principal stress
max in-plane stress
min in-plane stress
intpt 2
intpt 3
Done
Animate
Eigen First: 1 Last: 27 Inc: 1 Time: 100.001 State: 27
Animate
Loop
25 S
F
8.498e-01
7.284e-01
6.070e-01
4.856e-01
3.642e-01
2.428e-01
1.214e-01
0.000e+00
Drag slider to set state
Fast Renderer

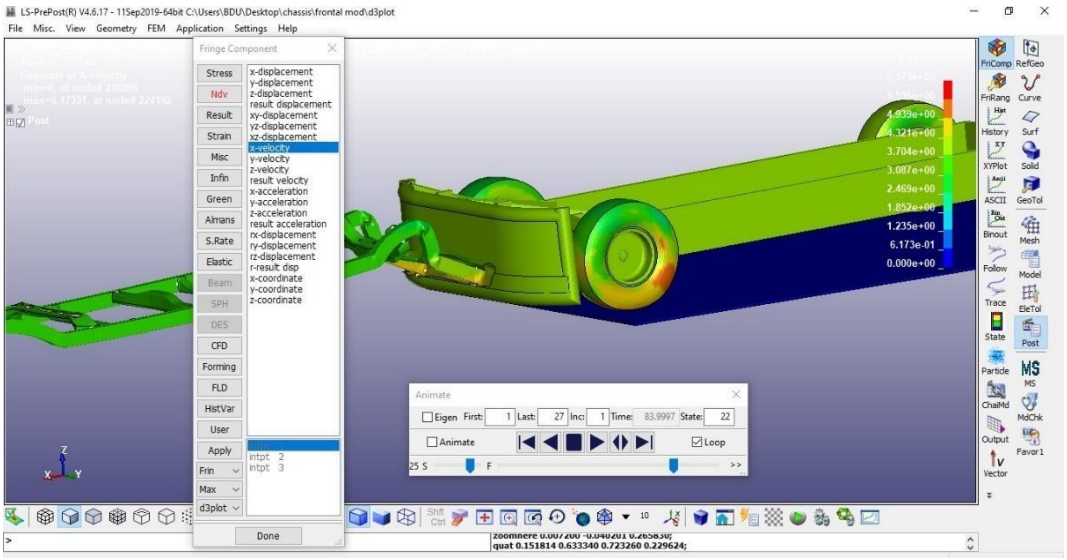
LS-PrePost(R) V4.6.17 - 11Sep2019-64bit C:\Users\BDU\Desktop\chassis\frontal mod\d3plot
File Misc. View Geometry FEM Application Settings Help
Fringe Component
Stress
Ndv
Result
Strain
Misc
Infin
Green
Almans
S.Rate
Elastic
Beam
SPH
DES
CFD
Forming
FLD
HistVar
User
Apply
Frin
Max
d3plot
x-displacement
y-displacement
z-displacement
result displacement
xy-displacement
yz-displacement
xz-displacement
x-velocity
y-velocity
z-velocity
result velocity
x-acceleration
y-acceleration
z-acceleration
result acceleration
rx-displacement
ry-displacement
rz-displacement
r-result disp
x-coordinate
y-coordinate
z-coordinate
intpt 2
intpt 3
Done
Animate
Eigen First: 1 Last: 27 Inc: 1 Time: 83.9997 State: 22
Animate
Loop
25 S
F
4.939e+00
4.321e+00
3.704e+00
3.087e+00
2.469e+00
1.852e+00
1.235e+00
6.173e-01
0.000e+00

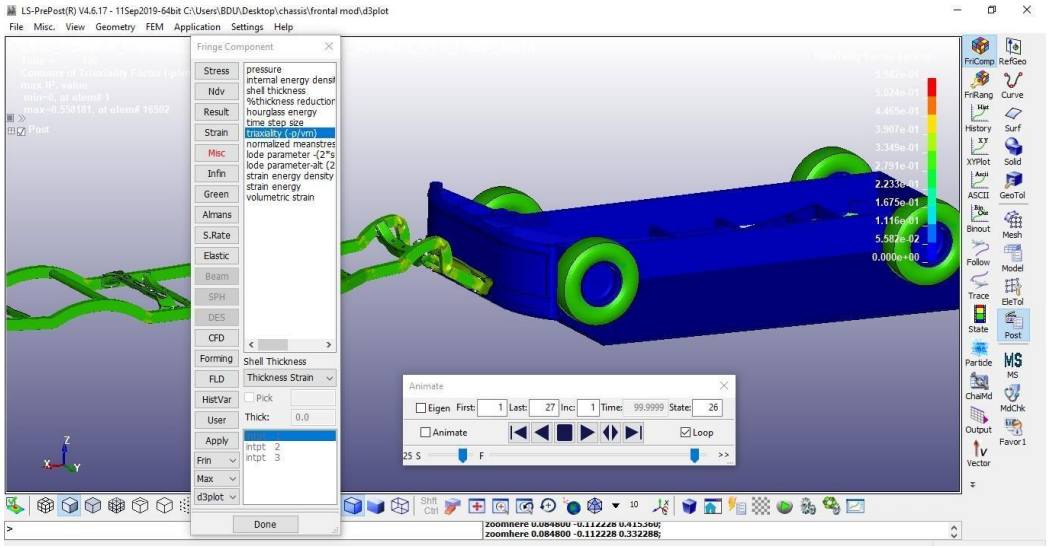
LS-PrePost(R) V4.6.17 - 11Sep2019-64bit C:\Users\BDU\Desktop\chassis\frontal mod\d3plot
File Misc. View Geometry FEM Application Settings Help
Fringe Component
Stress
Ndv
Result
Strain
Misc
Infin
Green
Almans
S.Rate
Elastic
Beam
SPH
DES
CFD
Forming
FLD
HistVar
User
Apply
Frin
Max
d3plot
pressure
internal energy densi
shell thickness
%thickness reduction
hourglass energy
time step size
Triaxiality (sy/vm)
normalized meanstres
lode parameter -(2*s
lode parameter-alt (2
strain energy density
strain energy
volumetric strain
Shell Thickness
Thickness Strain
Pick
Thick:
0.0
intpt 2
intpt 3
Done
Animate
Eigen First: 1 Last: 27 Inc: 1 Time: 99.9999 State: 26
Animate
Loop
25 S
F
2.233e-01
1.675e-01
1.116e-01
5.582e-02
0.000e+00

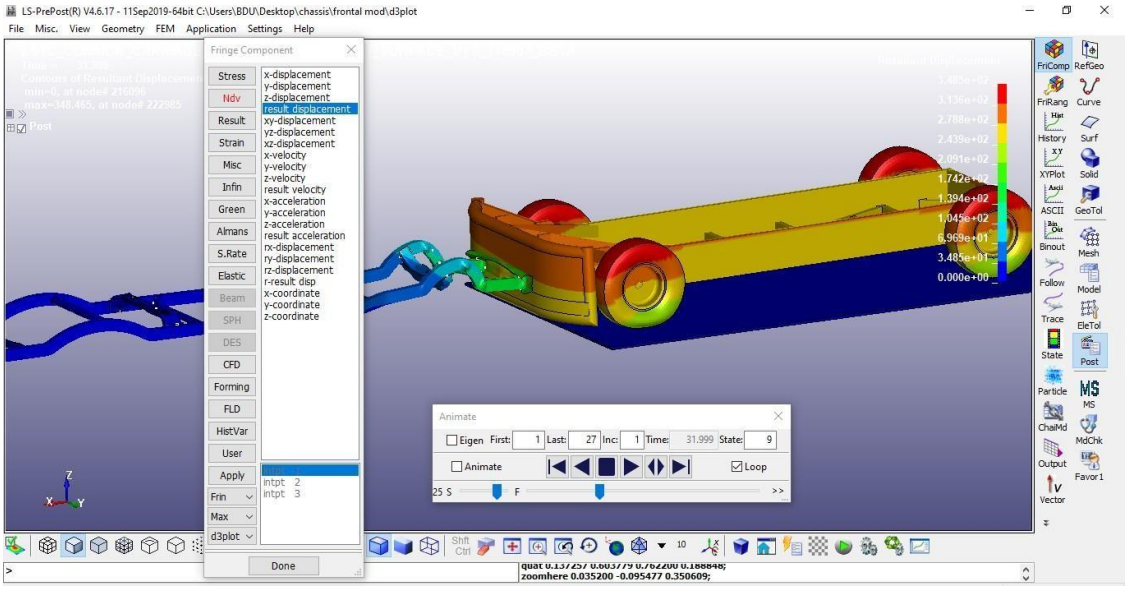
LS-PrePost(R) V4.6.17 - 11Sep2019-64bit C:\Users\BDU\Desktop\chassis\frontal mod\d3plot
File Misc. View Geometry FEM Application Settings Help
Fringe Component
Stress
Ndv
Result
Strain
Misc
Infin
Green
Almans
S.Rate
Elastic
Beam
SPH
DES
CFD
Forming
FLD
HistVar
User
Apply
Frin
Max
d3plot
x-displacement
y-displacement
z-displacement
result displacement
xy-displacement
yz-displacement
xz-displacement
x-velocity
y-velocity
z-velocity
result velocity
x-acceleration
y-acceleration
z-acceleration
result acceleration
rx-displacement
ry-displacement
rz-displacement
r-result disp
x-coordinate
y-coordinate
z-coordinate
intpt 1
intpt 2
intpt 3
Done
Animate
Eigen First: 1 Last: 27 Inc: 1 Time: 31.999 State: 9
Animate
Loop
FriComp
RefGeo
FriRang
Curve
History
Surf
XYPlot
Solid
ASCII
GeoTol
Binout
Mesh
Follow
Model
Trace
EleTol
State
Post
Particle
MS
ChalMd
MdChk
Output
Favor1
Vector
zoomhere 0.035200 -0.095477 0.350609;